



SOLID CONTACT ION SELECTIVE ELECTRODES BASED ON CARBON NANOTUBES

Gastón Adrián Crespo Paravano

ISBN: 978-84-693-6428-4

Dipòsit Legal: T-1630-2010

ADVERTIMENT. La consulta d'aquesta tesi queda condicionada a l'acceptació de les següents condicions d'ús: La difusió d'aquesta tesi per mitjà del servei TDX (www.tesisenxarxa.net) ha estat autoritzada pels titulars dels drets de propietat intel·lectual únicament per a usos privats emmarcats en activitats d'investigació i docència. No s'autoritza la seva reproducció amb finalitats de lucre ni la seva difusió i posada a disposició des d'un lloc aliè al servei TDX. No s'autoritza la presentació del seu contingut en una finestra o marc aliè a TDX (framing). Aquesta reserva de drets afecta tant al resum de presentació de la tesi com als seus continguts. En la utilització o cita de parts de la tesi és obligat indicar el nom de la persona autora.

ADVERTENCIA. La consulta de esta tesis queda condicionada a la aceptación de las siguientes condiciones de uso: La difusión de esta tesis por medio del servicio TDR (www.tesisenred.net) ha sido autorizada por los titulares de los derechos de propiedad intelectual únicamente para usos privados enmarcados en actividades de investigación y docencia. No se autoriza su reproducción con finalidades de lucro ni su difusión y puesta a disposición desde un sitio ajeno al servicio TDR. No se autoriza la presentación de su contenido en una ventana o marco ajeno a TDR (framing). Esta reserva de derechos afecta tanto al resumen de presentación de la tesis como a sus contenidos. En la utilización o cita de partes de la tesis es obligado indicar el nombre de la persona autora.

WARNING. On having consulted this thesis you're accepting the following use conditions: Spreading this thesis by the TDX (www.tesisenxarxa.net) service has been authorized by the titular of the intellectual property rights only for private uses placed in investigation and teaching activities. Reproduction with lucrative aims is not authorized neither its spreading and availability from a site foreign to the TDX service. Introducing its content in a window or frame foreign to the TDX service is not authorized (framing). This rights affect to the presentation summary of the thesis as well as to its contents. In the using or citation of parts of the thesis it's obliged to indicate the name of the author.

UNIVERSITAT ROVIRA I VIRGILI

SOLID CONTACT ION SELECTIVE ELECTRODES BASED ON CARBON NANOTUBES

Gastón Adrián Crespo Paravano

ISBN: 978-84-693-6428-4/DL:T-1630-2010

Solid Contact Ion Selective Electrodes Based on Carbon Nanotubes

Doctoral Thesis
Gastón A. Crespo

Tarragona, 2010



UNIVERSITAT
ROVIRA I VIRGILI

DEPARTMENT OF ANALYTICAL CHEMISTRY
AND ORGANIC CHEMISTRY

Solid Contact Ion Selective Electrodes Based on Carbon Nanotubes

Doctoral Thesis
Gastón A. Crespo

Tarragona, 2010



UNIVERSITAT
ROVIRA I VIRGILI

DEPARTMENT OF ANALYTICAL CHEMISTRY
AND ORGANIC CHEMISTRY

Solid Contact Ion Selective Electrodes Based on Carbon Nanotubes

Doctoral Thesis
Gastón A. Crespo

Tarragona, 2010



UNIVERSITAT
ROVIRA I VIRGILI

DEPARTMENT OF ANALYTICAL CHEMISTRY
AND ORGANIC CHEMISTRY

Solid Contact Ion Selective Electrodes Based on Carbon Nanotubes

Doctoral Thesis supervised by
Prof. F. Xavier Rius Ferrús

Tarragona, 2010



UNIVERSITAT
ROVIRA I VIRGILI

DEPARTMENT OF ANALYTICAL CHEMISTRY
AND ORGANIC CHEMISTRY

Solid Contact Ion Selective Electrodes Based on Carbon Nanotubes

Tribunal members:

Prof. Johan Bobacka (Åbo Akademi Univ.)

Prof. Angel Ríos Castro (Castilla y la Mancha Univ.)

Prof. Julian Alonso Chamarro (Autónoma Barcelona Univ.)

Prof. Ioanis Katakis (Rovira I Virgili Univ.)

Dr. Santiago Macho (Rovira I Virgili Univ.)

External examiners:

Prof. Livia Nagy (Pécs Univ.)

Prof. Robert Gyurcsányi (Technology and Economics Budapest Univ.)

Tarragona, 2010



UNIVERSITAT
ROVIRA I VIRGILI

DEPARTMENT OF ANALYTICAL CHEMISTRY
AND ORGANIC CHEMISTRY



UNIVERSITAT
ROVIRA I VIRGILI

**DEPARTAMENT DE QUÍMICA
ANALÍTICA I QUÍMICA ORGÀNICA**

Campus Sescelades
Marcel·lí Domingo, s/n
43007 Tarragona
Tel. 34 977 55 95 62
Fax 34 977 55 84 46
e-mail: fxavier.rius@urv.cat

F. Xavier Rius Ferrús, Professor of Analytical Chemistry at the Department of Analytical Chemistry and Organic Chemistry at the Universitat Rovira i Virgili,

CERTIFIES

that the Doctoral Thesis entitled: "Solid Contact Ion Selective Electrodes Based on Carbon Nanotubes", submitted by Gastón A. Crespo Paravano to obtain the degree of Doctor by the Universitat Rovira i Virgili, has been carried out under my supervision, in the Department of Analytical Chemistry and Organic Chemistry at the Universitat Rovira i Virgili, and all the results presented in this thesis were obtained in experiments conducted by the above mentioned student.

Tarragona, 4 May 2008

Professor F. Xavier Rius Ferrús

Acknowledgments

Firstly, I would really like to thank *Prof. F. Xavier Rius* for the opportunity to undertake my PhD study in his group and for having confidence in me. Both his scientific and personal teachings have been really important in my personal development. I appreciate the active cooperation of *Dr. Santiago Macho* and for looking after me in during my first years in Tarragona. My credits also go to the Spanish Ministry of Education and Science for supporting this thesis.

Secondly, a special thank you to my friend, *Dr. Francisco Andrade* who has been one of the most important guides in my first steps in the human and research world, since 2002 when we met at the University of Buenos Aires. I would like to express my thanks for his encouragement in each moment of my life, especially, for when things got more than a little tough.

Thirdly, my uttermost respect to my *Mum, Dad, my brother Cristian and my Grandma*. Without them, I would have never reached where I am now. Their support and devotion to me, is reflected in this thesis.

I would like to thank:

Professor Ernö Pretsch being really open and friendly towards me. Our meetings both in Tarragona and ETH University have been essential both in the thesis and my carrier development. In addition, thanks for the valuable information provided throughout the years.

Professor Ari Ivaska for having made possible my stay in his group in Abo Academi University, Finland. Also to *Professor Johan Bobacka* for his scientific support during my stay and in the subsequent years. Thanks to each member of the Laboratory of Analytical Chemistry, Åbo Akademi University, you made me feel at home.

Professor Bernhard Wehrli for having allowed my stay in his institute (Swiss Federal Institute of Aquatic Science & Technology – EAWAG - ETH University). Many thanks to my “old” friend *Matthias Kirf* who introduced me to environmental science. We have lived some very nice moments together in Tarragona and Lucerne.

Professor Robert Gyurcsanyi for having made possible my stay in his group in Budapest University of Technology and Economics. I enjoyed our useful discussions about nano-potentiometry.

Professor Geza Nagy and Livia Nagy for having made possible my stay in University of Pecs.

All Chemometrics, Qualimetrics and Nanosensor group members, especially, *Ali Duzgün* who has always been at my side from the beginning of my PhD. In the same way, I thank my friends *Enrique Parra, Dr. Pascal Blondeau, Xavier Rius’ son, Gary Shea, Oscar Sandrine, Ricardo Acosta and Cristian Galvani* for making each day better.

My best acknowledgments to my friend, *Jordi Ampurdanés* (soon *Dr. Ampurdanés*) for his unconditional help both in the lab and in this thesis. His enthusiastic personality is honorable to have in each laboratory. We have enjoyed many moments in these past few years together performing rather than performing science.

A big thanks *Valeria Russo*, who has helped me a lot in the design of the thesis. Also, *Dr. Pablo Ramos* for all the moments enjoyed, especially, in the first years in Tarragona.

Thank you to *Liliana* from the Fomec Laboratory of UBA University, who has supported me during these four years in Spain.

Finally, I would like to express my deep and sincere gratitude to my future wife, *Dr Noelia Barrabés* who has supported me in each moment of wonderful last year. This thesis would not have been finished without her help. Thank you for having trust in me, for encouraging me and finally for making me feel important and happy to be at your side.

Agredecimientos

En primer lugar me gustaría agradecer al *Prof. F. Xavier Rius* por haberme concedido la oportunidad de realizar mis estudios de doctorado en su grupo de investigación y por haber confiado en mí en todo momento. Sus enseñanzas tanto científicas como personales han sido realmente importantes en mi desarrollo personal. Mi aprecio hacia *Dr. Santiago Macho* por su activa cooperación científica y por haberme ayudado intensivamente durante mis primeros años en Tarragona. Mis agradecimientos al ministerio Español de Educación y Ciencia por haber financiado mis estudios doctorales.

En segundo lugar, un especial "gracias" a mi amigo, *Dr. Francisco Andrade* quien ha sido el conductor más importante en mis primeros pasos en el mundo de la investigación y también en el mundo de las personas, desde aquel invierno del 2002 cuando nos conocimos en la UBA. Agradecer por la continua motivación en cada momento de mi vida, especialmente, en aquellos donde la llovizna se transforma en tormenta.

En tercer lugar mi mayor y profundo respeto hacia mi *Mamá, Papá*, mi hermano *Cristian* y mi *Abuela*. Obviamente, sin ellos, yo nunca hubiera llegado a donde estoy ahora. Su soporte y cariño incondicional hacia mí es reflejado en cada párrafo de esta tesis.

Del mismo modo me gustaría agradecer a las siguientes personas:

Profesor Ernö Pretsch quien ha sido una persona muy abierta y amigable en todo momento. Nuestras reuniones en Tarragona y en la ETH han sido realmente importantes en la tesis como así también para mi carrera profesional. Además, gracias por todas las investigaciones reportadas a través de largos años.

Profesor Ari Ivaska por haber permitido mi estancia en su grupo en la Universidad de Åbo Akademi, Finlandia. Mis sinceros agradecimientos hacia el *Profesor Johan Bobacka* por su ayuda científica durante mi estancia y en los posteriores años. Gracias a cada miembro del Laboratorio de Química Analítica de la Universidad de Åbo Akademi por haber hacerme sentido como en casa.

Profesor Bernhard Wehrli por haber permitido my estancia en el instituto Federal Suizo de Ciencia y Tecnología Acuática (EAWAG- ETH). Muchísimas gracias a mi "viejo" amigo *Mathias Kirf* quien me ha introducido en la ciencia ambiental. Gracias por los lindos momentos que hemos juntos en Tarragona y Lucerne.

Profesor Robert Gyurcsanyi por haber posibilitado mi estancia en su grupo de investigación de la Universidad Tecnológica y Económica de Budapest. He disfrutado de las provechosas discusiones que mantuvimos sobre la nanopotentiometría.

Profesores Geza Nagy y Livia Nagy por haber posibilitado mi estancia en su grupo de investigación en la Universidad de Pecs.

A todos los miembros del grupo de Quimiometría, Cualimetría y Nanosensores de la URV. Especialmente a *Ali Duzgün* quien ha estado siempre a mi lado desde los comienzos de mis estudios de doctorado. También agradecer a mis amigos *Enrique Parra, Pascal Blondeau, Xavi Rius Gary Shea, Oscar Sandrine, Ricardo Acosta* y *Cristian Galvani* por hacerme sentir mejor cada día.

Mis mejores agradecimientos a mi amigo, *Jordi Ampurdanés* (próximamente *Dr. Ampurdanés*) por su incondicional ayuda tanto en el laboratorio como en el desarrollo de esta tesis. Su entusiasta personalidad es digna de poseer en cada laboratorio. Muchos momentos en estos últimos tres años hemos disfrutado dentro y fuera del ámbito científico.

Gracias a *Valeria Russo* quien me ayudado en el diseño de la tesis. También al *Dr. Pablo Ramos* por los buenos momentos vividos especialmente en el primer año.

Mis agradecimientos a *Liliana* quien ha estado en todo momento alentándome y apoyándome a la distancia.

Finalmente, me gustaría expresar mí mas profundos y sinceros agradecimientos a mi futura esposa, la *Dra. Noelia Barrabés* quien siempre me ha estado alentando en cada momento de este maravilloso último año. Esta tesis no podría haber sido finalizada sin su ayuda. Muchas gracias por haber confiado en mí, por su soporte y lo más importante, por hacerme sentir feliz a su lado.

UNIVERSITAT ROVIRA I VIRGILI

SOLID CONTACT ION SELECTIVE ELECTRODES BASED ON CARBON NANOTUBES

Gastón Adrián Crespo Paravano

ISBN:978-84-693-6428-4/DL:T-1630-2010

UNIVERSITAT ROVIRA I VIRGILI

SOLID CONTACT ION SELECTIVE ELECTRODES BASED ON CARBON NANOTUBES

Gastón Adrián Crespo Paravano

ISBN:978-84-693-6428-4/DL:T-1630-2010

UNIVERSITAT ROVIRA I VIRGILI

SOLID CONTACT ION SELECTIVE ELECTRODES BASED ON CARBON NANOTUBES

Gastón Adrián Crespo Paravano

ISBN:978-84-693-6428-4/DL:T-1630-2010

*"Lento en mi sombra, la penumbra hueca
exploro con el báculo indeciso,
yo, que me figuraba el Paraíso
bajo la especie de una biblioteca"
JLB (1960, El hacedor)*

UNIVERSITAT ROVIRA I VIRGILI

SOLID CONTACT ION SELECTIVE ELECTRODES BASED ON CARBON NANOTUBES

Gastón Adrián Crespo Paravano

ISBN:978-84-693-6428-4/DL:T-1630-2010

UNIVERSITAT ROVIRA I VIRGILI

SOLID CONTACT ION SELECTIVE ELECTRODES BASED ON CARBON NANOTUBES

Gastón Adrián Crespo Paravano

ISBN:978-84-693-6428-4/DL:T-1630-2010

UNIVERSITAT ROVIRA I VIRGILI

SOLID CONTACT ION SELECTIVE ELECTRODES BASED ON CARBON NANOTUBES

Gastón Adrián Crespo Paravano

ISBN:978-84-693-6428-4/DL:T-1630-2010

Table of contents

Summary	1
Resumen	3
1. Introduction	7
1.1. State of the art	9
1.2. Objectives	13
1.3. References	13
2. The principles	17
2.1. Introduction	19
2.2. Chemical sensors	19
2.3. Ion selective electrodes	19
2.3.1. Ion selective membrane	19
2.3.1.1. Polymeric matrix	20
2.3.1.2. Lipophilic ion exchangers	20
2.3.1.3. Ionophores	21
2.3.2. Generation of Nernstian response	22
2.3.3. Analytical performance parameters	25
2.3.3.1. Sensitivity	25
2.3.3.2. Selectivity	26
2.3.3.3. Limit of detection	28
2.3.3.4. Stability	28
2.3.4. Solid contact ion selective electrodes	29
2.3.4.1. Conditioning	30
2.4. General properties of Carbon Nanotubes	32
2.5. References	33
3. Experimental section	37
3.1. Introduction	39
3.2. Reagents	39
3.2.1. Carbon nanotubes	39
3.2.2. Membrane components	39
3.2.2.1. Ionophores	39
3.2.2.2. Lipophilic salts	39
3.2.2.3. Acrylic backbone	39
3.2.3. Other reagents	41
3.3. Procedures	41
3.3.1. Purification of carbon nanotubes	41
3.3.2. Deposition of carbon nanotubes	42

3.3.2.1. Spraying	42
3.3.2.2. Electrophoretic deposition	43
3.3.2.3. Drop casting	43
3.3.3. Development of the ion selective electrodes	44
3.3.3.1. PVC home-made electrode	44
3.3.3.2. Glassy carbon home-made electrode	44
3.3.3.3. Copper home-made electrode	45
3.3.3.4. Nano home-made electrode	45
3.3.4. Ion-Selective membrane preparation	46
3.3.4.1. Acrylic matrix	46
3.3.4.2. Ion selective membrane preparation	46
3.3.5. Deposition of the membrane	46
3.3.5.1. Dip coating	46
3.3.5.2. Drop casting	46
3.3.5.3. Back-filling	47
3.3.6. Conditioning	47
3.3.7. Microscopic characterization	47
3.3.7.1. Scanning electron microscopy	47
3.3.7.2. Transmission electron microscopy	47
3.3.8. Electrochemical characterization	48
3.3.8.1. Electrochemical impedance spectroscopy	48
3.3.8.2. Cyclic voltammetry	48
3.3.8.3. Chronopotentiometry	48
3.3.8.4. Potentiometry	49
3.4. References	49
4. Carbon Nanotubes as efficient transducer in potentiometric sensors	51
4.1. Introduction	53
4.2. "Ion-Selective Electrodes Using Carbon Nanotubes as Ion-to-Electron Transducers"	53
4.2.1. Abstract	53
4.2.2. Keywords	53
4.2.3. Introduction	54
4.2.4. Experimental section	55
4.2.4.1. Ion selective membrane	55
4.2.4.2. Electrode development	55
4.2.4.3. Electrochemical impedance spectroscopy	55
4.2.4.4. Chronopotentiometric measurements	56
4.2.4.5. Electromotive force measurements	56
4.2.5. Results and discussion	57
4.2.5.1. Impedance spectroscopy of Cu/SWCNTs on PVC support	58
4.2.5.2. Impedance of SWCNT/K ⁺ -ISEs	60
4.2.5.3. Water layer test	61
4.2.5.4. Potentiometric performance characteristics	61

4.2.5.5. Chronopotentiometry	63
4.2.6. Conclusions	64
4.2.7. Acknowledgments	65
4.2.8. References	66
4.2.9. Supporting information	67
5. Transduction mechanism of the carbon nanotubes	71
5.1. Introduction	73
5.2. "Transduction mechanism of carbon nanotubes in solid-contact ISE"	73
5.2.1. Abstract	73
5.2.2. Keywords	74
5.2.3. Introduction	74
5.2.4. Experimental section	75
5.2.5. Results and discussion	77
5.2.5.1. Characterization by cyclic voltammetry	77
5.2.5.2. Characterization by electrochemical impedance spectroscopy	78
5.2.5.3. Equivalent circuit	80
5.2.5.4. Resistance	81
5.2.5.5. Capacitance	82
5.2.5.6. Diffusion	83
5.2.5.7. Physical transduction mechanism	83
5.2.6. Conclusions	85
5.2.7. Acknowledgments	85
5.2.8. References	86
6. Applications	89
6.1. Introduction	91
6.2. "Solid contact pH-selective electrode using multi-walled carbon nanotubes"	92
6.2.1. Abstract	92
6.2.2. Keywords	92
6.2.3. Introduction	93
6.2.4. Experimental section	94
6.2.4.1. Chemicals	94
6.2.4.2. Preparation of methacrylate/acrylate polymers	94
6.2.4.3. Development of the solid-contact pH ISE	95
6.2.4.4. Ion selective membrane preparation	95
6.2.4.5. Instruments and EMF measurements	95
6.2.4.6. Impedance spectra of MWCNT based hydrogen ion sensor	96
6.2.4.7. Chronopotentiometric measurements	96
6.2.5. Results and discussion	96
6.2.6. Conclusions	100
6.2.7. Acknowledgments	101
6.2.8. References	102

6.3. "Determination of choline and derivatives with a solid-contact-ion-selective electrode based on octaamide cavitand and carbon nanotubes"	104
6.3.1. Abstract	104
6.3.2. Keywords	105
6.3.3. Introduction	105
6.3.4. Experimental	107
6.3.4.1. Chemical reagents and material	107
6.3.4.2. Preparation of the electrode	107
6.3.4.3. Ion-selective membrane synthesis and deposition	108
6.3.4.4. Conditioning of the electrode	108
6.3.5. Electrochemical measurements	109
6.3.5.1. Potentiometric measurements	109
6.3.5.2. Chronopotentiometric measurements	109
6.3.5.3. Impedance measurements	110
6.3.5.4. Water layer test	110
6.3.6. Results and discussion	110
6.3.6.1. Potentiometric measurements	110
6.3.6.2. Chronopotentiometric measurements	112
6.3.6.3. Impedance measurements	113
6.3.6.4. Water layer test	113
6.3.7. Conclusions	115
6.3.8. Acknowledgments	115
6.3.9. References	116
6.4. Robust potentiometric sensors to determine ionic gradients in aquatic environments	118
6.4.1. Introduction	118
6.4.2. Experimental section	119
6.4.2.1. Development of waterproof electrodes	119
6.4.2.2. Potentiometric measures	121
6.4.3. Results and discussion	122
6.4.3.1. Calibration of the electrodes	122
6.4.3.2. Light sensitivity test	123
6.4.3.3. <i>In-situ</i> measurements	124
6.4.4. Conclusions	125
6.4.5. Acknowledgments	125
6.4.6. References	126
6.5. Potentiometric sensors for the <i>on-line</i> monitoring of a catalytic denitrification process	127
6.5.1. Introduction	127
6.5.2. Experimental section	129
6.5.2.1. Manufacturing of the sensors	129
6.5.2.2. Membrane cocktail preparation	129
6.5.2.3. Reagents	130
6.5.2.4. Instrumentation	130
6.5.3. Results and discussion	131

6.5.3.1. Flow calibration of the electrodes	131
6.5.3.2. Control of a catalytic reaction	133
6.5.4. Conclusions	135
6.5.5. References	136
7. Miniaturization	139
<hr/>	
7.1. Introduction	141
7.2. "Nanomeric solid-contact ion-selective electrodes using carbon nanotubes as transducers"	142
7.2.1. Abstract	142
7.2.2. Introduction	142
7.2.3. Experimental section	144
7.2.3.1. Reagents and materials	144
7.2.3.2. Electrode construction	144
7.2.3.3. Silanization	145
7.2.3.4. Carbon Nanotubes dispersion	146
7.2.3.5. Carbon Nanotubes deposition	146
7.2.3.6. Membrane preparation	147
7.2.3.7. Electrode assembly	147
7.2.3.8. Electrochemical measurements	148
7.2.3.8.1. Potentiometric measurements	148
7.2.3.8.2. Impedance measurements	148
7.2.3.8.3. Resistance measurements	148
7.2.4. Results and discussion	148
7.2.5. Conclusions	151
7.2.6. Acknowledgments	152
7.2.7. References	152
8. Conclusions	155
<hr/>	
8.1. Conclusions	157
8.2. Future prospects	158
8.3. References	159
Appendices	161
<hr/>	
Appendix 1. Glossary	163
Appendix 2. Equations	169
Appendix 3. Complementary information of chapter 3	171
Appendix 4. Complementary information of chapter 6 (6.5)	173
Appendix 5. Short CV	177

UNIVERSITAT ROVIRA I VIRGILI

SOLID CONTACT ION SELECTIVE ELECTRODES BASED ON CARBON NANOTUBES

Gastón Adrián Crespo Paravano

ISBN:978-84-693-6428-4/DL:T-1630-2010

UNIVERSITAT ROVIRA I VIRGILI

SOLID CONTACT ION SELECTIVE ELECTRODES BASED ON CARBON NANOTUBES

Gastón Adrián Crespo Paravano

ISBN:978-84-693-6428-4/DL:T-1630-2010

UNIVERSITAT ROVIRA I VIRGILI

SOLID CONTACT ION SELECTIVE ELECTRODES BASED ON CARBON NANOTUBES

Gastón Adrián Crespo Paravano

ISBN:978-84-693-6428-4/DL:T-1630-2010

Summary

The aim of this thesis is the development of solid contact ion selective electrodes, ISEs, where the transducer layer is made of a network of carbon nanotubes.

Potentiometric classical ion selective electrodes (ISEs) have been used for analytical applications since the beginning of 1900's. Determination of pH by a glass membrane ion selective electrode emerged at the beginning, being the first ISEs developed. pH glass electrode is still one of the most useful and robust sensors for routine measurements both in laboratories and industries.

Throughout the years, new technologies, ideas and designs have been developed and incorporated successfully in the potentiometric fields so as to provide answers to the new society's needs. Therefore, the ion selective electrodes developed in this thesis are a step further in the progress of ISEs and must be considered as products of the scientific envisioning, growth, and interdisciplinary cooperation of many research teams over many years of continuous efforts.

The sensing part can be regarded nowadays as well developed, although it has been during only the last few years when considerable improvements have taken place in the development of new polymeric membranes, ionophores and lipophilic ions. Moreover, the understanding of the theoretical sensing mechanism has been a powerful solid backbone in the rise of ISEs.

Miniaturization of classical ISEs requires making all solid contact electrodes to avoid the intrinsic drawbacks of the inner solution. In this manner, the transduction layer has been the focus of attention for the two last decades. New solid contact transducers having the capacity to convert an ionic current into an electronic current have been emerging. Within them, conducting polymers have played an important role in the transduction of the potentiometric signal, being the most used in solid contact ion selective electrodes (SC-ISEs) up to now. However, the behaviour of conducting polymers can be further improved. For instance, their sensitivity to light one of main operational issues yet to be solved.

In the present context of searching for new materials able to transduce potentiometric signals we selected and tested carbon nanotubes (CNTs). CNTs, which were rediscovered by Iijima in 1991, display excellent electronic properties in terms of signal transduction. In addition, due to their chemical reactivity CNTs can be easily functionalized with receptors or other functional groups. In fact, depending on the type of functionalization the macroscopic and microscopic properties of CNTs can be drastically changed. This nanostructured material had not been used previously as a solid contact material in ISEs.

The main aim of this thesis is to demonstrate that CNTs can act as a clean and efficient transducer in SC-ISEs overcoming the drawbacks displayed by the previously assayed solid contact

materials. The developed electrodes were used in different conditions to determine several ions in different sample types, demonstrating the capabilities of this nanostructured material.

The thesis has been structured in different chapters, each one containing the following information:

- **Chapter 1** provides a short historical overview of potentiometric ISEs. The evolution from the "classical ISEs" to the SC-ISEs is briefly illustrated. Once the motivation for this thesis is described, the general and specific objectives of the thesis are reported.
- **Chapter 2** reports the scientific foundations of the developed electrodes. All components of the ISE, sensing layer, transducers and detection systems are introduced. Analytical performance characteristics of ISEs are also described.
- **Chapter 3** corresponds to the experimental part. Reagents, protocols, procedures and instruments used in the thesis are reported.
- **Chapter 4** provides the demonstration that CNTs can act as a transducer layer in SC-ISEs. The first SC-ISEs based on CNTs are characterized by electrochemical and optical techniques.
- **Chapter 5** contains the experimental results that lead to the elucidation of the possible transduction mechanism of CNTs in SC-ISEs. Electrochemical impedance spectroscopy (EIS) is employed as the main characterization technique.
- **Chapter 6** is composed of four sections reporting different analytical applications. In the first section, the common pH electrode is developed using a solid contact technology based on CNTs. In the second section, the development of SC-ISEs based on a new synthetic ionophore selective to choline, and CNTs as transducers is shown. In the third section, watertight and pressure-resistant SC-ISEs based on CNTs are developed and tested in aquatic research to obtain information about the gradient profiles along the depth of the lakes. In the fourth section, SC-ISEs based on CNTs are adapted for the *on-line* control of a denitrification catalytic process.
- **Chapter 7** reports the possibilities of miniaturization of the SC-ISEs based on CNTs to reach a nanometric electrode. Potentiometric and optical characterizations are described in this section. Moreover, a discussion about the limitations of the real miniaturization in potentiometry is undertaken.
- **Chapter 8** points out the conclusions of the thesis. In addition, future prospects are suggested.
- Finally, several appendices are added to complete the doctoral thesis.

Resumen

El principal objetivo de esta tesis es el desarrollo de electrodos selectivos de iones de contacto sólido, ESIs-CS, utilizando como capa transductora una red compuesta de nanotubos de carbono.

Los electrodos potenciométricos selectivos de iones se han sido utilizados en aplicaciones analíticas desde comienzos de 1900. La determinación de pH mediante electrodos de vidrio selectivo de iones fue el primer ESI desarrollado. Hoy en día, el electrodo de vidrio para la determinación de pH es todavía uno de los sensores más útiles y robustos utilizados en mediciones rutinarias tanto en laboratorios como en industrias.

A lo largo de los años, se han desarrollado nuevas tecnologías, ideas y diseños, y se han incorporado satisfactoriamente en el campo potenciométrico proporcionando soluciones a las necesidades en continua evolución de la sociedad. De esta manera, los electrodos selectivos de iones desarrollados en esta tesis son un paso más en el progreso de los ESIs y considerarse como el producto de una sólida base científica, del crecimiento y de la cooperación interdisciplinaria de diversos grupos de investigación durante varios años.

La parte del sensor donde tiene lugar el reconocimiento químico y donde se genera el potencial dependiente de la muestra en estudio en los ESIs se puede considerar, en estos días, ampliamente desarrollada, aunque considerables mejoras han tenido lugar durante los últimos años, especialmente en el desarrollo de nuevas membranas poliméricas, ionóforos e iones lipofílicos. Sobre todo, el estudio y la comprensión del mecanismo teórico del sensor ha sido muy importante en el crecimiento y desarrollo de los ESIs.

El concepto de electrodos selectivos de iones de estado sólido surge en el proceso de miniaturización de los ESIs clásicos, como requisito vital para evitar las intrínsecas desventajas de la solución interna. De esta forma, la capa transductora ha sido el principal punto de atención durante dos décadas. Así, se han desarrollado nuevos transductores de contacto sólido con la capacidad de convertir una corriente iónica en una corriente electrónica. Entre ellos, los polímeros conductores han jugado un importante papel en la transducción de la señal potenciométrica, siendo éstos los más empleados en los electrodos selectivos de iones de contacto sólido (ESIs-CS). Sin embargo el comportamiento de los polímeros conductores puede mejorarse. Por ejemplo, la sensibilidad hacia la luz de estos materiales es un inconveniente todavía no resuelto.

En este contexto de investigación de nuevos materiales capaces de actuar como transductor de una señal potenciométrica, se han escogido y estudiado los nanotubos de carbono (NTCs) como transductores. Los NTCs fueron redescubiertos por Ijima en 1991, y muestran excelentes propiedades electrónicas en términos de traducción de señal. Además, debido a su reactividad

química, los NTCs pueden funcionalizarse fácilmente con receptores u otros grupos funcionales. De hecho, sus propiedades macroscópicas y microscópicas pueden afectarse drásticamente dependiendo del tipo y grado de funcionalización. Este material nanoestructurado no había sido previamente utilizado como transductor en ISEs.

El principal propósito de esta tesis es demostrar que los nanotubos de carbono pueden actuar de forma eficiente como transductor en electrodos selectivos de iones de estado sólido logrando vencer las desventajas de los transductores previamente mencionados. Los electrodos desarrollados se usaron en diferentes condiciones para determinar distintos iones en diversos tipos de sistemas, demostrando las extraordinarias capacidades de este material nanoestructurado.

Esta tesis se ha estructurado en capítulos que contienen la siguiente información:

El **Capítulo 1** proporciona una breve visión histórica de los electrodos potenciométricos selectivos de iones. Se ilustra la evolución desde los "clásicos ESIs" hasta los actuales "ESIs-CS". Además se señalan en esta sección los objetivos generales y específicos.

El **Capítulo 2** contiene las bases científicas de los electrodos desarrollados. Se introducen todos los componentes que integran un ESI, tales como: capa reconocedora, capa transductora y sistema de detección. A continuación se describen los parámetros analíticos de calidad de los ESIs.

El **Capítulo 3** describe la parte experimental. Se recogen los reactivos, protocolos, procedimientos e instrumentos usados a lo largo de la tesis.

El **Capítulo 4** provee de la demostración de que los NTCs pueden actuar eficientemente como capa transductora en SC-ISEs. Se caracteriza el primer ESI-CS integrado por NTCs mediante técnicas ópticas y electroquímicas.

El **Capítulo 5** contiene los resultados experimentales que permiten la posible elucidación del mecanismo de transducción de los NTCs en los ESIs-CS. Espectroscopía de Impedancia Electroquímica (ESI) es utilizada como la principal técnica de caracterización.

El **Capítulo 6** está integrado por cuatro secciones con diferentes aplicaciones analíticas. En la primera sección, se desarrolla un electrodo de pH que usa NTCs como nueva tecnología transductora en ESIs-CS. En la segunda sección se muestra el desarrollo de un ESI-CS integrado por un ionóforo sintético selectivo a colina, y NTCs como transductores. En la tercera sección, se desarrollan y prueban ESIs-CS basados en NTCs, resistentes a altas presiones y totalmente herméticos, en investigaciones acuáticas con la finalidad de obtener información sobre los gradientes de concentración de iones en función de la profundidad de un lago. En la cuarta sección ESIs-CS basados en NTCs se adaptan para el control *on-line* de un proceso catalítico de desnitrificación.

El **Capítulo 7** presenta la posibilidad de la miniaturización de los ESIs-CS basados en NTCs logrando obtener un electrodo nanométrico. Se muestran en esta sección la caracterización óptica y potentiométrica. Además, se discuten las limitaciones de la miniaturización real de los ESIs en potenciometría.

El **Capítulo 8** contiene las conclusiones de la tesis. Adicionalmente, se sugieren las perspectivas futuras del trabajo presentado.

Finalmente, se añaden algunos apéndices como complemento de la tesis doctoral.

UNIVERSITAT ROVIRA I VIRGILI

SOLID CONTACT ION SELECTIVE ELECTRODES BASED ON CARBON NANOTUBES

Gastón Adrián Crespo Paravano

ISBN:978-84-693-6428-4/DL:T-1630-2010



CHAPTER 1
INTRODUCTION

UNIVERSITAT ROVIRA I VIRGILI

SOLID CONTACT ION SELECTIVE ELECTRODES BASED ON CARBON NANOTUBES

Gastón Adrián Crespo Paravano

ISBN:978-84-693-6428-4/DL:T-1630-2010

1.1. State of the art

Potentiometry as an analytical technique emerged at the beginning of the last century through the joint development of suitable measuring instruments and the introduction of new electrochemical sensing mechanisms. Through the years improvement of the measuring instruments from the old voltmeters, galvanometers and electrometers [1], which did not display enough resolution for many of today's applications, was accomplished. As a consequence of that technological race, potentiometers with high precision, in terms of the magnitude of current flowing through the electronic circuit, are available nowadays. In contrast to the measuring instruments and the data acquisitions tools, research on electrochemical sensing mechanism and their components has been evolving continuously [2].

Potentiometric detection is by far one of the most inexpensive and easiest to use techniques within a wide range of other electroanalytical techniques. As a consequence, potentiometric measurements are frequently recorded as routine essays in control or research laboratories. The main targets of detection are usually cations such as hydronium, alkaline, alkaline-earth metal ions and several anions.

Looking at the process of electrochemical sensing, potentiometric ion selective electrodes (ISEs) can be studied from different points of view depending on which part or configuration of the electrode is selected. As is well known today, an ion selective electrode is basically composed for an ion selective membrane (ISM), a transducer element, an electrical conductor and an inert body protecting the conductor from the external parasitic noise. Furthermore, several kinds of ion selective membranes have been developed and recommended for analytical applications. However, only liquid and polymeric ion selective membranes based on carrier and ion exchanger are studied here.

During 1960's and 1970's breakthroughs concerning the ion selective membrane took place originating the modern carrier-based ISEs. Firstly, Moore et al [3] had found out that several antibiotics showed ion transport properties in the mitochondrial cell. Simon's group took advantage of this knowledge and included for the first time the antibiotic inside the membrane demonstrating that these antibiotics induce *in vitro* selectivities similar to those observed *in vivo* [4]. Secondly, at the same time, host-guest chemistry was emerging. Pedersen and Lehn synthesized macrocyclic compounds (polyethers and macroheterobicyclic) able to act as complex agents for alkali ions [5, 6]. In the following years, these synthetic receptors started to be included in ISMs [7]. Finally, the liquid ion exchanger membranes concept was introduced by Ross to detect calcium ions [8]. Later, polyvinyl chloride (PVC) polymers were introduced as the matrix in carrier-ISMs [9, 10]. Nonetheless, at that time ionic sites were not explicitly incorporated in the membrane, although later on, it was demonstrated that they were presented as PVC impurities [11, 12].

In the subsequent two decades, many researchers developed and characterized successful selective neutral and charged carriers for several analytes. Pretsch's group was pioneering in this area [2]. In the same way, the incorporation of many of them in ISEs provided attractive applications in other fields such as clinical analysis [13, 14]. On the other hand, the unravelling of carrier-ISM mechanism for internal solution electrodes had clearly been the major focus of attention during this time. Principally, Morf's, Pretsch's and Ivaska's groups played an important role elucidating the principles of ISEs [15]. Nevertheless, the sensing mechanism has been widely explained by different models and the complexity of these models is related to the number and the kind of suppositions employed [16].

PVC and plasticizers (DOS or n-NPOE) are the main components of the most common ion selective membranes. Up until now, they have been used for several practical reasons. First, easy and quick preparation is needed. Second, the membranes are easily deposited by drop casting onto the electrode surface. Finally, the conditioning process, before the potentiometric calibration is reached completely, both in the surface and the bulk of the membrane. However, some drawbacks have also arisen due to their large diffusional constant [17]. PVC membranes can up-take water from the sample decreasing the performance parameters of the sensor. Moreover, leaching out of the plasticizers rendered the membrane incompatible for measurements *in vivo* inducing an inflammatory response [18].

Polymeric membranes free of plasticizers emerged as interesting and promising matrices attempting to overcome the problems shown by PVC membranes. Hall's group developed the first acrylic membranes based on n-butyl acrylate and methyl methacrylate suitable to act as matrix in ion selective membranes [19]. Subsequently, Bakker's group also reported another acrylic membrane with different monomers such as methyl methacrylate and decyl methacrylate [20]. The larger diffusional constant of the acrylic matrices in contrast to the PVC matrix improved the limit of detection, the life-time of the sensor and the quality of the potentiometric signal. In addition, the water uptake is dramatically reduced [21]. In order to decrease the high resistance present in acrylic membranes, lipophilic salts are usually employed (ETH 500).

As previously mentioned, the transducer element is an essential part of any sensor. The electrochemical event developed on the phase boundary (sample/membrane) must be transformed into an electronic current. After that, the suitable electronic processing enables the recording of the pertinent analytical signal.

Internal solution ion selective electrodes (IS-ISEs) are known as classical ISEs, where the internal solution in conjunction with a silver/silver chloride wire acts as transducer. This redox couple and the electrolyte solution participate actively in the Faradaic process that successfully transduces the ionic current into an electronic current [16]. In fact, the same process occurs in the reference electrodes.

Nevertheless, when the ion selective membrane is sandwiched between two solutions, the sample and the inner electrolyte, a transmembrane ionic flux appears and diffusional potential is generated across the bulk membrane [22]. Consequently, the transmembrane ionic flux can flow from the inner electrolyte to the sample or vice versa depending on the concentration of the primary analyte. As a consequence, very low limits of detection are impossible to reach due to the contamination of the sample. Especially in measurements with actual test samples, IS-ISEs display drawbacks that limit their performance. Usually, these electrodes should be used in a vertical position to avoid the incorrect electrical contact and the shedding of the internal solution. Likewise, other usual parameters such as pressure, temperature, light and presence of gases influence the stability of the potentiometric signal. In addition dry-storage must be avoided to keep the shelf-life of the electrode. However, the largest obstacle is clearly the possibility to achieve a true miniaturization of these electrodes [23].

As a consequence of these drawbacks, ion selective electrodes based on internal solid contact (SC-ISEs) were considered again after three decades since their initial use. SC-ISEs appeared firstly around 40 years ago, although named as coated wire electrodes (CWE) [24, 25]. Obviously, the exchange of the classical internal solution by a platinum wire was an interesting approach. However, these electrodes showed potential instabilities due to the lack of an efficient signal transduction. Primordially, this inefficient transduction influences the long-term stability of the sensor, although the electrodes could be used for short and fast tests. The mechanism involved in the transduction of CWE is not yet well understood, though a poor capacitive mechanism (blocked interface) could fit with the experiment results.

Many researchers have paid attention to new transducer materials in order to obtain SC-ISEs with stable electrode potential. For this purpose, it is necessary to have sufficiently fast and reversible ion-to-electron transduction in the solid state without any contribution from parasitic side reactions [16].

In this way, in the early 1990's, several components of the conducting polymers family (CP) were introduced as a promising transducers triggering the new wave of SC-ISEs [26]. The solid contact concept has been widely accepted within the ISE community since the publication of the paper by Sutter *et al.* in 2004 which showed that the detection limit of all-solid-state ISEs could be extended to the subnanomolar range by using electropolymerised conducting polymers [27].

SC-ISEs based on conducting polymers such as polyaniline (PANI) [28] polyindole [29], poly(3-octylthiophene) (POT) [30] and poly(3,4- ethylenedioxythiophene) (PEDOT) [31] have been reported.

Bobacka's group participated actively in the elucidation of the transduction mechanism in conducting polymers. Polypyrrole (PPy), polythiophene (PT), polyaniline (PANI) and their derivatives,

consist of a polycationic backbone and charge-compensating ions. Depending on the charge and mobility of the incorporated ions (doping process), conducting polymers behave as anion or cation exchangers [32]. Therefore, when ions approach or move away to the doped CP backbone redox processes are established and the ion-to-electron transduction takes place. Moreover, due to the high redox capacitance, stable SC-ISE can be obtained. PEDOT was thoroughly characterized by different electrochemical techniques helping to the detailed elucidation of the mechanism involved in the sensing [33, 34].

Nevertheless, conducting polymers show some disadvantages related to secondary reaction with redox interferences as well as large sensitivity to CO_2 and O_2 [16]. The formation of a water film between the conducting polymer and the membrane, which is especially critical for measurements in the low limit of detection range and for the stability of the sensor, has been investigated recently [35, 36]. Additionally, one of the most serious drawbacks is their marked light-sensitivity [27].

On the other hand, the generation of fluxes from the membrane to the conducting polymer or vice versa cannot be avoided because of the intrinsic mechanism of the CP transduction. Therefore, the membrane and the sample can be contaminated influencing the "ultimate limit of detection". Despite the fact that conducting polymers have been efficiently used as transducer for a long time, some of their properties could be improved.

After the great revolution into the materials science during 1990's, new materials were disseminated into others field. These materials have been employed in many applications since the end of the 1990's until now.

At the beginning of our research, in May of 2006, nanostructured materials had never been used as transducers in ion selective electrodes. In this way, we tested carbon nanotubes (CNTs) as ion-to electron transducer giving origin to the introduction of nanostructured solid contact ion selective electrodes. As will be shown throughout this thesis, carbon nanotubes can be used as clean and efficient ion-to-electron transducer in solid contact ion selective electrodes.

1.2. Objectives

The general objective of this thesis is the development, characterization and application of solid contact ion selective electrodes (SC-ISEs) based on a layer of carbon nanotubes (CNTs) as ion-to-electron transducer.

This general objective is detailed in a series of specific objectives:

1. Demonstration that a layer of purified single wall carbon nanotubes can be employed as efficient ion-to-electron transducer in SC-ISEs.
2. Elucidation of the transduction mechanism involved in SC-ISEs based on carbon nanotubes.
3. Study of the influence of different types of carbon nanotubes as ion-to-electron transducers such as single-wall or multi-wall carbon nanotubes.
4. Implementation of a new synthetic ionophore selective to choline and derivatives in SC-ISEs based on carbon nanotubes as ion-to-electron transducer.
5. Miniaturization of SC-ISEs based on carbon nanotubes.
6. Testing, in a preliminary way, SC-ISEs based on CNTs in monitoring online processes and environmental applications.

The main added value of this thesis is to explore the capability of carbon nanotubes to transduce the electrochemical event originated at the interface sample-membrane to an electrical signal. This thesis attempts for the first time to implement nanostructured material as the transducer layer in potentiometric solid contact ion selective sensors, to explain their sensing mechanism and to demonstrate their applicability in actual test samples.

1.3. References

- [1] Hildebrand, J.H., *Some applications of the hydrogen electrode in analysis, research and teaching*. Journal of the American Chemical Society, 1913. 35 847-871.
- [2] Bakker, E. and E. Pretsch, *Modern Potentiometry*. Angewandte Chemie-International Edition, 2007. 46(30) 5660-5668.
- [3] Moore, C. and B.C. Pressman, *Mechanism of action of valinomycin on mitochondria*. Biochemical and Biophysical Research Communications, 1964. 16(3) 562-567.
- [4] Stefanac, Z. and W. Simon, *Ion specific electrochemical behavior of macrotretrolides in membranes*. Microchemical Journal, 1967. 12(1) 125-132.

- [5] Pedersen, C.J., *Cyclic polyethers and their complexes with metal salts*. Journal of the American Chemical Society, 1967. 89 (26) 7017-7036.
- [6] Lehn, J.M. and J.P. Sauvage, *Cation and cavity selectivities of alkali and alkaline-earth cryptates*. Journal of the Chemical Society D-Chemical Communications, 1971.(9) 440-441.
- [7] Ammann, D., W. Simon, and E. Pretsch, *Synthetic, electrically neutral carrier for Ca²⁺*. Tetrahedron Letters, 1972. (24) 2473-2476.
- [8] Ross, J.W., *Calcium-selective electrode with liquid ion exchanger*. Science, 1967. 156 (3780) 1378-1379.
- [9] Fiedler, U. and J. Ruzicka, *Selectrode - universal ion-selective electrode-Valinomycin-based potassium electrode with nonporous polymer membrane and solid-state inner reference system*. Analytica Chimica Acta, 1973. 67(1) 179-193.
- [10] Pick, J., E. Pungor, M. Vasak, and W. Simon, *Potassium-selective silicone-rubber membrane electrode based on a neutral carrier*. Analytica Chimica Acta, 1973. 64(3) 477-480.
- [11] Buhlmann, P., S. Yajima, K. Tohda, K. Umezawa, S. Nishizawa, and Y. Umezawa, *Studies on the phase boundaries and the significance of ionic sites of liquid membrane ion-selective electrodes*. Electroanalysis, 1995. 7(9) 811-816.
- [12] Yajima, S., K. Tohda, P. Buhlmann, and Y. Umezawa, *Donnan exclusion failure of neutral ionophore-based ion-selective electrodes studied by optical second-harmonic generation*. Analytical Chemistry, 1997. 69(10) 1919-1924.
- [13] Osswald, H.F., R.E. Dohner, T. Meier, P.C. Meier, and W. Simon, *Flow-through system of high stability for measurement of ion activities in clinical-chemistry*. Chimia, 1977. 31(2) 50-53.
- [14] Ma, S.C., V.C. Yang, and M.E. Meyerhoff, *Heparin-responsive electrochemical sensor - a preliminary study*. Analytical Chemistry, 1992. 64(6) 694-697.
- [15] Bakker, E., P. Buhlmann, and E. Pretsch, *Polymer membrane ion-selective electrodes - What are the limits*. Electroanalysis, 1999. 11(13) 915-933.
- [16] Bobacka, J., A. Ivaska, and A. Lewenstam, *Potentiometric ion sensors*. Chemical Reviews, 2008. 108(2) 329-351.
- [17] Michalska, A.J., C. Appaih-Kusi, L.Y. Heng, S. Walkiewicz, and E.A.H. Hall, *An experimental study of membrane materials and inner contacting layers for ion-selective K⁺ electrodes with a stable response and good dynamic range*. Analytical Chemistry, 2004. 76(7) 2031-2039.
- [18] Lindner, E., V.V. Cosofret, S. Ufer, T.A. Johnson, R.B. Ash, H.T. Nagle, M.R. Neuman, and R.P. Buck, *In-vivo and in-vitro testing of microelectronically fabricated planar sensors designed for applications in cardiology*. Fresenius Journal of Analytical Chemistry, 1993. 346(6-9) 584-588.
- [19] Heng, L.Y. and E.A.H. Hall, *Methacrylate-acrylate based polymers of low plasticiser content for potassium ion-selective membranes*. Analytica Chimica Acta, 1996. 324(1) 47-56.
- [20] Qin, Y., S. Peper, and E. Bakker, *Plasticizer-free polymer membrane ion-selective electrodes containing a methacrylic copolymer matrix*. Electroanalysis, 2002. 14(19-20) 1375-1381.

- [21] Veder, J.P., R. De Marco, G. Clarke, R. Chester, A. Nelson, K. Prince, E. Pretsch, and E. Bakkert, *Elimination of undesirable water layers in solid-contact polymeric ion-selective electrodes*. Analytical Chemistry, 2008. 80(17) 6731-6740.
- [22] Bakker, E., P. Buhlmann, and E. Pretsch, *Carrier-based ion-selective electrodes and bulk optodes. 1. General characteristics*. Chemical Reviews, 1997. 97(8) 3083-3132.
- [23] Lindner, E. and R.E. Gyurcsanyi, *Quality control criteria for solid-contact, solvent polymeric membrane ion-selective electrodes*. Journal of Solid State Electrochemistry, 2009. 13(1) 51-68.
- [24] Cattrall, R.W. and H. Freiser, *Coated Wire Ion Selective Electrodes*. Analytical Chemistry, 1971. 43(13) 1905-1906.
- [25] Cattrall, R.W., S. Tribuzio, and H. Freiser, *Potassium-Ion Responsive Coated Wire Electrode Based on Valinomycin*. Analytical Chemistry, 1974. 46(14) 2223-2224.
- [26] Cadogan, A., Z.Q. Gao, A. Lewenstam, A. Ivaska, and D. Diamond, *All-solid-state sodium-selective electrode based on a calixarene ionophore in a poly(vinyl chloride) membrane with a polypyrrole solid contact*. Analytical Chemistry, 1992. 64(21) 2496-2501.
- [27] Lindfors, T., *Light sensitivity and potential stability of electrically conducting polymers commonly used in solid contact ion-selective electrodes*. Journal of Solid State Electrochemistry, 2009. 13(1) 77-89.
- [28] Han, W.S., M.Y. Park, K.C. Chung, D.H. Cho, and T.K. Hong, *All solid state hydrogen ion selective electrode based on a tribenzylamine neutral carrier in a poly(vinyl chloride) membrane with a poly(aniline) solid contact*. Electroanalysis, 2001. 13(11) 955-959.
- [29] Pandey, P.C. and R. Prakash, *Characterization of electropolymerized polyindole-Application in the construction of a solid-state, ion-selective electrode*. Journal of the Electrochemical Society, 1998. 145(12) 4103-4107.
- [30] Bobacka, J., M. McCarrick, A. Lewenstam, and A. Ivaska, *All-solid-state poly(vinyl chloride) membrane ion-selective electrodes with poly(3-octylthiophene) solid internal contact*. Analyst, 1994. 119(9) 1985-1991.
- [31] Bobacka, J., T. Lahtinen, J. Nordman, S. Haggstrom, K. Rissanen, A. Lewenstam, and A. Ivaska, *All-solid-state Ag⁺-ISE based on [2,2,2]p,p,p-cyclophane*. Electroanalysis, 2001. 13(8-9) 723-726.
- [32] Bobacka, J., A. Ivaska, and A. Lewenstam, *Potentiometric ion sensors based on conducting polymers*. Electroanalysis, 2003. 15(5-6) 366-374.
- [33] Bobacka, J., A. Ivaska, and A. Lewenstam, *Plasticizer-free all-solid-state potassium-selective electrode based on poly(3-octylthiophene) and valinomycin*. Analytica Chimica Acta, 1999. 385(1-3) 195-202.
- [34] Bobacka, J., A. Lewenstam, and A. Ivaska, *Electrochemical impedance spectroscopy of oxidized poly(3,4-ethylenedioxythiophene) film electrodes in aqueous solutions*. Journal of Electroanalytical Chemistry, 2000. 489(1-2) 17-27.
- [35] Sutter, J., E. Lindner, R.E. Gyurcsanyi, and E. Pretsch, *A polypyrrole-based solid-contact Pb²⁺-selective PVC-membrane electrode with a nanomolar detection limit*. Analytical and Bioanalytical Chemistry, 2004. 380(1) 7-14.
- [36] Sutter, J. and E. Pretsch, *Response behavior of poly(vinyl chloride)- and polyurethane-based Ca²⁺-selective membrane electrodes with polypyrrole- and poly(3-octylthiophene)-mediated internal solid contact*. Electroanalysis, 2006. 18(1) 19-25.

UNIVERSITAT ROVIRA I VIRGILI

SOLID CONTACT ION SELECTIVE ELECTRODES BASED ON CARBON NANOTUBES

Gastón Adrián Crespo Paravano

ISBN:978-84-693-6428-4/DL:T-1630-2010



CHAPTER 2
THE PRINCIPLES

UNIVERSITAT ROVIRA I VIRGILI

SOLID CONTACT ION SELECTIVE ELECTRODES BASED ON CARBON NANOTUBES

Gastón Adrián Crespo Paravano

ISBN:978-84-693-6428-4/DL:T-1630-2010

2.1. Introduction

This chapter presents an overview of the principles of ion selective electrodes starting from the ion selective membrane (recognition part) and finishing on the carbon nanotubes properties (transducer element). Analytical parameters involved in the characterization of the sensor are also discussed in detail.

2.2. Chemical sensors

A chemical sensor is a self-contained integrated device that is capable of providing specific quantitative or semi-quantitative chemical information using a recognition element which is retained in direct spatial contact with a transduction element [1]. Moreover, depending on the operating principle of the transducer, chemical sensors can be classified in several groups. Within them, electrochemical sensors transform an electrochemical event into an electrical signal (mainly current or voltage).

2.3. Ion selective electrodes

Ion selective electrodes (ISEs) belong to the electrochemical sensors, specifically to the potentiometric sensors subgroup, which is one of the oldest types of chemical sensors [2].

Ion selective electrodes similarly to the rest of the sensors are composed of three different parts. The first one corresponds to the ion selective membrane (ISM) (recognition layer) where the selective receptor and the ion exchanger, which is involved in the establishment of the potentiometric signal, are placed. The second one, the most relevant in the thesis, is the transducer element or transducer layer responsible for converting ionic current to electronic current or vice-versa. Finally, the detection system is composed, in our case, for the potentiometric cell (ion-selective or indicator electrode, reference electrode and potentiometer).

2.3.1. Ion selective membrane

Ion selective membrane is an essential part of the ISEs. Several kinds of ion selective membranes have been developed including solid state membranes, glass membranes [3], liquid ion exchanger membranes, neutral carrier liquid and neutral carrier polymeric membrane [4]. From all of them, neutral carrier liquid and neutral carrier polymeric membranes will be discussed here. These ion selective membranes are basically composed of a polymeric or liquid matrix, the carrier (ionophore) and the ion exchanger.

2.3.1.1. Polymeric matrix

The polymeric matrix provides mechanical stability to the membrane. The components are inert and insoluble in water. Due to the lipophilic environment provided by the membrane, a distribution of ions in the two phases (hydrophobic membrane/aqueous sample) is accomplished. Usually, poly(vinyl-chloride) (PVC) with or without plasticizers was historically used as matrix [5, 6]. The plasticizers are employed as a solvent enabling the achievement of a homogenous membrane. Solvent polymeric membranes contain about 33 % (w/w) of PVC and 66 % (w/w) of plasticizers. Bis(2-ethylhexyl sebacate) (DOS with apolar properties) or o-nitrophenyl octyl ether (o-NPOE with polar properties) are the commonest plasticizers employed. Nonetheless, several disadvantages have been reported regarding the PVC-plasticized matrix. For instance, leaching out the plasticizer causes contamination of the sample, reduces the life-time of the sensor and provides instability to the signal [7, 8]. In addition, PVC membranes readily up-take water generating a thin layer water between the membrane and the internal contact that is detrimental for some performance analytical parameters. From the manufacturing point of view, PVC membranes are easier to prepare and deposit than other membranes developed previously.

Attempting to overcome these drawbacks, new membranes based on n-butyl acrylate (n-BA), methyl (MMA) and decyl methacrylate (DMA) have emerged [9-13]. The absence of plasticizer and ionic impurities as well as the low diffusional constant of the membrane give the sensor longer stability and a lower limit of detection.

2.3.1.2. Lipophilic ion exchangers

The use of the lipophilic ion or ion exchanger is an important requirement to obtain a Nernstian response and guarantee the permselectivity of the membrane, also known as Donnan exclusion. This means that the co-extraction process (primary ions with their respective counter ions entering the membrane from the solution) is minimized as much as possible and only the exchange process of the primary ion is theoretically permitted. Therefore, the concentration of primary ion due to the co-extraction is negligible compared to the total primary ion concentration inside the membrane phase. Then, the concentration of total primary ion inside the membrane is sample-independent. In the same way, membranes without lipophilic ions incorporated do not respond to changes in the activity of the sample [4, 14, 15].

Sodium tetraphenylborate (NaTPB), Potassium tetrakis[p-chlorophenylborate (KTpCIPB) and Potassium tetrakis[3,5-bis(trifluoromethyl)phenyl]borate (KTFPB) are used as cation exchanger (R⁻) whereas tridodecylmethylammonium (TDMACl) chloride is used as anion exchanger (R⁺) (Figure 2.1). On the one hand, due to their highly sterically shielded negative or positive charge, the ion exchangers cannot form specific ion pairs. In contrast, ion pair formation of non-shielded ions may induce a loss of selectivity in the sensor [16]. On the other hand, the leaching out of

the cation exchanger for PVC membrane ($D=10^{-6} \text{ cm}^2\text{s}^{-1}$) is quite negligible being around 1% in 30 days for PVC membrane. Moreover, it is assumed that there is not a concentration gradient of exchanger inside the membrane.

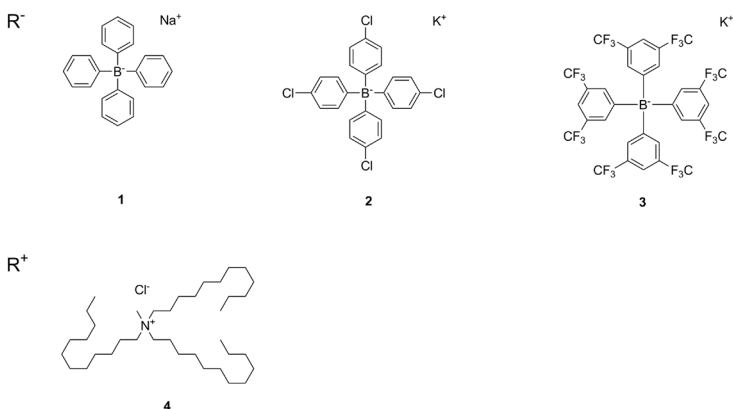


Figure 21 – Chemical structure of lipophilic anions (R⁻): 1-Sodium tetraphenylborate(NaTPB); 2-Potassium tetrakis(p-chlorophenyl)borate (KTPCPB); 3-Potassium tetrakis[3,5-bis(trifluoromethyl)phenyl]borate (KTFPB) and lipophilic (R⁺): 4- Tridodecylmethylammonium chloride (TDMACl) cation, commonly used in ISEs.

2.3.1.3. Ionophores

Lipophilic ionophores or ligand agents play a unique and important role related to the selectivity of the membrane. The primary ion must be bound to the ionophore more strongly than other interfering ions. Therefore, the ionophores are synthesized according to the nature of each analyte (charge and size) as well as considering the ability to form supramolecular assembly (host-guest) by hydrogen bonds, metal coordination and hydrophobic/lipophilic forces (**Figure 2.2**).

In the same way, other factors must be considered in order to obtain a successful ionophore for ISEs applications. They are only mentioned in this sub-chapter. i) Thermodynamic: The interaction ionophore-analyte is related to the equilibrium constant (β_{il}). The value of the formation constant is really flexible with a range from 10^4 to $10^{10} \text{ kg}\cdot\text{mol}^{-1}$ for 1:1 stoichiometry [17]. ii) Kinetic: The total ionic exchange current must be high compared to the current flowing through the membrane. To avoid kinetic limitations, the free energy from the activation of the complexation process and the hydration competition are key factors to be considered when designing ionophores. Moreover, an ionophore should be a flexible structure such as valinomycin that shows a conformation change when the cation is attached at the ligand [18]. iii) Lipophilicity: The higher the p_c factor [$p_c = C_{\text{total [org]}} / C_{\text{total [aq]}}$] the lower the leaching out rate.

The selectivity values of membranes containing only ion exchanger (without ionophore) is determined by the hydration free energy of the sample ions. When the ionophore is added, the selectivity starts depending on the formation constant (β_{IL}) being the most relevant process to obtain a selective sensor.

For optimal working conditions, membranes based on neutral ionophores require the addition of a lipophilic ion whose charge must be opposite to that of the analyte.

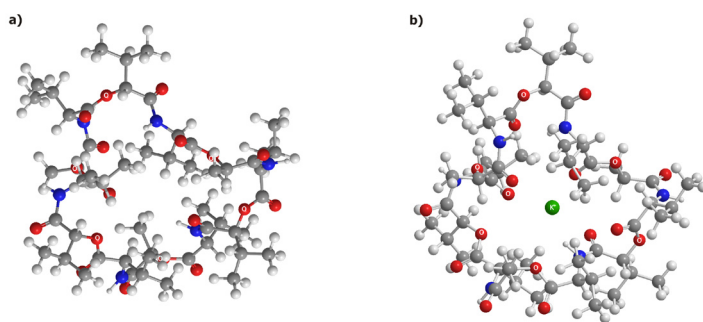


Figure 2.2 - a) Valinomycin chemical structure optimized in non polar solvent b) Valinomycin-Potassium complex structure optimized in the same conditions. Valinomycin is a flexible structure and its chemical conformation change is influenced by both the polarity of the solvent and the interaction with potassium ion. Six ether oxygen functions interact with the metallic center.

2.3.2. Generation of Nernstian response

The potentiometric cell is composed of two electrodes: the ion selective electrode and the reference electrode [4] (**Figure 2.3**). The electromotive force (EMF), measured under nearly zero-current conditions between the two electrodes, is the sum of phase boundary potentials across the cell. Considering, there are few sample-dependent phase boundary potentials (membrane potential, E_M ; liquid junction potential of the reference electrode, $E_{D,ref}$), the EMF expression is highly simplified.

$$EMF = E_M + E_{D,ref} + E_{const} \quad (2.1)$$

The liquid junction potential ($E_{D,ref}$) originates from the different ionic mobilities at the phase boundary between sample solution and bridge electrolyte. Its minimization can be achieved, when highly concentrated salts with similar mobilities like $LiAcO$, KCl and NH_4NO_3 are employed. Fortunately, this potential can be calculated by the Henderson formalism if the composition of the sample is known [19]. Additionally, activities are calculated using the Debye approximation [20].

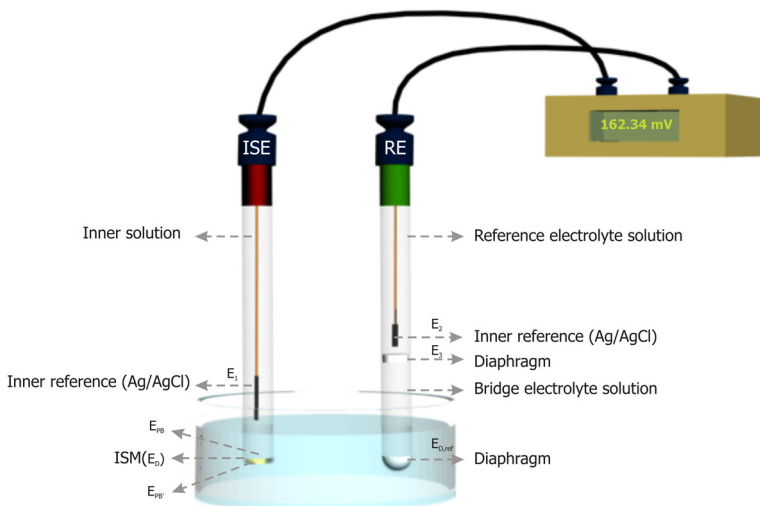


Figure 2.3 - Potentiometric cell composed for a reference electrode (RE, right) and an internal solution ion selective electrode (ISE, left). The *EMF* (162.34 mV) is the sum of all the phase boundary involved in the cell. E_2 , E_3 and $E_{D,ref}$ correspond to the potentials generated in the RE whereas E_1 , E_{PB} , $E_{PB'}$ and E_D correspond to the potentials generated in the ISE part.

The generation of the sensing mechanism in the ion selective membrane has been the source of a large discussion for at least 30 years. Basically there are several models that attempt to explain the mechanism using different factors and suppositions. Several models ranging from basic ones to others showing a high degree of complexity have been proposed. Bobacka and co-workers [2] summarize in his review the advantages and drawbacks of each model. Obviously, one must keep in mind that, the larger the number of suppositions, the easier the mathematical tools involved. In this thesis, we have focused our attention on the transducer layer. Therefore, one of the simplest sensing mechanisms is adopted here to interpret the potentiometric measurements (phase boundary potential- total equilibrium models) [21].

In fact, in all models considered, the membrane potential is divided into the sum of three potentials: the boundary potential between the inner solution or inner solid contact and the membrane, E_{PB} ; the diffusion potential inside the membrane, E_D and the phase boundary potential between the membrane/sample solution $E_{PB'}$.

$$E_M = E_{PB} + E_D + E_{PB'} \quad (2.2)$$

At this point, two suppositions are needed to simplify the border effects that are always difficult to model. i) Diffusion potential contribution (E_D) due to the ion migrations inside the mem-

brane are ignored. Therefore, electroneutrality in the bulk membrane is assumed, except for the thin layer in contact with the solution. In addition, the internal phase boundary E_{PB} is considered constant. As a result, membrane potential depends only on the phase external phase boundary potential in contact with the sample ($E_M = E_{PB}$) (2.3). ii) Electrochemical equilibrium is assumed at the sample/membrane. Also, the concentration and potential profiles inside the membrane are independent of the time and length, except on the phase boundary. Consequently, electrochemical potentials developed by Guggenheim [22] can be applied for an ion i present in both phases arriving at the well-known Nernstian equation (Appx 2, equation 2.19, 2.20, 2.21).

$$E_M = E_{PB} = \frac{\mu_{i(aq)}^0 - \mu_{i(org)}^0}{n_i F} + \frac{RT}{n_i F} \ln \frac{a_{i(aq)}}{a_{i(org)}} \quad (2.4)$$

$$\mu_{i(aq)}^0 - \mu_{i(org)}^0 = \Delta G_{tr}^{0,w \rightarrow m} = RT \ln k_i \quad (2.5)$$

Equations (2.4) and (2.5) provide a mathematical model that successfully explains the generation of the potential at the interface being $\Delta G_{tr}^{0,w \rightarrow m}$ the free standard energy of the distribution process of ion i between two phases and k_i correspond to the "single ion distribution coefficient". Subsequently, E_M will be converted into an analytical signal with valuable information concerning the activity of the target ion in the test solution [$a_{i(aq)}$].

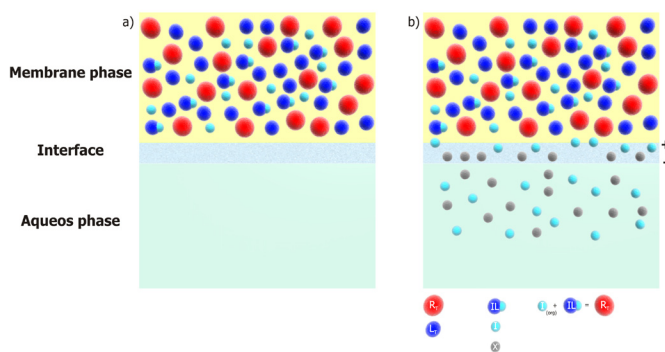


Figure 2.4 – Phase boundary sensing mechanism is illustrated. **a)** The membrane has an ideal behaviour and it is not in contact with a solution at the first instant. **b)** The membrane is placed in contact with an aqueous solution which has a primary ion and a counterion (I^+ and X^-). The charge separations between cations and anions into the interface membrane/aqueous solution are generated due to the difference in the free hydration energies.

Moreover, the phase boundary potential at the interface between membrane and sample solution appears as a consequence of charge separations due to the partition of cations and anions between the organic membrane and the aqueous sample. In general, the solvation energies of the anions and cations in the two phases (membrane and sample solution) are different. Conse-

quently, the cation for instance, has a greater tendency to pass into the membrane phase than the anion, appearing an electrical double layer at the interface (charge separation). Furthermore, this phenomenon occurs in a thin layer around 10 nm from the membrane surface, where the electroneutrality condition is not fulfilled (Figure 2.4).

After these considerations, equations (2.4) and (2.5) can be re-written considering (Appx 2, equation 2.22-2.27) membranes with or without ionophore (L) as a function of the total ion-exchanger sites (R_T), the activity coefficients for i (γ_i), single ion distribution coefficient (k_i), number of charges (n_i), formation constant between the ionophore and the ion i (β_{iL}) and the constant s equal to 59.1 mV at 25 °C.

Without ionophore:

$$E_{PB} = E_i^0 + \frac{s}{n_i} \log a_{i(aq)} = \frac{s}{n_i} \log \frac{n_i k_i}{\gamma_{i(org)} R_T} + \frac{s}{n_i} \log a_{i(aq)} \quad (2.6)$$

With ionophore:

$$E_{PB} = E_i^0 + \frac{s}{n_i} \log a_{i(aq)} = \frac{s}{n_i} \log \frac{nk_i \beta_{iL} \left(L_T - \frac{R_T}{n} \right)}{\gamma_{i(org)} R_T} + \frac{s}{n} \log a_{i(aq)} \quad (2.7)$$

The activity of ion $a_{i(org)}$ in the membrane is included into the constant term. In fact, owing to the electroneutrality condition and the relatively high concentration of lipophilic ion exchanger, $a_{i(aq)}$ is buffered. Therefore, the phase boundary potential depends only on the activity of the ion i in the aqueous phase.

It should be noted that the difference between equation (2.6) and (2.7) concerning the E_i^0 potential, responsible to shift Nernstian curves to parallel lines. As was mentioned in the first part of this chapter, when the ion exchanger is the only component placed inside the membrane E_i^0 will depend on the free energy of salvation of the ion in both phases. However, when the ionophore is incorporated, E_i^0 depends also on the complexation constant and the free energy.

2.3.3. Analytical performance parameters

There are four main parameters commonly used to characterize a quantitative sensor, namely sensitivity, stability, selectivity and limit of detection. All of them there are summarized in this section.

2.3.3.1. Sensitivity

The sensitivity of the ion selective electrodes is calculated from the slope of the calibration curve. As the relation between the instrumental signal and the logarithmic activity of the target

ion is well established by the Nernst equation, the theoretical sensitivity is defined by RT/n_iF ($59.2/n_i$ [mV.dec⁻¹] at 25°C). It can be seen that the sensitivity depends on the number of charges. Then, sensitivity gives us information about the proper functioning of the electrode. Nevertheless, super and sub Nernstian sensitivity can be often obtained, although they are not discussed here.

2.3.3.2. Selectivity

Ion selective electrodes usually work ideally within a limited range of different ion concentrations in solution. Outside of this range, the presence of other ions present in the solution in small concentrations can start to interfere with the potentiometric signal. Therefore, the evaluation of the selectivity coefficients K_{ij}^{pot} is mandatory to know the behavior of the sensor in actual test samples. Theory and the experimental determination of the selectivity have been discussed for a long time [23, 24].

Equation 2.8 shows the expression for the selectivity coefficient K_{ij}^{pot} for a primary ion (i) and an interference (j). It is derived from the Nicolski-Eisenman formalism (equation 2.15). K_{ij}^{pot} is a unitless coefficient that represents the times that the activity of the interfering j ion (modulated by the exponent (n_i/n_j)) gives the same potential value as the activity of the target ion i previously defined. I and J correspond to the pure phases of the primary and interference ions. It means that each pure phase only has either the primary or the interference ion.

$$K_{ij}^{pot} = \frac{a_i(I)}{a_j(J)^{n_i/n_j}} \quad (2.8)$$

Consequently, this equation is of practical use only if two activity values are known. In order to improve the usefulness of equation 2.8, it can be re-written in standard potential terms according to equation 2.9 (Appx 2, equations 2.28-2.31).

$$K_{ij}^{pot} = e^{\frac{n_i F}{RT} (E_j^0 - E_i^0)} \quad (2.9)$$

As a result, the selectivity coefficient can be worked out by the difference between the standard potentials of the separately measured of the primary ion and the interference under study. Moreover, unbiased selectivity coefficients are obtained only if the standard potential has been calculated with ISE exhibiting a Nernstian response for both ions [18, 23]. This methodology to obtain the selective coefficient is known as "separated solution method (SSM)" and it has been widely used in this thesis. Other methods have also been reported such as "fixed interference method (FIM)" or "matched potential method (MPM)", although the Nernstian response for all ions must be accomplished in all of them [24].

In order to describe a little bit more the parameters involved in the K_{ij}^{pot} , the selectivity coefficient expression can be written in another simplified way [25]. Equation 2.10 clearly shows that K_{ij}^{pot} depends on the ion exchanger constant and the formation constants of both ions (primary ion and interference ion). In fact, the exchanger constant, (K_{ij}) is a quotient between the free energies of solvation of i and j (k_i, k_j) in each phase (2.11).

$$K_{ij}^{pot} = K_{ij} \frac{\beta_{jL}}{\beta_{iL}} \quad \text{with} \quad K_{ij} = \frac{k_j^{z_i/z_j}}{k_i} \quad (2.10) \quad (2.11)$$

Nevertheless, an extension of equation (2.10) is illustrated in the next equations according to the concentration of all components of the membrane either with or without ionophore. Equation (2.12) shows the selectivity coefficient expression without ionophore as a function of: the total lipophilic ion sites (R_T), the distribution constant of each ion between the organic and the aqueous phases (k_i, k_j) and the activity coefficients for each ion (γ_i, γ_j). In the simple case that, the number of charge of both ions is the same and both activity coefficients are near to the unit, the potentiometric selectivity coefficient is equal to the exchanger constant (K_{ij}) (Appx 2, equations 2.32, 2.33).

$$K_{ij}^{pot} = \frac{\gamma_i R_T}{k_i n_i} \left(\frac{k_j n_j}{\gamma_j R_T} \right)^{n_i/n_j} \quad \text{if } n_i = n_j \text{ and } \gamma_i \cong \gamma_j \cong 1 \text{ then } K_{ij}^{pot} = \frac{k_j}{k_i} \quad (2.12)$$

Similarly, equation (2.13) and (2.14) display the selectivity coefficient expression, incorporating the ionophore inside the membrane, as a function of the total lipophilic ion sites (R_T), the distribution constant of each ion between the organic and the aqueous phases (k_i, k_j), the activity coefficients for each ion (γ_i, γ_j), the formation constant between the ionophore and both ions (β_{iL}, β_{jL}) and the total concentration of ionophore (L_T). In this case, if the number of charge of both ions is the same and both activity coefficients are near to the unit, then the potentiometric selectivity coefficient is equal to the product of the exchanger constant (K_{ij}) and the formation constants (Appx 2, equation 2.33-2.36).

$$K_{ij}^{pot} = \frac{\gamma_i R_T}{n_i \beta_{iL} k_i (L_T - R_T / n_i)} \left(\frac{n_j \beta_{jL} k_j (L_T - R_T / n_j)}{\gamma_j R_T} \right)^{n_i/n_j} \quad (2.13)$$

$$\text{if } n_i = n_j \text{ and } \gamma_i \cong \gamma_j \cong 1 \text{ then } K_{ij}^{pot} = \frac{k_j \beta_{jL}}{k_i \beta_{iL}} = K_{ij} \frac{\beta_{jL}}{\beta_{iL}} \quad (2.14)$$

On the other hand, the potential recorded for a mix of ions of the same charge can be written according to the Nicolski-Eisenman formalism (2.15) [3, 26].

$$E = E_i^0 + \frac{RT}{n_i F} \ln \left(a_i(IJ) + K_{ij}^{pot} a_j(IJ)^{z_i/z_j} \right) \quad (2.15)$$

However, if the sample contains ions of different charge the phase boundary potential must be calculated according to the Nicolski-Eisenman-Bakker new formalism (Appx 2, Equation 2.37) [27].

2.3.3.3. Limit of detection

Ion selective electrodes display upper and lower limits of detection. According to IUPAC these limits are defined by the cross section of the two extrapolated linear segments of the calibration curve [28]. However, another definition for lower detection limit has been proposed for ISEs showing super-Nernstian response. In this case, the limit of detection limit corresponds to the analyte activity when the potential is deviated in $(RT/n_i F) \ln 2$ (17.8 mV for monovalent ions) from the Nernstian slope [29]. If the ISEs show Nernstian response both definitions are valid.

In addition, the membrane processes involved in the determination of the lower detection limit (LDL) have been studied in many articles [30]. There are two process related to LDL degeneration. First, fluxes from the membrane to the sample (theoretically non existing in solid contact electrodes due to the absence of the inner solution). Second, the interferences from other ions present in the sample solution.

In absence of the first process and for ideal membranes, the ultimate lower detection limit would be reached. It is defined, when 50% of the primary ions are replaced by interfering ions in the organic phase [31]. This corresponds approximately to the equation (2.16).

$$a_i(DL) = K_{ij}^{pot} a_j^{n_i/n_j} \quad (2.16)$$

On the other hand, the upper limit of detection (ULD) is reached when the permselectivity is lost. The coextraction of primary ions with their counterions increases the concentration of primary ions inside the membrane. Usually, the coextraction process is originated either by the presence of a high concentration of the primary analyte in the sample side or by lipophilic counterions entering the membrane.

2.3.3.4. Stability

The evaluation of the potentiometric signal along short and long time periods is one of most important parameters in order to characterize ion selective electrodes. The quality of the transducer is also reflected by the stability of the sensor. Usually, the stability is expressed as a drift in $\mu\text{V}\cdot\text{h}^{-1}$ or $\text{mV}\cdot\text{h}^{-1}$ units.

2.3.4. Solid contact ion selective electrodes

Internal solution ion selective electrodes (IS-ISEs) have always shown a high stability provided by the liquid/solid transduction system. The transduction is established by coupling ionic conductivity of the membrane and internal filling solution chloride with the electronic conductivity of the internal reference half-cell (Ag/AgCl) via a reversible redox reaction (Ag/Ag⁺) (equation 2.17).



In other words, this type of ion-to-electron transduction is a Faradaic process, with a redox capacitance (C_{redox}) associated to it. When the current i flows across the system for a time t , a change of potential ΔE_C is modulated by the redox capacitance of the process. (equation 2.18). Nonetheless, Equation 2.18 is a simplification of the transduction phenomena.

$$\frac{\Delta E_C}{\Delta t} = \frac{i}{C_{redox}} \quad (2.18)$$

In addition, the higher the redox capacitance, the smaller the potential change is for a given current and ion flux, i.e., for a given rate of an electrochemical side reaction. This means that a high capacitance stabilizes the potential of the solid contact itself but does not eliminate the ion flux associated with side reactions [2].

Consequently, thorough studies have been performed using this internal reference system in ISEs. Fortunately, the models developed for them are also applicable to solid contact ion selective electrode (SC-ISEs) with few exceptions.

SC-ISE is an asymmetrical sensor, where the membrane is in contact on one side with the solid transducer instead of the inner solution as in IS-ISEs, and on the other side in contact with the aqueous phase of the test sample. In this way, all components in the SC-ISEs are solid, making an all-solid-state sensor (Figure 2.5).

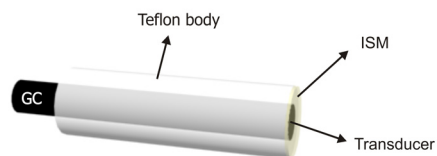


Figure 2.5 – Scheme of general solid contact ion selective electrodes (SC-ISEs). The membrane is sandwiched between the electrical conductor (GC in this case coated by a Teflon body) and the aqueous phase.

The present thesis deals with solid state ion selective electrodes. Therefore, we will focus our attention towards these types of electrodes, omitting the well known properties of the IS-ISEs. The incorporation of a solid transducer instead of the internal solution generates a range of new opportunities. The most relevant properties are herewith listed [32, 33];

1. Possibilities of miniaturization (micro, nano and planar electrodes).
2. Increase of electrode physical robustness.
3. Possibilities of measurement in any position (not only vertically).
4. Easy preparation and handling.
5. Negligible trans-membrane flux.
6. Improvement of lower limit of detection.
7. Improvement of life-time of the sensor.
8. Dry storage.
9. Working under pressure or temperature.

The first SC-ISEs, labeled, coated wire electrode (CWE) did not display a well defined transduction mechanism [34]. As a consequence, instabilities in the potentiometric signal due to a lack of proper transduction were observed. In this case, the redox capacitance, present in electrodes having an internal liquid solution, was replaced by an ultra-low double layer capacitance. For this reason, the research to find out efficient transducers materials has been a challenge up to now [2].

As mentioned in the first chapter, conducting polymers have played an important role throughout the last two decades as transducers in SC-ISEs. The transduction mechanism involved in CP is analogous to the reference system used in IS-ISE, even though in this case the redox process takes place on the doped-conducting polymer. CPs display a wide range of redox capacitance values. For instance, poly(3-octylthiophene) (POT) has a low redox capacitance (more sensitive to current flow) whereas poly(3,4- ethylenedioxythiophene) (PEDOT) has a high redox capacitance (less sensitive to current flow) [2].

Nevertheless, several drawbacks related to light-sensitivity, redox secondary reaction, pH sensitivity, gas-sensitivity to CO_2 and O_2 and the presence of a water layer, affect the stability of the transducer and thereby of the instrumental signal of the sensor. For this reason, nanostructured materials such as carbon nanotubes have been researched and implemented in ion selective electrodes in an attempt to overcome the drawbacks shown by the ion-to-electron transducers.

2.3.4.1 Conditioning

There are two basic steps to achieve a well-conditioning of the membranes proper to reach low limit of detections [33]: i) Membranes are placed in a relatively concentrated solution (10^{-3}

or 10^{-2} M) of the primary ion. The exchange between interference ion (j) and the primary ion (i) is reached according the high concentration gradient existing between the bulk solution and the membrane. **Figure 2.6a** shows the concentration profile of the complex ionophore-primary ion, $[IL]_{org}$ inside the membrane as function of the thickness, concentration of the bulk solution and lipophilic ionic sites. In fact, it can be observed as the primary ion concentration on the phase boundary (c_i) and the bulk concentration of the solution ($c_{i,bulk}$) are practically the same at the end of the process. The primary ion gradient ($\Delta c_i/\Delta x$), from the bulk solution to the membrane, is always decreasing until the membrane is fully-conditioned. The process is rate-limited depending on thickness, diffusional constant of the ions in the membrane, value of the gradient and potentiometric selectivity coefficients. Therefore, acrylic membranes ($D \approx 10^{-12}$ $\text{cm}^2 \cdot \text{s}^{-1}$) need a longer time than PVC membranes ($D \approx 10^{-8}$ $\text{cm}^2 \cdot \text{s}^{-1}$). Usually, 24 hours are used, although in this period, the membrane is not fully-conditioned.

ii) After the first step of conditioning, the electrodes must be washed with MQ-water and placed in a diluted solution of the primary analyte (10^{-8} or 10^{-9} M) for 48 hs. The aim of this stage is to achieve the concentration of the primary ion on the phase boundary as lower as possible without leaching out of the membranes components. **Figure 2.6b** illustrates the theoretic case which a low concentration of primary on the phase boundary is achieved and the membrane even is full-conditioned without internal gradients. In other words the concentration of the primary ion or $[IL]_{org}$ inside the membrane phase is constant and the profiles are planes (**Figure 2.6b**). Therefore, lower limit of detection can be achieved with this methodology.

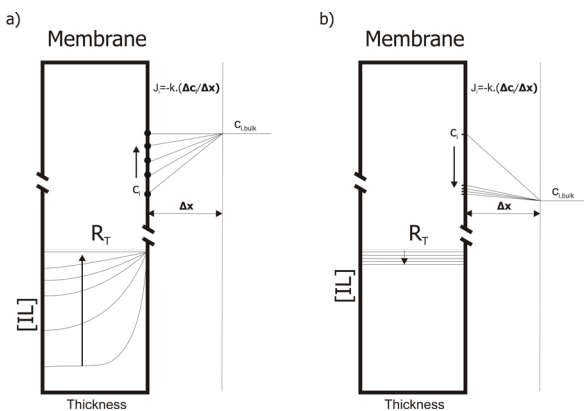


Figure 2.6 – **a**) First step of the conditioning process consists of placing the SC-ISEs in a concentrated solution of the primary ion (10^{-3} - 10^{-2} M) for 24 hours. R_T (concentration of ionic sites), $[IL]$ (concentration of complex inside the membrane), c_i (phase boundary concentration of i), $c_{i,bulk}$ (concentration of i in the aqueous phase), Δx (thickness of diffusional layer in the aqueous phase), k (diffusion coefficient [nM^2/s]) and J_i (flux of i [nM/s]); **b**) Second step of the conditioning consists of placing the SC-ISEs into a dilute solution of the primary ion (10^{-8} - 10^{-9} M) for 24-48 hs.

2.4. General properties of Carbon Nanotubes

The excellent electrical, mechanical and optical properties of carbon nanotubes (CNTs) (a relatively new allotropic form of pure carbon) have been studied extensively. In particular, the electrical and electronic properties are especially relevant in our case.

Carbon nanotubes are classified depending on the number of walls in their molecular structure. Single (SWCNTs) and multi wall carbon nanotubes (MWCNTs) are the commonest structures reported, though there are other architectures such as bamboo, torus, rings or nanobuds.

The molecular structure of a SWCNT can be visualized as a graphene sheet of carbon atoms rolled into a seamless cylinder with a typical diameter of 1.5 nm and a length of up to tens of micrometers (Figure 2.7) [35]. As an ideal quasi-1D structure with an atomically monolayered surface and extended curved π -bonding configuration, an individual SWCNT can exhibit semi-conducting, metallic or semimetallic behaviour [36]. Depending on the chirality of the wrap, the resulting SWNTs can be either metallic (mSWNT) or semiconducting (sSWNT). In a random sample of SWNTs, it is predicted that one third will be metallic, whilst the remaining two thirds will be semiconducting (with a band gap proportional to $1/d$, where d is the diameter of the tube of the order of 0.5 eV) [37]. Whereas multi-walled carbon nanotubes (MWCNTs) are concentric tubes of rolled-up graphene separated by the interlayer distance of graphite (0.34 nm) [38], as shown in Figure 2.7. With MWCNTs, only one of the concentric tubes needs to have a metallic character for the overall electronic properties to be essentially metallic [39].

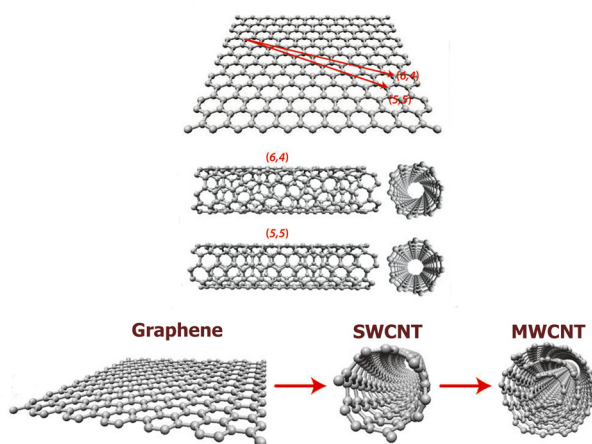


Figure 2.7 – Chemical structures of SWCNTs and MWCNTs are obtained from the fold of either one, or several graphene sheets in some defined directions respectively. The wrapping vectors in this case are (6,4) originating semiconducting SWCNTs and (5,5) generating metallic SWCNTs.

2.5. References

- [1] Thevenot, D.R., K. Toth, R.A. Durst, and G.S. Wilson, *Electrochemical biosensors: Recommended definitions and classification - (Technical Report)*. Pure and Applied Chemistry, 1999. 71(12) 2333-2348.
- [2] Bobacka, J., A. Ivaska, and A. Lewenstam, *Potentiometric ion sensors*. Chemical Reviews, 2008. 108(2) 329-351.
- [3] Eisenman, G., D.O. Rudin, and J.U. Casby, *Glass electrode for measuring sodium ion*. Science, 1957. 126(3278) 831-834.
- [4] Morf, W., *The principles of Ion-selective Electrodes and of Membrane Transport*. Elsevier Vol. 2. 1981, Amsterdam-Oxford-New York.
- [5] Moody, G.J., R.B. Oke, and J.D.R. Thomas, *Calcium-sensitive electrode based on a liquid ion exchanger in a poly(vinyl-chloride) matrix*. Analyst, 1970. 95(1136) 910-918.
- [6] Ammann, D., W. Simon, and E. Pretsch, *Synthetic, electrically neutral carrier for Ca²⁺*. Tetrahedron Letters, 1972. (24) 2473-2476.
- [7] Peper, S., I. Tsagkatakis, and E. Bakker, *Cross-linked dodecyl acrylate microspheres: novel matrices for plasticizer-free optical ion sensing*. Analytica Chimica Acta, 2001. 442(1) 25-33.
- [8] Reinhoudt, D.N., J.F.J. Engbersen, Z. Brzozka, H.H. Vandenvlekkert, G.W.N. Honig, H.A.J. Holterman, and U.H. Verkerk, *Development of durable K⁺-selective chemically-modified field-effect transistors with functionalized polysiloxane membranes*. Analytical Chemistry, 1994. 66(21) 3618-3623.
- [9] Heng, L.Y. and E.A.H. Hall, *Methacrylate-acrylate based polymers of low plasticiser content for potassium ion-selective membranes*. Analytica Chimica Acta, 1996. 324(1) 47-56.
- [10] Heng, L.Y. and E.A.H. Hall, *Producing "self-plasticizing" ion-selective membranes*. Analytical Chemistry, 2000. 72(1) 42-51.
- [11] Heng, L.Y. and E.A.H. Hall, *Methacrylic-acrylic polymers in ion-selective membranes: achieving the right polymer recipe*. Analytica Chimica Acta, 2000. 403(1-2) 77-89.
- [12] Heng, L.Y. and E.A.H. Hall, *Taking the plasticizer out of methacrylic-acrylic membranes for K⁺-selective electrodes*. Electroanalysis, 2000. 12(3) 187-193.
- [13] Qin, Y., S. Peper, and E. Bakker, *Plasticizer-free polymer membrane ion-selective electrodes containing a methacrylic copolymer matrix*. Electroanalysis, 2002. 14(19-20) 1375-1381.
- [14] Buhlmann, P., S. Yajima, K. Tohda, K. Umezawa, S. Nishizawa, and Y. Umezawa, *Studies on the phase boundaries and the significance of ionic sites of liquid membrane ion-selective electrodes*. Electroanalysis, 1995. 7(9) 811-816.
- [15] Buhlmann, P., S. Yajima, K. Tohda, and Y. Umezawa, *EMF response of neutral-carrier based ion-sensitive field-effect transistors with membranes free of ionic sites*. Electrochimica Acta, 1995. 40(18) 3021-3027.
- [16] Bakker, E. and E. Pretsch, *Lipophilicity of tetraphenylborate derivatives as anionic sites in neutral carrier-based solvent polymeric membranes and lifetime of corresponding ion-selective electrochemical and optical sensors*. Analytica Chimica Acta, 1995. 309(1-3) 7-17.

- [17] Bakker, E., M. Willer, M. Lerchi, K. Seiler, and E. Pretsch, *Determination of complex-formation constants of neutral cation-selective ionophores in solvent polymeric membranes*. Analytical Chemistry, 1994. 66(4) 516-521.
- [18] Bakker, E., P. Buhlmann, and E. Pretsch, *Carrier-based ion-selective electrodes and bulk optodes. 1. General characteristics*. Chemical Reviews, 1997. 97(8) 3083-3132.
- [19] Henderson, P., *Thermodynamics of the liquid chain*. Zeitschrift Fur Physikalische Chemie--Stoichiometrie Und Verwandtschaftslehre, 1907. 59(1) 118-127.
- [20] Debye, P. and E. Huckel, *The theory of electrolytes I. The lowering of the freezing point and related occurrences*. Physikalische Zeitschrift, 1923. 24 185-206.
- [21] Bakker, E., *Generalized selectivity description for polymeric ion-selective electrodes based on the phase boundary potential model*. Journal of Electroanalytical Chemistry, 2010. 639(1-2) 1-7.
- [22] Guggenheim, E.A., *The conceptions of electrical potential difference between two phases and the individual activities of ions*. Journal of Physical Chemistry, 1929. 33(6) 842-849.
- [23] Bakker, E., *Determination of improved selectivity coefficients of polymer membrane ion-selective electrodes by conditioning with a discriminated ion*. Journal of the Electrochemical Society, 1996. 143(4) L83-L85.
- [24] Bakker, E., E. Pretsch, and P. Buhlmann, *Selectivity of potentiometric ion sensors*. Analytical Chemistry, 2000. 72(6) 1127-1133.
- [25] Bakker, E. and E. Pretsch, *Modern Potentiometry*. Angewandte Chemie-International Edition, 2007. 46(30) 5660-5668.
- [26] Ross, J.W., *Calcium-selective electrode with liquid ion exchanger*. Science, 1967. 156(3780) 1378-1379.
- [27] Bakker, E., R.K. Meruva, E. Pretsch, and M.E. Meyerhoff, *Selectivity of polymer membrane-based ion-selective electrodes-self-consistent model describing the potentiometric response in mixed ion solutions of different charge*. Analytical Chemistry, 1994. 66(19) 3021-3030.
- [28] Guilbault, G.G., *Recommendations for publishing manuscripts on ion-selective electrodes*. Pure and Applied Chemistry, 1981. 53(10) 1907-1912.
- [29] Sokalski, T., T. Zwickl, E. Bakker, and E. Pretsch, *Lowering the detection limit of solvent polymeric ion-selective electrodes. 1. Modeling the influence of steady-state ion fluxes*. Analytical Chemistry, 1999. 71(6) 1204-1209.
- [30] Bakker, E. and E. Pretsch, *Potentiometric sensors for trace-level analysis* (vol 24, pg 199, 2005). Trac-Trends in Analytical Chemistry, 2005. 24(5) 459-459.
- [31] Nagele, M., E. Bakker, and E. Pretsch, *General description of the simultaneous response of potentiometric ionophore-based sensors to ions of different charge*. Analytical Chemistry, 1999. 71(5) 1041-1048.
- [32] Lindner, E. and R.E. Gyurcsanyi, *Quality control criteria for solid-contact, solvent polymeric membrane ion-selective electrodes*. Journal of Solid State Electrochemistry, 2009. 13(1) 51-68.
- [33] Chumbimuni-Torres, K.Y., N. Rubinova, A. Radu, L.T. Kubota, and E. Bakker, *Solid contact potentiometric sensors for trace level measurements*. Analytical Chemistry, 2006. 78(4) 1318-1322.

- [34] Cattrall, R.W. and H. Freiser, *Coated Wire Ion Selective Electrodes*. Analytical Chemistry, 1971. 43(13) 1905-1906.
- [35] Iijima, S. and T. Ichihashi, *Single-Shell Carbon Nanotubes of 1-Nm Diameter*. Nature, 1993. 363(6430) 603-605.
- [36] Zhou, W.Y., X.D. Bai, E.G. Wang, and S.S. Xie, *Synthesis, Structure, and Properties of Single-Walled Carbon Nanotubes*. Advanced Materials, 2009. 21(45) 4565-4583.
- [37] Saito, R., G. Dresselhaus, and M.S. Dresselhaus, *Physical Properties of Carbon Nanotubes*. 1998. London Imperial College Press.
- [38] Iijima, S., *Helical Microtubules of Graphitic Carbon*. Nature, 1991. 354(6348) 56-58.
- [39] Dumitrescu, I., P.R. Unwin, and J.V. Macpherson, *Electrochemistry at carbon nanotubes: perspective and issues*. Chemical Communications, 2009(45) 6886-6901.

UNIVERSITAT ROVIRA I VIRGILI

SOLID CONTACT ION SELECTIVE ELECTRODES BASED ON CARBON NANOTUBES

Gastón Adrián Crespo Paravano

ISBN:978-84-693-6428-4/DL:T-1630-2010



CHAPTER 3
EXPERIMENTAL
SECTION

UNIVERSITAT ROVIRA I VIRGILI

SOLID CONTACT ION SELECTIVE ELECTRODES BASED ON CARBON NANOTUBES

Gastón Adrián Crespo Paravano

ISBN:978-84-693-6428-4/DL:T-1630-2010

3.1. Introduction

This chapter contains information related to the experimental part of the thesis including protocols and devices used. Firstly, a list of reagents is introduced. Secondly, the development of the electrodes is detailed, starting from the transducer layer (CNTs) and finishing with the ion selective membrane (ISM) recognition layer. Finally, microscopic and electrochemical characterization techniques employed along the thesis are reported.

3.2. Reagents

3.2.1. Carbon nanotubes

- Single wall carbon nanotubes SWCNTs with 95% purity (outer diameter 1-2 nm and length 10-20 μm) were purchased from Carbolex Inc.
- Multi-wall nanotubes (MWCNTs) with 95 % purity (outer diameter of 10–20 nm, and length of around 50 μm) were obtained from Heji, Inc.

3.2.2. Membrane components

3.2.2.1. Ionophores

Valinomycin, tri-n-dodecylamine (TTDA), 4-Nonadecylpyridine (ETH 1907), N,N-dicyclohexyl-N',N'-dioctadecyl-diglycolic diamide (ETH 5234, calcium ionophore IV), Cyanoaqua-cobyrinic acid heptakis(2-phenylethyl ester) (Nitrite ionophore I), Nonactin (Ammonium ionophore III), 9,11,20,22-Tetrahydrotetabenzo [1,3,8,10]tetraazacyclotetradecine-10,21-dithione (Nitrate ionophore IV) were purchased from Sigma. Octaamide cavitand was provided from Ballester's group (Figure 3.1-3.2).

3.2.2.2. Lipophilic salts

Potassium tetrakis(4-chlorophenyl)borate (KTCBP), potassium tetraakis[3,5-bis(trifluoromethyl)phenyl]borate (KTFPB), sodium tetrakis[3,5-bis(trifluoromethyl)phenyl]borate (NaTFPB), tridodecylmethylammonium chloride (TDMACl) and Tetrakis(4-chlorophenyl)borate tetradodecylammonium salt (ETH 500) were purchased from Sigma Aldrich.

3.2.2.3. Acrylic backbone

Methyl methacrylate (MMA), n-butyl acrylate (nBA), radical precursor previously re-crystallized in warm methanol (AIBN), benzene, petroleum ether (80-100°C), hexane and dichloromethane were acquired from Sigma.

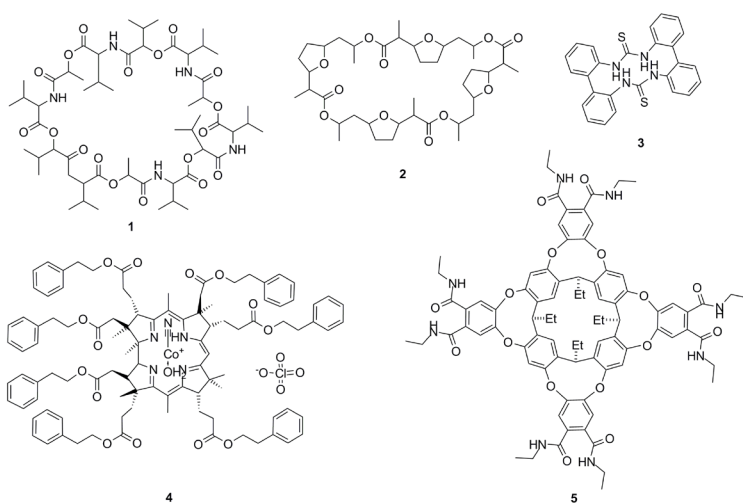


Figure 3.1 – Chemical structure of ionophores used. 1-Valinomycin (Potassium Ionophore); 2-Nonactin (Ammonium ionophore III); 3-Nitrate ionophore V; 4-Nitrite ionophore I; 5- Octaamide cavitand (Choline ionophore).

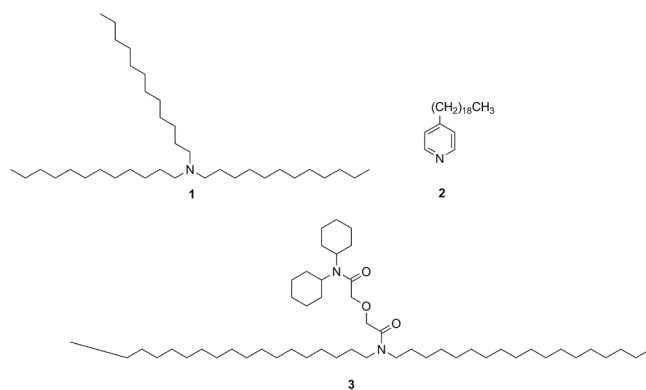


Figure 3.2 – Other ionophores used. 1-TTDA (Hydrogen ionophore I); 2- ETH 1907 (Hydrogen ionophore II); 3- ETH 5234 (Calcium ionophore IV).

3.2.3. Other reagents

2-nitrophenyloctylether (o-NPOE), tri-N-butylchlorosilane, sodium dodecylsulfate (SDS), tetrahydrofuran (THF), nitric and sulfuric acids.

All salts used in the thesis were analytical grade (KCl, NaCl, CaCl₂, MgCl₂, LiCl, NaNO₃, NH₄NO₃, NaNO₂, ClOCl, AChOCl, d-(+)-glucosamine hydrochloride (C₆H₁₃NO₅·HCl), trimethylamine hydrochloride (C₃H₉N·HCl), l-alanine hydrochloride (C₃H₇NO₂·HCl), acetyl-l-carnitine (C₉H₁₇NO₄). All the solutions were prepared using deionised water (18.2 MΩ cm specific resistance) obtained from Milli-Q PLUS (Millipore Corporation, Bedford, MA, USA).

3.3. Procedures

3.3.1. Purification of carbon nanotubes

There are many articles reporting different purification processes of carbon nanotubes depending basically on the application required. In this thesis, only two complete purification processes were used. They are named as weak and strong purification according to the degree of the carboxylation achieved. Both processes are composed of two sub-stages namely dry and wet step methods (Figure 3.3). Oxidation of the amorphous carbon, minimizing the nanotubes's loss, is achieved through the dry step. Carbon nanotubes are heated up to 360°C under an oxygen atmosphere for 90 min [1]. An amount of carbon nanotubes (200 mg) are put inside quartz tubular reactor (4cm x 120 cm, Afora) and heated by a horizontal split tube furnace (HST/600, Carbolite). At the same time, a dry air current flows (100 cm³.min⁻¹, Carbueros Metálicos) through the tube.

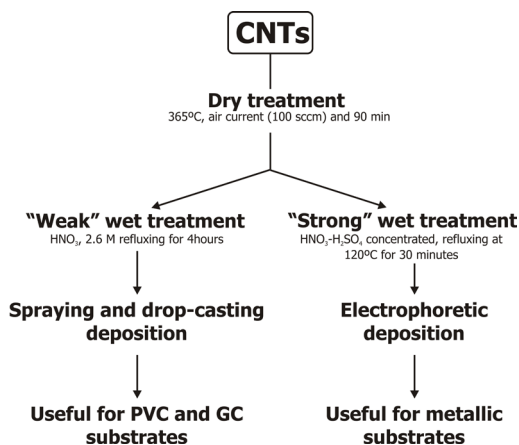


Figure 3.3 – Scheme of the different purification and deposition processes used.

The consequence of the second stage, the wet step, are basically the elimination of metallic particles, the shortening of the carbon nanotubes and the generation of new carboxylic groups (-COOH) on the carbon nanotubes. In the weak purification, 100 mg of SWCNTs or MWCNTs are introduced in 200 mL of HNO_3 2.6 M in refluxing for 4 hours [2]. The resulting CNTs are weakly carboxylated. On the other hand, in the strong purification 100 mg of SWCNTs or MWCNTs are introduced in 4 mL of sulfonitric mixture (3 mL of concentrated HNO_3 , 65 % and 1 mL of concentrated H_2SO_4 , 98 %) for 30 minutes at 120°C [3]. The resulting CNTs are strongly carboxylated. Later on, CNTs are filtered and washed with distilled water until to reach a neutral pH. After this, CNTs are dried in the oven at 100°C and are then ready to use. As a summary, the stronger the acid conditions the shorter the CNTs and therefore higher carboxylated CNTs are obtained. The procedures and results are well reported in the literature. The elementary analysis shows an appreciable increment of the oxygen percentage up to 6 % wt.

3.3.2. Deposition of carbon nanotubes

3.3.2.1. Spraying

SWCNTs and MWCNTs without any treatment, and low carboxylated SWCNTs and MWCNTs were deposited onto the PVC and glassy carbon (GC) substrates by spraying technique [4]. 10 mg of CNTs were powdered by a miller and dispersed in 10 ml of 1 % wt of sodium dodecyl sulphate (SDS). The dispersion was homogenized by tip-sonicator for 30 min (amplitude 60 %, cycle 0.5, Ultraschallprozessor UP200S, Dr. Hielscher). After a few seconds to settle, only the superior fraction is transferred to the compartment placed on the spray-gun. The electrodes are placed at 30 cm in perpendicular line. The deposition was achieved in successive steps. After spraying the dispersion of CNTs for 2 seconds, the layer was dried by a hot-gun, thoroughly washed with water and dried again. The aim of this last step was to eliminate as much as possible the SDS on the electrode. The process was repeated 35 times obtaining a thickness around 35 μm (Figure 3.4).



Figure 3.4 – Scheme of deposition of the CNTs by spraying technique onto a glassy carbon substrate.

3.3.2. Electrophoretic deposition

Highly carboxylated SWCNTs and MWCNTs have been deposited by electrophoretic deposition (EPD) on metallic surfaces. After the strong purification process new carboxyl groups are formed on the end of the tube as well as on the wall defects. Therefore, CNTs become ionized molecules and they acquire migratory properties when they are introduced into an electrical field [5].

0.075g MWCNTs was dissolved in 10 ml of milli Q water. The suspension was ultrasonicated in an ultrasonic bath (J.P.Selecta Ultrasonics) for 15 min and subsequently centrifugated (3000 rpm for 15 min) producing well dispersed and stable CNTs dispersion. Before each deposition it is highly recommendable to sonicate the dispersion in a ultrasonic bath again. Working electrode and counter electrode (separation 1 cm each other) are placed in the electrophoretic cell that contains the CNTs dispersion. DC-Power supply (Isotech IPS 1810H) is properly connected at both electrodes. Working electrode must be connected at the positive electrical pole. At the same time, an electrometer is placed in series with the power supply; it is used as an amperimeter. Several potential differences and periods of time are applied to the CNTs dispersions depending strongly on the substrate material and the active area. The smaller the surface area, the shorter the deposition time.

Electrophoretic deposition has two great advantages over spraying methods. Firstly, CNTs can be dispersed without using any surfactant. Secondly, CNTs can be deposited in a simple way on an irregular, tiny and rough surface without any problems. This deposition technique was also employed to develop macro ion selective electrodes (Figure 3.5).

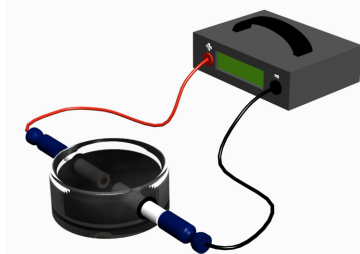


Figure 3.5 – Electrophoretic deposition of CNTs onto the macro copper substrate.

3.3.2.3. Drop casting

Low carboxylated SWCNTs were deposited by drop casting. 10 mg of SWCNTs were dispersed onto 10 mL of dimethylformamide (DMF) [6]. A small volume of the dispersion, around 50 μ L, was placed on the active surface. This technique is not often use in this thesis due to the lower evaporation of the DMF and it's handling difficulties. In fact, SWCNTs seem to be coated with an oily film when visually inspected under the microscope.

3.3.3. Development of the ion selective electrodes

3.3.3.1. PVC home-made electrode

In order to develop a carbon nanotube based electrode in which the carbon nanotubes not only acted as transducers but also as electrical conductors, a non-conducting substrate such as the PVC cover of an electrical cable was used. The copper electrical conductor was removed from the cable leaving the PVC tube (1.5 mm internal \varnothing , 3 mm external \varnothing) that was subsequently cut into pieces of approx. 20 mm pieces long. A pipette tip was introduced inside the tube and the distal end was sealed with a drop of common silicon. Only about 10 mm of the PVC tube is coated with CNTs, and the other half part is protected with a teflon tape. At this moment, CNTs can be deposited by spraying onto the non-protected PVC substrate (**Figure 3.6**).

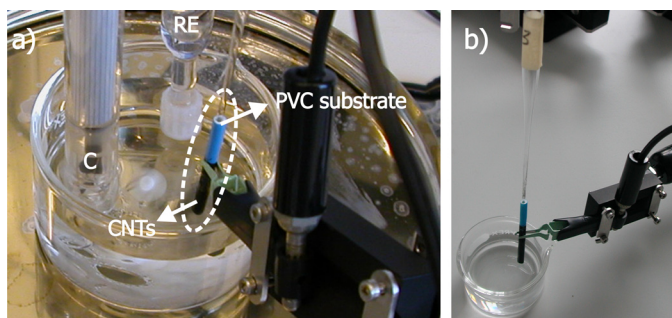


Figure 3.6 – PVC home-made solid contact electrode based on CNTs. **a)** Potentiometric measurement using PVC-home made SC-ISEs based on SWCNTs, reference electrode (RE). Conductometric electrode (C) recorded the conductivity of the solution. **b)** Full image of the SC-ISEs based on CNTs.

3.3.3.2. Glassy carbon home-made electrode

Polished glassy carbon (GC) rods (Sigradur®G, length 50 mm and diameter 3 mm) are used. The GC rods were inserted by mechanical pressure into a hard Teflon body. We used different Teflon body lengths depending on the specific applications. For laboratory probes, the electrical connections were directly made with a clamp in contact with the overhanging GC (Teflon body: length 40 mm and external diameter 6 mm, Amidata SA). For other applications, the exterior of the GC rod was fully protected with a larger Teflon or PVC body (length 80 mm and external diameter 6 mm, Amidata SA). On one of the distal ends, a gold plug male was screwed in becoming the new electrical contact. The junction between GC and the gold plug was done using a metallic silver paste dissolved (EPO-TEK H20E, EPOTEX®) in a small volume of solvent. After that, CNTs were deposited on the opposite distal end of the electrode by spraying technique (**Figure 3.7**).



Figure 3.7 – GC home-made electrode coated by a Teflon body.

3.3.3.3. Copper home-made electrode

A Similar procedure to 3.3.3.2 was used to develop copper electrodes. Copper rods (length 50 mm and diameter 3 mm, Amidata) were polished using abrasive paper (Carbimet 600/P1200, Buehler) and subsequently treated with alumina of different grain-size (30, 5, 1 and 0.03 μm Micropolish II, Buehler). Teflon or PVC bodies (length 40-80 mm and diameter 6 mm, Amidata SA and Broncesval SA) were employed to build up these macroelectrodes. Both spraying and electrophoretic deposition techniques were used to deposit CNTs onto these substrates.

3.3.3.4. Nano home-made electrode

Quartz capillaries with internal filament (Internal Diameter 0.7 mm and Outer Diameter 1 mm, Sutter Instruments) were used in the fabrication of nanoelectrodes. A Sutter 2000 puller machine was employed to make the nano-pipettes. Two program lines enabled to obtain nanopipettes with 2 mm long sharp tips and approx. 200 nm of external diameter. The program lines are related to several factors involved in the puller process, such as temperature of the laser, heating time and time and force of the pulling. (First line: 575 3 35 145 75; second line: 425 0 15 128 200). Later, the nanopipettes were silanized using gas-phase of tri-N-butylchlorosilane.

Platinum, gold, copper, titanium and carbon fiber wires (diameter 25 μm , Goodfellow) were used as electrical conducting substrates. MWCNTs were deposited on these surfaces by electrophoretic technique.

3.3.4. Ion-Selective membrane preparation

3.3.4.1. Acrylic matrix

The procedure for synthesizing the matrix of methyl methacrylate (MMA) and n-butyl acrylate (nBA) was adopted from Heng and Hall with some modifications [7]. The method is based on free radicals polymerization. This was accomplished by adding 0.40 g of MMA, 5.54 g of nBA and 2.88 mg of AIBN acting as initiator, to 3 mL of dry benzene. The MMA-nBA mixture was degassed with nitrogen for 15 minutes. Subsequently, the mixture was heated for 12 hours at 80 °C under a nitrogen atmosphere. The MMA-nBA copolymer was then isolated by precipitation with petroleum ether and purified in the same solvent. After vigorous agitation, the viscous matrix was partially dissolved in 25 mL of dichloromethane. The dissolved part was collected in another recipient. The process is repeated three times. Later, the dissolved part collected was precipitated in 500 mL of analytical grade hexane. The transparent and sticky matrix was dried for two days under a vacuum before use. After each synthesis process the final acrylic matrix was characterized by ¹H RMN. The area under both triplets at 0.93 and 3.5 ppm ratio must be around ten (Appx 3, Figure 1).

3.3.4.2. Ion selective membrane preparation

For macroelectrodes, all ion selective membranes were prepared in the same way: i) ionophore 15-30 mmol/kg depending on the stoichiometric ratio between the ionophore and the primary analyte. ii) lipophilic anion or cation, 40-60 % mol of ionophore. iii) In some cases, 20 mmol/kg of ETH 500 iv) 100-200 mg of the acrylic matrix. The components were dissolved in 1-2 mL of dichloromethane and the mixture was mixed in a vortex for 1 hour.

On the other hand, for nano-electrodes, the following steps of the ion selective membrane preparation were modified in order to avoid obtaining a large total resistance. In this way the cocktail is only composed by: i) 63.9 mmol/kg of calcium IV ionophore ii) lipophilic anion 50 % mol of ionophore iii) 45.32 mg of o-NPOE.

3.3.5. Deposition of the membrane

3.3.5.1. Dip coating

Dip coating was used for PVC home-made electrodes. The electrode was dipped three times into the cocktail. The electrode was dried in a normal atmosphere overnight. Thicknesses around 45-50 μm were obtained.

3.3.5.2. Drop casting

Drop casting was used for macroelectrodes with a Teflon or PVC body. 150 μL (3x50 μL) of the cocktail was placed on the electrode. A short plastic tube was used as a recipient to hold the

liquid membrane. The membrane was dried inside the dichloromethane atmosphere; therefore, the slow evaporation of the solvent avoided the formation of undesired bubbles.

3.3.5.3. Back-filling

The nanopipette corresponding to the home-made electrode described in 3.3.3.4 was back-filled with the cocktail. Only one small drop was needed to fill the volume required.

3.3.6. Conditioning

In order to reach a low limit of detection of the SC-ISEs, two basic steps were accomplished [8]: i) The membranes were placed in a relatively concentrated solution (10^{-3} or 10^{-2} M) of the primary ion for 24 hs. ii) After the first step of conditioning, the electrodes had to be washed with MQ-water and placed in a diluted solution of the primary analyte (10^{-8} or 10^{-9} M) for 48 hs.

When the lower limit of detection was determined, this procedure was accomplished. However, calibration curves for a common and rapid test could be obtained either without the second stage or reducing the time.

3.3.7. Microscopic characterization

3.3.7.1 Scanning electron microscopy

Environmental Scanning Electron Microscopy (E-SEM, Quanta 600, FEI, Hillsboro) was used to characterize the CNT's layer deposited onto the electrodes by the spraying technique. Either teflon or PVC electrode with the CNTs layer were attached to the support inside the E-SEM chamber. Parameters (potential, pressure and working distance) were characterized in each case to obtain the maximum resolution possible of the images. Ion selective membranes were also checked by E-SEM inspection. The thickness of the membranes was measured in the same way.

Scanning Electron Microscopy (SEM, JSM 6400 Jeol) was used to characterize the electrophoretic deposition of the CNTs onto the metallic wires. The size of the nanometric cavity on the quartz pipette was also measured using this technique.

3.3.7.2. Transmission electron microscopy

SWCNTs and MWCNTs structures were characterized by Transmission Electron Microscope (TEM, JEOL model 1011). SWCNTs or MWCNTs were dispersed in a solvent (DMF or water depending the type of CNTs). Several drops of the dispersion were placed in a line grating substrate. After drying out, the sample was analyzed by TEM.

TEM images provided information about the quality of the purification process. Amorphous carbon bundles or metallic particles were observed either between or inside of the CNTs. Diam-

eters and lengths of the individual tubes were measured with high precision to check the shortening process involved in the strong wet purification stage. TEM was also a useful technique to characterize the dispersion of the CNTs.

3.3.8. Electrochemical characterization

3.3.8.1. Electrochemical impedance spectroscopy

Electrochemical measurements were performed by using a one-compartment, three electrode electrochemical cell. The working electrode, the counter electrode (glassy carbon rod) and the reference electrode (Ag/AgCl/KCl (3 M) single junction electrode Model 6.0733.100, Metrohm) were placed in the cell maintaining the same configuration in all the experiments. Impedance measurements were recorded using an Autolab general purpose electrochemical system, Autolab frequency response analyzer system (AUT20.FRA2-AUTOLAB, Eco Chemie, B.V) and electrochemical Analyzer/Workstation (Model 600 Series, CH Instruments). The impedance spectra was recorded in the frequency range 100 kHz-10 mHz by using a sinusoidal excitation signal that was superimposed on a current circuital potential value (E_{dc}). All E_{dc} potentials were referred to the reference electrode. The electrodes that consisted only of a layer of carbon nanotubes were studied using excitation amplitude of 10 mV. However, for the electrodes containing the selective membrane, an amplitude of 100 mV was used in order to enhance the signal/noise ratio.

Impedance measurements are usually recorded in a concentrated electrolyte solution of the primary analyte from 10^{-3} up to 10^{-1} M. In some cases the cell solution was purged with argon or oxygen depending on the experiment and all measurements were performed at room temperature. The impedance spectra were then fitted to an equivalent electrical circuit by using the CH or the Autolab impedance analysis software.

3.3.8.2. Cyclic voltammetry

The cyclic voltammograms (CV) were recorded in the same way as the electrochemical impedance measurements (see 3.4.2.1). Three cycles in the potential range -0.5 V to 0.5 V at a scan rate of 0.1 V/s were performed in each case. The cell solution containing 0.1 M of KCl was purged with argon or oxygen.

3.3.8.3. Chronopotentiometry

Constant-current chronopotentiometry was performed by using the same instrumentation and electrodes as described above for EIS. A constant current of a 1-5 nA was applied to the working electrode for 60-100 s followed by an inverse current of the same absolute value for the same amount of time under simultaneous recording of the electrode potential. The measurements were performed in a primary analyte solution of 0.1 M at room temperature.

3.3.8.4. Potentiometry

Keithley 6514 electrometer and Lawson multichannel high input resistance ($10^{15}\Omega$) were used to record electromotive forces (EMF). A double-junction Ag/AgCl/KCl (3 M) reference electrode (type 6.0729.100, Methrom AG) containing a 0.1-1 M LiAcO electrolyte bridge was used. The measurements were performed in stirred solutions at room temperature. Potential values were corrected for liquid-junction potentials according to the Henderson equation. Activity coefficients were calculated by the Debye-Hückel approximation.

3.4. References

- [1] Furtado, C.A., U.J. Kim, H.R. Gutierrez, L. Pan, E.C. Dickey, and P.C. Eklund, Debundling and dissolution of single-walled carbon nanotubes in amide solvents. *Journal of the American Chemical Society*, 2004. 126(19) 6095-6105.
- [2] Zhang, J., H.L. Zou, Q. Qing, Y.L. Yang, Q.W. Li, Z.F. Liu, X.Y. Guo, and Z.L. Du, Effect of chemical oxidation on the structure of single-walled carbon nanotubes. *Journal of Physical Chemistry B*, 2003. 107(16) 3712-3718.
- [3] Cho, J., K. Konopka, K. Rozniatowski, E. Garcia-Lecina, M.S.P. Shaffer, and A.R. Boccacini, Characterisation of carbon nanotube films deposited by electrophoretic deposition. *Carbon*, 2009. 47(1) 58-67.
- [4] Kaempgen, M. and S. Roth, Transparent and flexible carbon nanotube/polyaniline pH sensors. *Journal of Electroanalytical Chemistry*, 2006. 586(1) 72-76.
- [5] Boccacini, A.R., J. Cho, J.A. Roether, B.J.C. Thomas, E.J. Minay, and M.S.P. Shaffer, Electrophoretic deposition of carbon nanotubes. *Carbon*, 2006. 44(15) 3149-3160.
- [6] Agui, L., P. Yanez-Sedeno, and J.M. Pingarron, Role of carbon nanotubes in electroanalytical chemistry - A review. *Analytica Chimica Acta*, 2008. 622(1-2) 11-47.
- [7] Heng, L.Y. and E.A.H. Hall, Producing "self-plasticizing" ion-selective membranes. *Analytical Chemistry*, 2000. 72(1) 42-51.
- [8] Chumbimuni-Torres, K.Y., N. Rubinova, A. Radu, L.T. Kubota, and E. Bakker, Solid contact potentiometric sensors for trace level measurements. *Analytical Chemistry*, 2006. 78(4) 1318-1322.

UNIVERSITAT ROVIRA I VIRGILI

SOLID CONTACT ION SELECTIVE ELECTRODES BASED ON CARBON NANOTUBES

Gastón Adrián Crespo Paravano

ISBN:978-84-693-6428-4/DL:T-1630-2010



**CHAPTER 4
CARBON
NANOTUBES
AS EFFICIENT
TRANSDUCER IN
POTENTIOMETRIC
SENSORS**

UNIVERSITAT ROVIRA I VIRGILI

SOLID CONTACT ION SELECTIVE ELECTRODES BASED ON CARBON NANOTUBES

Gastón Adrián Crespo Paravano

ISBN:978-84-693-6428-4/DL:T-1630-2010

4.1. Introduction

This chapter demonstrates that carbon nanotubes can be used as ion-electron transducer. It is clearly depicted through electrochemical and optical techniques. A first approach to introduce nanostructured materials on the potentiometric field is achieved using simple and inexpensive materials. Thus, new great research opportunities have been opened up from this discovery.

4.2. “Ion-Selective Electrodes Using Carbon Nanotubes as Ion-to-Electron Transducers”

Analytical Chemistry. 2008, *80*, 1316-1322

Gastón A. Crespo, Santiago Macho and F. Xavier Rius*

Department of Analytical and Organic Chemistry, Rovira i Virgili University,
43007 Tarragona, Spain.

4.2.1. Abstract

This study developed a new type of all-solid-state ion selective electrode based on a transducing layer of a network of single-walled carbon nanotubes (SWCNTs). The extraordinary capacity of carbon nanotubes to promote electron transfer between heterogeneous phases made the presence of electroactive polymers or any other ion-to-electron transfer promoter unnecessary. The new transducer layer was characterized by environmental scanning electron microscopy (ESEM) and electrochemical impedance spectroscopy (EIS). The stability of the electrical potential of the new solid-contact electrode was examined by performing current-reversal chronopotentiometry and the influence of the interfacial water film was assessed by the potentiometric water layer test. The performance of the new electrode was evaluated by determining K^+ with an ion selective membrane that contained the well known valinomycin ion-carrier. The new electrode have a Nernstian slope (58.4 mV/decade), dynamic ranges of four logarithmic units and selectivities and limits of detection comparable to other solid-contact electrodes. The short response time (less than 10 seconds for activities higher than $10^{-5.5}M$) and the stability of the signal over several days makes these new electrodes very promising candidates for attaining true miniaturization.

4.2.2. Keywords

Ion selective electrodes, ion-to-electron transducers, solid-contact electrodes, carbon nanotubes, potentiometric potassium determination.

4.2.3. Introduction

Because of their intrinsic advantages of miniaturization and straightforward fabrication, ion selective electrodes (ISE) with internal solid contact have been recognized as the means by which the next ISE generation will be constructed¹. The introduction of conducting polymers as internal ion-to-electron transducers has greatly improved the stability of the potential of the first coated-wire electrodes^{2,4}. In this case the internal redox system consists of an electroactive polymer layer. However, several factors influence the stability of the redox system within the conducting polymer. Drifts may occur because of the presence of protonable functional groups, the formation of a water film between the membrane and the inner contact, and the influence of some gases⁴. Moreover, the doping of the conducting polymer for each application needs to be fine tuned if the ion-to-electron transduction between the selective membrane and the conducting wire is to be optimized^{2,3}.

The extraordinary properties of carbon nanotubes derive from their chemical structure. They are particularly suited to nanosensing with electrochemical fields because of their surface-to-volume ratio, the presence of mobile electrons on the surfaces of the nanotubes and their extraordinary capacity to promote electron transfer between heterogeneous phases⁵. These properties have led to carbon nanotubes being used as components of field effect transistors^{6,7}, capacitors⁸ or nanoelectrode arrays in voltammetric analysis⁹. However, to date they have not been tested as transducers in potentiometric analysis. Kaemppgen *et al* used carbon nanotubes as a backbone structure in pH electrodes to support polyaniline¹⁰. Taking advantage of its conducting characteristics, they used the conducting polyaniline in a double role, as recognition layer (since the oxonium ions interact with the amine groups) and a transducer.

Transduction through carbon nanotubes means that there are no redox reactions at the interface between the membrane and the inner electronic contact. Nevertheless, there is a Nernstian response. This may be attributed to the charge transfer capacities of the SWCNTs. However, other effects such as the presence of a water layer that may appear at the membrane-SWCNT interface may also contribute to the response signal. Water and redox-active gases such as O₂ can diffuse through the membrane and build an oxygen half-cell in a similar way to that suggested by early studies^{11,12}. Additionally, the presence of gases with acid-base properties such as CO₂ can also influence the pH of the water layer and thus affect the stability of the electromotive force response¹³.

In this communication, we report that carbon nanotubes can act as active ion-to-electron transducers in potentiometric electrodes. Specifically, we demonstrate the transducing capacities of single-walled carbon nanotubes, SWCNTs, by developing an all-solid-contact ion-selective electrode for K⁺ that does not need the presence of conducting polymers. The electrical performance of the new internal solid contact material was characterized by electrochemical imped-

ance spectroscopy (EIS). In addition, the stability of the derived solid-contact electrode and the influence of the interfacial water layer were examined by performing current-reversal chronopotentiometry¹⁴ and the potentiometric water test, respectively. Finally, the main performance characteristics of the new electrode were estimated.

4.2.4. Experimental section

4.2.4.1. Ion selective membrane

The membrane contained 2.0 wt.% (18.1 mmol kg⁻¹) of valinomycin, 0.5 wt.% (10.0 mmol kg⁻¹) of the lipophilic anion potassium tetrakis(4-chlorophenyl)borate and 97.5 wt.% of monomers methyl methacrylate (MMA) and n-butyl acrylate (nBA) in proportion 1:10 respectively, according to a described procedure¹⁵. The membrane was prepared by dissolving 200 mg of membrane components in 2.0 mL of methylene chloride.

4.2.4.2. Electrode development

The electrode is built by spraying an aqueous suspension (10⁻² wt. %) of the purified SWCNTs¹⁶ containing 1 wt. % of sodium dodecyl sulfate onto a non-conducting PVC rod (3 mm external diameter) that serves as mechanical support. The carbon nanotubes were deposited in successive steps. After spraying the dispersion of nanotubes for 2 seconds, the layer of SWCNTs was dried, thoroughly washed with water and dried again. The process was repeated between five and six times. An ion-selective membrane containing valinomycin, as ion-carrier for K⁺, was deposited (about 45 μm thick) onto the SWCNT network by dip-coating into a methylene chloride solution. The electrical contact was established by direct contact of the SWCNT layer with a metal clamp, as shown in **Figure 4.1**. The recorded potential did not change after the layer of carbon nanotubes had been contacted at least ten times. Electrodes without the SWCNT layer were prepared in complete analogy.

4.2.4.3. Electrochemical Impedance Spectroscopy

Electrochemical Impedance Spectroscopy (EIS) was performed by using an Electrochemical Analyzer/Workstation (Model 600 Series, CH Instruments., UK). Impedance was measured by using a one-compartment three-electrode cell where the electrode under study was connected as the working electrode. The reference electrode was a Ag/AgCl/KCl (3 M), and the auxiliary electrode was a platinum wire. The impedance spectra were recorded in the frequency range 100 kHz-10 mHz by using a sinusoidal excitation signal that was superimposed on a constant direct current potential, E_{dc} = 0.2 V. The electrodes that consisted only of the layer of carbon nanotubes (active area = 0.14 cm²) were studied using an excitation amplitude of 10 mV. However, for the electrodes containing the membrane selective to K⁺, with impedances over 10 MΩ, an amplitude of 100 mV was used in order to enhance the signal/noise ratio. The measurements were taken in

a solution of 0.1 M KCl at room temperature (22 ± 2 °C). The impedance spectra were fitted to an equivalent electrical circuit by using the CH impedance analysis software.

4.2.4.4. Chronopotentiometric measurements

A constant current of a few nanoamperes was applied to the working electrode for 100 s followed by a reversed current of the same magnitude for the same length of time and the EMF was measured in a solution of KCl 0.1 M at room temperature (22 ± 2 °C). These measurements were recorded by using a one compartment three-electrode cell to which the electrode under study was connected as the working electrode. The reference electrode was a Ag/AgCl/KCl (3 M), and the auxiliary electrode was a platinum wire.

4.2.4.5. Electromotive force measurements

Electromotive forces (EMF) were measured at room temperature (22 ± 2 °C) in unstirred solutions with a Keithley high input impedance voltmeter. A double-junction Ag/AgCl/KCl (3 M) reference electrode (type 6.0729.100, Methrom AG) containing a 1M LiAcO electrolyte bridge was used. The experiments were performed in a 100 mL glass beaker pretreated overnight in 10^{-4} M HNO_3 . All EMF values were corrected for liquid-junction potentials according to the Henderson equation. Activity coefficients were calculated by the Debye–Hückel approximation.

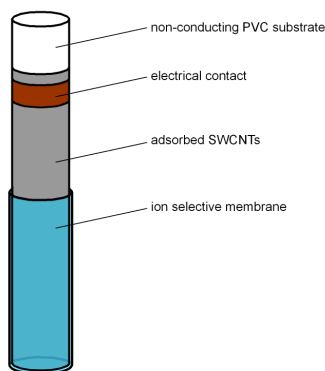


Figure 4.1 - Scheme of the ion selective electrode. The valinomycin-containing K^+ ion selective membrane is placed on a network of SWCNT that acts as the transducer layer. The SWCNT layer is adsorbed onto a non-conducting PVC rod and contacted to the electrical wire.

4.2.5. Results and discussion

A layer approximately $25\mu\text{m}$ thick that contained the network of SWCNTs is obtained by using the procedure described. Carbon nanotubes showed good mechanical adhesion of the PVC support. The nanotube network was characterized by environmental scanning electron microscopy (ESEM). ESEM has several advantages over conventional SEM because of its capacity to work in milder conditions. **Figure 4.2** shows the ESEM image of the SWCNT network where the nanotubes are well interconnected since they are deposited in the 'spaghetti' way. The electrode was designed to avoid contact between the ion selective membrane and the electrical conducting wire, thus demonstrating the capacity of the carbon nanotubes to transduce the electrochemical potential generated at the membrane-solution interface. Electrodes prepared with an identical procedure without the SWCNT layer provided no electrical signal. **Figure 4.3** shows a schematic representation of the electrodes studied where the SWCNT networks play the role of the ion-to-electron transducer with no redox reaction.

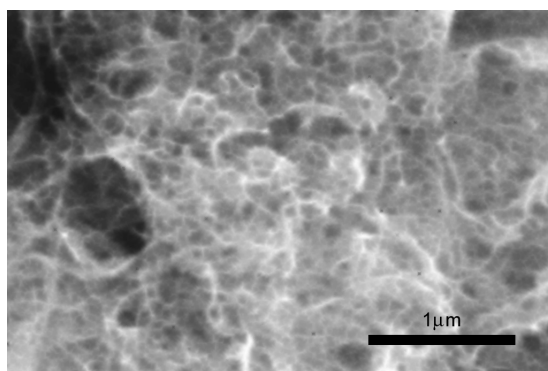


Figure 4.2 - ESEM image of the carbon nanotube transducer layer.

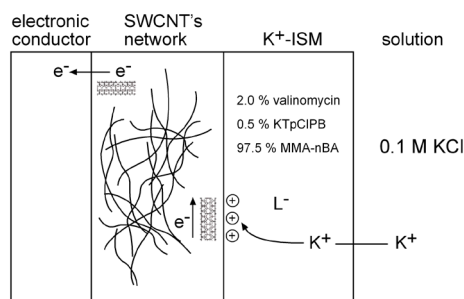


Figure 4.3 - Schematic representation of the electrodes studied in this work, showing the different layers and the role of SWCNTs as ion-to-electron transducers. K^+ -ISM: potassium ion selective membrane; L^- = TpClPB^- : tetrakis(4-chlorophenyl) borate anion, MMA-nBA: polymer made of the monomers methyl methacrylate and n-butyl acrylate.

4.2.5.1. Impedance spectroscopy of Cu/SWCNTs on PVC support

Figure 4.4 shows typical electrochemical impedance spectroscopy results of the Cu/SWCNTs on a PVC support electrode in 0.1 M KCl solution. Figure 4.4A shows the complex plane impedance plot. The system has multiple components and contains more significant constituents than when conducting polymers were used as ion-to-electron transducers in contact with electronic conductors¹⁷. One of the main constituents is the ohmic resistance, which for a standard SWCNT network size (0.14 cm² active area, 25 μm thickness and 12 mm from the active area to the electronic contact) is $R_e = 1.1 \text{ k}\Omega$. It should be considered that when the proposed electrode design is used (Figure 4.1), the network itself acts as electronic conductor. The Bode plot (Figure 4.4B) indicates that this resistance is located in the region of high-intermediate frequencies (in the range 10 kHz to 100 Hz).

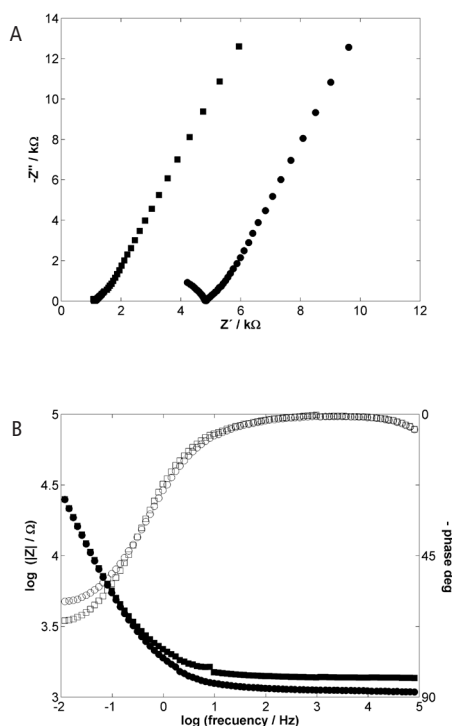


Figure 4.4 - Electrochemical impedance spectroscopy results of the Cu/SWCNTs on PVC support electrode in 0.1 M KCl solution. Experimental conditions: $E_{dc} = 0.2 \text{ V}$, Frequency range = 100 kHz-10 mHz, Amplitude = 10 mV. A) Complex plane impedance plot at two different distances between the active surface and electrical contact. (♦) 12 mm and (■) 27.5 mm. B) Bode plot for the same experiments performed in A): the filled symbols are the log Z-log f changes. The empty symbols are the phase changes.

The magnitude of this resistance varies with the distance between the active surface and the electrical contact (**Figure 4.4**) as expected, which shows that the conductance characteristics of the network of SWCNTs is the major contribution to the ohmic resistance. Results were similar when the thickness of the SWCNT layer was varied (see **Figure 4.1.si** in supporting information).

Another component of the resistance has its origin at the interface between the SWCNT network and the metallic conductor in the upper part of the electrode. Changes in the nature of the metallic contact by using copper, Pt or glassy carbon as electronic conductors give rise to very small changes in the intersection with the real impedance axis that fall within the uncertainty of the measurements (see **Figure 4.2.si** in supporting information). Finally, the solution resistance becomes apparent when the spectrum is recorded at different concentrations of the KCl solution (**Fig 3.si** in supporting information). The estimated value, $R_s = 145 \Omega$, is in agreement with the value found, $R_s = 150 \Omega$, for a conducting polymer transducer in an identical 0.1M KCl solution ¹⁷.

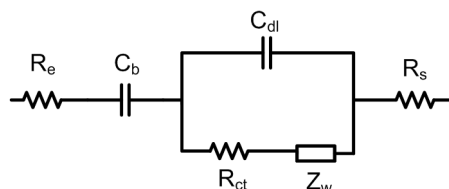


Figure 4.5 - Equivalent electrical circuit for the Cu/SWCNTs on PVC support electrodes. R_e : electronic resistance; C_b : bulk electronic capacitance; C_{dl} : double-layer capacitance; R_{ct} : charge-transfer resistance; Z_w : Warburg diffusion impedance; R_s : solution resistance.

The Bode plot in **Figure. 4.4B** also suggests that capacitive components are present in the network of SWCNTs. The change of phase at high frequencies may be due to a double-layer capacitance in parallel with the charge-transfer resistance at the interface between the SWCNT network and the ionic solution. Eleven impedance spectra were fitted to several equivalent circuits by using the non-linear least-squares method. **Figure 4.5** shows the equivalent circuit for which the fitting was best (average error, $\chi^2 = 0.04$). The value estimated for the double layer capacitance was $C_{dl} = 302 \mu\text{F}$. The charge transfer resistance was found to be in the $\text{n}\Omega$ range, indicating the high transfer capacity of the carbon nanotubes and facilitating the mechanism of the ion-to-electron transduction in this nanostructured material. Note that although potassium ions encountered a resistance to diffusing into the polymer when conducting polymers were used, we found neither an appreciable diffusional resistance nor the related low-frequency diffusional capacitance when carbon nanotubes were used. The absence of a high frequency semicircle also suggests that the electronic charge transfer is fast at both the electronic conductor-SWCNT interface and the SWCNT network-solution interface ¹⁸.

The presence of the bulk capacitance component, $C_b = 4.6$ mF, is detected by the phase change and a straight line with a slope near -1 in the $\log Z$ - $\log f$ plot in the low frequency region. This capacitance increases when the thickness of the SWCNT layer is increased. Therefore, it is assigned to the bulk property. This high value for the low-frequency capacitance suggests that the SWCNTs can act as ion-to-electron transducers displaying both high exchange current and potential stability¹⁸. According to the equivalent circuit used (Figure 4.5), the overall capacitance of the SWCNT layer is mainly dictated by the lowest capacitance found (i.e. the double layer capacitance), which is compatible with the overall capacitance value obtained by chronopotentiometry.

4.2.5.2. Impedance of SWCNT/ K^+ -ISEs

The impedance spectrum of the electrodes made by depositing the valinomycin polymeric membrane onto the carbon nanotube layer acting as inner transducer, SWCNT/ K^+ -ISEs, displays a single high frequency semicircle (Figure 4.6). This slightly depressed high frequency semicircle is related to the bulk resistance, R_{bulk} , of the ion-selective membrane in parallel with its geometric capacitance, C_{bulk} . For the SWCNTs/ K^+ -ISEs studied here, the total resistance R_{bulk} was between 13.5 and 18 $M\Omega$, (membrane thickness ca. 45 μm and 80 μm , respectively). The absolute value of this resistance and its variation with the thickness of the polymeric layer clearly shows that the contribution of the ion selective membrane outweighs the resistance of the Cu/SWCNTs on the PVC support electrode studied above. A relatively high noise level appears in the low-frequency region of the complex impedance plane plot. The magnitude of this noise depends on the thickness of the ion-selective membrane, suggesting that it might be due to a bulk process in the membrane.

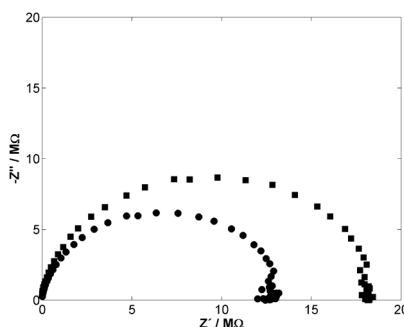


Figure 4.6 - Complex plane impedance plot of the SWCNT- K^+ ISE electrode in 0.1 M KCl solution. Experimental conditions: $E_{\text{dc}}=0.2$ V, Frequency range =100 kHz-10 mHz, Amplitude = 100 mV. Potassium selective membrane thickness: (●) 45 μm and (■) 80 μm .

The absence of a second semicircle in the low-frequency region indicates the lack of a second relaxation process in which a small double-layer capacitance is in parallel with a large charge-transfer resistance at the interface between the inner transducer and the ion selective

membrane¹⁸. As can be seen in **Figure 4.6**, this is clearly not our case, in agreement with the potential stability found in the chronopotentiometric results.

4.2.5.3. Water layer test

We assessed the presence and influence of a water layer at the interface between the polymeric membrane and the carbon nanotubes by means of the potentiometric water layer test⁴.¹⁹ The ISEs were initially conditioned in 0.1 M KCl for 24 hours and their response was then alternately measured in 0.1 M KCl, 0.1 M NaCl, and again in 0.1 M KCl. **Figure 4.7** shows a clear difference in the behavior of the coated wire electrode developed by simply coating a Cu wire with the polymeric potassium selective membrane, and the SWCNTs/K⁺-ISEs electrode. A moderate negative potential drift is initially observed when the new the SWCNTs/K⁺-ISEs electrode was used to take measurements in solutions of the primary ion KCl. However, a reduced positive potential drift is observed when measurements were made in solutions of the discriminating Na⁺ ion, which indicates that NaCl is hardly replaced by KCl in the water film formed between the ion selective membrane and the SWCNT layer. The final replacement of the test solution by the original 0.1 M KCl solution gives rise to an almost null negative potential drift. These results compare very favorably with those obtained for the coated-wire electrode, indicating that a reduced water layer is formed in our sensor. The highly hydrophobic character of the SWCNT network²⁰ could be the reason for the presence of this reduced water layer.

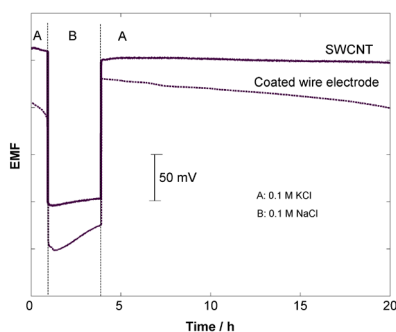


Figure 4.7 - Water layer test for the SWCNT/K⁺-ISE electrodes using carbon nanotubes as inner transducer (solid line) and the coated wire electrode made by depositing the K⁺ selective membrane on a bare Cu wire (dotted line). The measurements were recorded in 0.1 M KCl (A) and 0.1 M NaCl (B).

4.2.5.4. Potentiometric performance characteristics

We measured the $\log a_{K^+}$ dependence of the new electrodes by recording the EMF with the standard additions method. The magnitude of the recorded electromotive force does not depend on the size of the sensing area in contact with the test solution. Before each measurement, the

sensor device was immersed in a solution 0.01 M of KCl overnight in order to condition the electrode ²¹ and to ensure the same starting conditions. A linear range of four logarithmic units of potassium ion activity is obtained with five different electrodes, with a close to Nernstian slope corresponding to a sensitivity value of 58.1 mV/decade a_{K^+} . (standard deviation of the slope = 0.4 mV/decade a_{K^+}). The limit of detection calculated as the intersection of the two slope lines in **Figure 4.8** is $10^{-5.5}$.

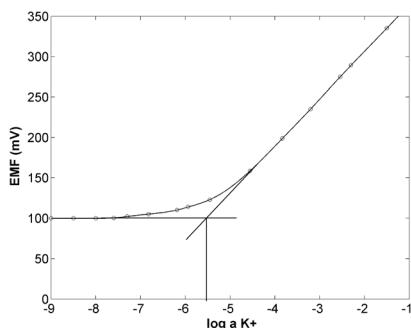


Figure 4.8 - EMF dependence on $\log a_{K^+}$ for valinomycin-containing ion selective membranes on a SWCNT inner layer contact, conditioned in 0.01 M KCl.

The selectivity of the electrode is mainly defined by the composition of the membrane used and directly related to the two-phase equilibria. The following upper limit potentiometric selectivity coefficients, $\log K_{KJ}^{pot} \pm$ statistical range ($n=3$), were obtained with the fixed interference method ²²: $\log K_{KLi}^{pot} = -3.6 \pm 0.3$, $\log K_{KNa}^{pot} = -4.6 \pm 0.2$, $\log K_{KCa}^{pot} = -2.1 \pm 0.4$, $\log K_{KNH4}^{pot} = -3.9 \pm 0.3$, $\log K_{KMg}^{pot} = -4.6 \pm 0.4$ which are comparable to their liquid-contact electrode counterparts. The absence of an inner solution favours the response time of the new solid-contact SWCNT-ISEs (**Figure 4.9**).

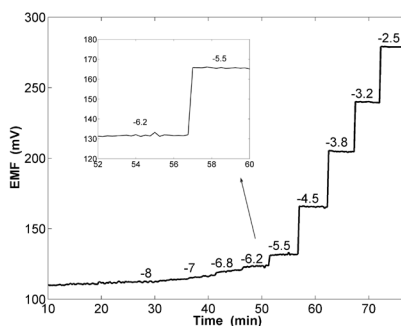


Figure 4.9 - Time response of the SWCNT/ K^+ -ISE electrodes. Expansions of selected ranges in inserts.

Particularly at low concentrations, the response is faster than for the electrodes that contain a similar membrane but liquid-contact. For example, when the concentration was increased from $10^{-6.2}$ to $10^{-5.5}$ M, the new electromotive force value was stable after 10 s.

The electrode developed shows a moderately stable response over time. It is known that, in long term use, leaching of ionophores from the membrane can seriously influence the detection limit ²³. **Figure 4.10** shows that, for the membrane used and with SWCNT as the internal layer, the loss in detection limit was restricted to one decade of activity values in 25 days. On the other hand, the E° , selectivity, and slope of the response show little variation so for electrodes used at above $10^{-4.5}$ M KCl, this is a reliable and reproducible system.

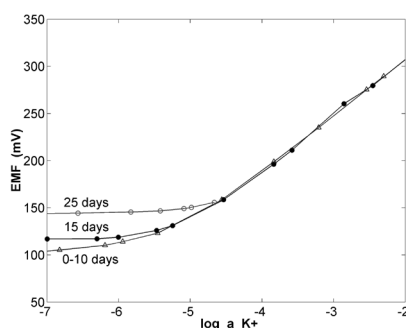


Figure 4.10 - Potentiometric response to different K^+ activities over time for SWCNT/ K^+ -ISE electrodes conditioned in 0.01 M KCl and stored in the same solution between uses.

4.2.5.5. Chronopotentiometry

We used reversal chronopotentiometry to evaluate the electrical capacity of the solid contact and the potential stability of the electrode developed ¹⁹. **Figure 4.11** shows a typical change in potential vs. time when currents of -1 and -5 nA are applied to the working electrode for 100 s followed by currents of +1 and +5 nA, respectively, for the same time interval. For comparison purposes, the same plot is represented for the coated wire electrode ($I = 1$ nA). The potential jump is related to the total resistance (R), according to Ohms law, $R = E/I$, where E represents the change in potential and I the current applied. The total resistances estimated for the electrodes developed are $R_{total} = 13.8$ M Ω ($I = 1$ nA) and 12.4 M Ω ($I = 5$ nA). From the same experimental plots, the stability of the potentials can be derived from the ratio $\Delta E/\Delta t$. The resulting values $\Delta E/\Delta t = 1.7 \cdot 10^{-5}$ V/s ($I = 1$ nA) and $\Delta E/\Delta t = 8.5 \cdot 10^{-5}$ V/s ($I = 5$ nA) are lower than the values obtained from the coated wire electrode developed under similar conditions ($\Delta E/\Delta t = 2.8 \cdot 10^{-4}$ V/s) ($I = 1$ nA). The experiments were repeated four times obtaining very similar results. Following the fundamental capacitor equation, $I = C dE/dt$, it can be readily seen that this potential drift is inversely proportional to the capacitance C of the electrode. The values obtained $C = 60 \mu F$ ($I =$

1 nA) and $C = 59 \mu\text{F}$ ($I = 5 \text{ nA}$) are in qualitative agreement with the overall capacitance obtained from the impedance spectroscopy study. These results corroborate the stability of the processes involved at the SWCNT-membrane interface.

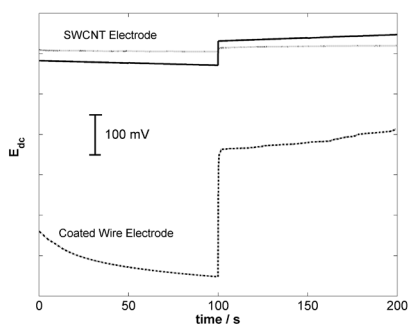


Figure 4.11 - Chronopotentiometric results. Upper part: SWCNT/ K^+ -ISE electrode. Solid line: applied current +5 nA for 100 s and -5 nA for 100 s. Dotted line: applied current +1 nA for 100 s and -1 nA for 100 s. Bottom part: Coated wire electrode, applied current +1 nA for 100 s and -1 nA for 100 s. Solution = 0.1 M KCl.

4.2.6. Conclusions

This work demonstrates that carbon nanotubes can be used as efficient transducers in solid-contact ion selective electrodes. The principles of ion-to-electron transduction in SWCNTs are not based on a redox reaction and ion exchange properties as in electroactive polymers but on the high charge transfer of carbon nanotubes. The high influence of the surrounding chemical environment on the conductance of carbon nanotubes make them very sensitive to the phase-boundary potential changes generated at the interface ion selective membrane-test solution. The charge transfer process between the ionic conducting membrane and the electronically conducting wire takes place without producing voltage instabilities. The high surface/volume ratio of SWCNTs may contribute to enlarging the contact area between the polymeric membrane and the nanotubes²⁴, minimizing the resistance at this interface as well. The hydrophobicity of the SWCNT layer may be the reason why a significant water layer is not detected in the ion-selective membrane or the transducer layer interface. The adverse influence of gases such as O_2 or CO_2 , that can remove electrons from or add electrons to the SWCNTs, is hindered in the absence of a water layer. The use of semiconducting SWCNTs generates a moderate ohmic resistance in the transduction layer. The optimizing process undertaken in our laboratory will emphasize the importance of using metallic or semiconductor SWCNTs and the relevance of the carboxylation process²⁵ to modify the electrical characteristics of the transducers. Although ion-selective microelectrodes containing an inner solution with sensor tip diameters in the micro- and sub-micrometer range have been known for decades, true miniaturization of potentiometric sensors is now affordable because the inner electrolyte solution or the conducting polymer have been

eliminated without creating instabilities. Moreover, the new type electrodes are very easy to build at very reasonable costs.

4.2.7. Acknowledgments

We thank the Spanish Ministry of Education and Science, MEC, for supporting the work through the project grant NAN2004-09306-C05-05. GAC also acknowledges MEC for the doctoral fellowship AP2006-04171.

Dedicated to Professor Ernő Pretsch, in thanks for his many years of expertise and guidance.

4.2.8. References

- (1) Pretsch, E. *Trac-Trends in Analytical Chemistry*. **2007**, *26*, 46-51.
- (2) Bobacka, J. *Electroanalysis*. **2006**, *18*, 7-18.
- (3) Michalska, A. *Analytical and Bioanalytical Chemistry*. **2006**, *384*, 391-406.
- (4) Sutter, J.; Pretsch, E. *Electroanalysis*. **2006**, *18*, 19-25.
- (5) Dai, H. J. *Accounts of Chemical Research*. **2002**, *35*, 1035-1044.
- (6) Tans, S. J.; Verschueren, A. R. M.; Dekker, C. *Nature*. **1998**, *393*, 49-52.
- (7) Martel, R.; Schmidt, T.; Shea, H. R.; Hertel, T.; Avouris, P. *Applied Physics Letters*. **1998**, *73*, 2447-2449.
- (8) Snow, E. S.; Perkins, F. K.; Houser, E. J.; Badescu, S. C.; Reinecke, T. L. *Science*. **2005**, *307*, 1942-1945.
- (9) Tu, Y.; Lin, Y. H.; Yantasee, W.; Ren, Z. F. *Electroanalysis*. **2005**, *17*, 79-84.
- (10) Kaempgen, M.; Roth, S. *Journal of Electroanalytical Chemistry*. **2006**, *586*, 72-76.
- (11) Cattrall, R. W.; Tribuzio, S.; Freiser, H. *Analytical Chemistry*. **1974**, *46*, 2223-2224.
- (12) Hulanicki, A.; Trojanowicz, M. *Analytica Chimica Acta*. **1976**, *87*, 411-417.
- (13) Vazquez, M.; Danielsson, P.; Bobacka, J.; Lewenstam, A.; Ivaska, A. *Sensors and Actuators B-Chemical*. **2004**, *97*, 182-189.
- (14) Bobacka, J.; Lewenstam, A.; Ivaska, A. *Journal of Electroanalytical Chemistry*. **2001**, *509*, 27-30.
- (15) Heng, L. Y.; Hall, E. A. H. *Analytica Chimica Acta*. **2000**, *403*, 77-89.
- (16) Furtado, C. A.; Kim, U. J.; Gutierrez, H. R.; Pan, L.; Dickey, E. C.; Eklund, P. C. *Journal of the American Chemical Society*. **2004**, *126*, 6095-6105.
- (17) Bobacka, J.; Lewenstam, A.; Ivaska, A. *Journal of Electroanalytical Chemistry*. **2000**, *489*, 17-27.
- (18) Bobacka, J. *Analytical Chemistry*. **1999**, *71*, 4932-4937.
- (19) Fibbioli, M.; Morf, W. E.; Badertscher, M.; de Rooij, N. F.; Pretsch, E. *Electroanalysis*. **2000**, *12*, 1286-1292.
- (20) Sun, Y. P.; Fu, K. F.; Lin, Y.; Huang, W. J. *Accounts of Chemical Research*. **2002**, *35*, 1096-1104.
- (21) Bakker, E. *Journal of the Electrochemical Society*. **1996**, *143*, L83-L85.
- (22) Bakker, E.; Pretsch, E.; Buhlmann, P. *Analytical Chemistry*. **2000**, *72*, 1127-1133.
- (23) Bakker, E.; Buhlmann, P.; Pretsch, E. *Talanta*. **2004**, *63*, 3-20.
- (24) Janata, J. *Proceedings of the Ieee*. **2003**, *91*, 864-869.
- (25) Lawrence, N. S.; Deo, R. P.; Wang, J. *Electroanalysis*. **2005**, *17*, 65-72.

4.2.9. Supporting information

Figure 4.1si shows important shifts in the resistance recorded. As expected, the thinner the SWCNT layer, the larger the resistance measured. The network originating from carbon nanotubes synthesized by chemical vapor deposition is approximately two-thirds semiconducting nanotubes and one-third metallic nanotubes. In this situation, the probability of finding a metallic pathway also increases with the thickness of the network.

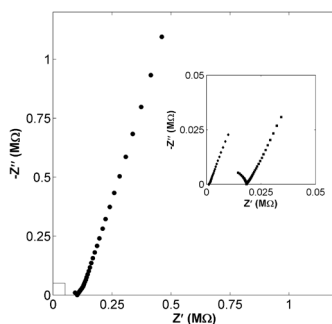


Figure 4.1si - Complex plane impedance plots obtained with the Cu/SWCNTs on PVC support electrode at different thickness of the SWCNT network. (●) 7.5 μm ($R=0.12 \text{ M}\Omega$), (■) 12.5 μm ($R=0.025 \text{ M}\Omega$) and (◆) 25 μm ($R=0.001 \text{ M}\Omega$).

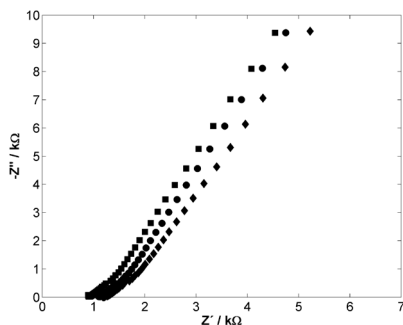


Figure 4.2si - Complex plane impedance plots of the Cu/SWCNTs on PVC support electrode in KCl 0.1 M with different electrical contacts (●) Copper; (■) Platinum; (◆) Glassy carbon. $E_{dc} = 0.2 \text{ V}$. Frequency range = 100 kHz-10 mHz, Amplitude = 10 mV. Thickness of the SWCNT layer = 25 μm .

These results indicate that this contact resistance is a minor component of the overall resistance recorded.

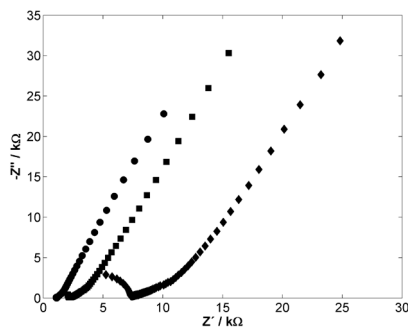


Figure 4.3si - Complex plane impedance plots obtained with the Cu/SWCNTs on PVC support electrode at different concentrations of supporting electrolyte (KCl): (●) 0.1 M ; (■) 0.01 M ; (◆) 0.001 M. $E_{dc} = 0.2$ V, Frequency range = 100 kHz-10 mHz, Amplitude = 10 mV. SWCNT layer thickness = 25 μm .

As shown in **Figure 4.3si**, the intersection with the real impedance axis at high frequencies shifts when the electrolyte concentration is changed. According to the estimated values, the overall resistance is therefore determined mainly by the ohmic resistance of the SWCNT network together with much lower values of the solution resistance.

UNIVERSITAT ROVIRA I VIRGILI

SOLID CONTACT ION SELECTIVE ELECTRODES BASED ON CARBON NANOTUBES

Gastón Adrián Crespo Paravano

ISBN:978-84-693-6428-4/DL:T-1630-2010

UNIVERSITAT ROVIRA I VIRGILI

SOLID CONTACT ION SELECTIVE ELECTRODES BASED ON CARBON NANOTUBES

Gastón Adrián Crespo Paravano

ISBN:978-84-693-6428-4/DL:T-1630-2010



**CHAPTER 5
TRANSDUCTION
MECHANISM
OF CARBON
NANOTUBES**

UNIVERSITAT ROVIRA I VIRGILI

SOLID CONTACT ION SELECTIVE ELECTRODES BASED ON CARBON NANOTUBES

Gastón Adrián Crespo Paravano

ISBN:978-84-693-6428-4/DL:T-1630-2010

5.1. Introduction

The main aim of this chapter is to show the transduction mechanism of carbon nanotubes in solid contact electrodes. The proposed mechanism was supported by the use of electrochemical impedance spectroscopy. In the same way, the non-faradaic process, involved in carbon nanotubes, is compared to the characteristic faradaic process exhibited in conducting polymers.

5.2. “Transduction mechanism of carbon nanotubes in solid contact ISE”

Analytical Chemistry. 2009, *81*, 676-681

Gastón A. Crespo,[†] Santiago Macho,[†] Johan Bobacka^{**} and F. Xavier Rius^{**}

[†]Department of Analytical and Organic Chemistry, Rovira i Virgili University,
43007Tarragona, Spain.

^{**}Chemistry Centre, Laboratory of Analytical Chemistry, Åbo Akademi University,
FIN-20500 Åbo-Turku, Finland

5.2.1 Abstract

Porous carbon materials and carbon nanotubes were recently used as solid-contacts in ion-selective electrodes and the signal transduction mechanism of these carbon-based materials are therefore of great interest. In this work the ion-to-electron transduction mechanism of carbon nanotubes are studied by using electrochemical impedance spectroscopy (EIS) and cyclic voltammetry (CV). Single-walled carbon nanotubes (SWCNT) are deposited on glassy carbon (GC) disk electrodes by repetitive spraying, resulting in SWCNT layers with thicknesses of 10, 35 and 50 μm .

The impedance spectra of these GC/SWCNT electrodes in contact with aqueous electrolyte solution show a very small resistance and a large bulk capacitance that is related to a large effective double layer at the SWCNT/electrolyte interface. Interestingly, the impedance response of GC/SWCNT is very similar to that of poly(3,4-ethylenedioxythiophene) (PEDOT) film electrodes studied earlier under the same experimental conditions. The same equivalent circuit is valid for both types of materials.

The reason is that both materials can be described schematically as an asymmetric capacitor where one side is formed by electronic charge (electrons/holes) in the SWCNT wall or along the conjugated polymer chain of PEDOT and the other side is formed by ions (anions/cations) in the solution (or in the ion-selective membrane when used as solid-contact in ISEs).

5.2.2. Keywords

Single-wall carbon nanotubes; ion-to-electron transduction; impedance; equivalent circuit.

5.2.3. Introduction

The new generation of ion-selective electrodes with internal solid-contact (SC-ISE) have attracted much attention in the last decade due to their important advantages over conventional ion selective electrodes with internal solution ^{1,2}. In the last years different research teams have focused their investigations on different materials that are able to convert effectively the ionic signal through the ion-selective membrane into an electronic signal ³.

Among these solid-contact materials, electroactive conducting polymers have been the most commonly used due to their ability to generate a high redox capacitance that confers a high stability to the recorded signal ⁴⁻⁷. The transduction mechanism of the conducting polymer poly(3,4-ethylenedioxythiophene) (PEDOT) was thoroughly studied by different electrochemical techniques, including electrochemical impedance spectroscopy (EIS) ^{5,8}.

Although, the advantages of conducting polymers with respect to other transducing materials are apparent, they may also display some drawbacks depending on the type of conducting polymer used ⁹. Under certain conditions conducting polymers may show chemical instability, undergo redox side-reactions with O₂ or respond to changes in pH that can be induced by CO₂ ^{9,10}. The possible formation of a water layer at the interface between the conducting polymer and the polymeric ion-selective membrane has also become an issue of concern ¹¹.

Nanostructured materials such as three-dimensionally ordered macroporous (3DOM) carbon ¹² and single-walled carbon nanotubes (SWCNT) ¹³ have appeared very recently as ion-to-electron transducers in SC-ISEs. SC-ISEs based on 3DOM as transducer were found to show excellent long-term potential stability and insensitivity to O₂ and light ¹². Furthermore, these carbon-based materials did not show any evidence of the formation of a water layer between the ion-selective membrane and the transducer ^{12,13}. Other performance parameters were comparable to the rest of the SC-ISEs ¹⁴. The nanostructured characteristics of these materials that are associated to their high surface to volume ratio, together with the inert character of the carbon structures, seem to be the intrinsic reasons for their outstanding transducing properties.

Specifically, SWCNT display some distinctive characteristics. They have been extensively studied from the theoretical point of view and their electronic characteristics well reported. All the atoms in SWCNT are located at the surface, therefore, the current flows at the surface and small variations of the local chemical environment can be detected. For this reason, SWCNT are also a suitable material for ultra small sensors. From the practical point of view, carbon nanotubes are easy to handle. Several procedures have been reported to clean them from impurities (for

instance, catalyst nanoparticles and amorphous carbon) and SWCNT can easily deposited on different surfaces by spraying or drop-casting. Moreover, the spaghetti like structure of the network of SWCNT can be deposited in a reproducible way and allows an easy interconnection among the nanotubes.

Carbon nanotubes also offer some additional characteristics that are relevant from the analytical point of view. These attributes represent an advantage over the electroactive polymers, the commonest material used as transducers up to date. Firstly, carbon nanotubes are very hydrophobic, therefore, it has been observed that practically no water layer is formed at the interface between the polymeric membrane and the network of carbon nanotubes. Secondly, carbon nanotubes do not involve redox reactions. This fact is of capital significance to avoid spurious side-reactions that might interfere in the EMF generated. This property, linked to the absence of a water layer makes the instrumental response of the SWCNT-based electrodes very stable and insensitive to electroactive reagents and finally, SWCNT are not sensitive to light. This offers a manufacturability advantage over several conducting polymers.

Although the high double-layer capacitance resulting from the large interface between the nanomaterial and the ion-selective membrane is the probable reason for the stable signals obtained, the transduction mechanism has not been studied so far. In this work, we study the electrochemical transduction properties of SWCNT by electrochemical impedance spectroscopy (EIS) and cyclic voltammetry (CV). The results are compared with those obtained earlier for poly(3,4-ethylenedioxythiophene) (PEDOT) under the same experimental conditions ⁸.

5.2.4. Experimental section

SWCNT with 95 % purity were obtained from Heji, while the rest of the reagents were analytical grade from Aldrich. All solutions were prepared using deionized water (18 M Ω cm specific resistance), obtained with a Milli-Q PLUS (Millipore Corporation, Bedford, MA). The working electrodes were home made in our laboratory. Glassy carbon (GC) (Sigradur[®]G, Germany) rod (length = 50 mm, diameter = 3 mm) was inserted in a Teflon body (length = 40 mm, outer diameter = 6 mm). The GC surface was polished with alumina of different sizes (25, 1 and 0.03 μ m, Buehler, USA). The resulting active surface was about 0.07 cm². The SWCNT were deposited by spraying an aqueous dispersion containing 10⁻² wt. % of the purified SWCNT ¹⁵ and 1 wt. % of sodium dodecyl sulphate (SDS) onto the polished GC surface, as shown in **Figure 5.1**. Prior to the deposition, the dispersion was homogenized by using a tip-sonicator (amplitude 60 %, cycle 0.5, Ultraschallprocessor UP200S, Dr. Hielscher) for 30 min. The deposition of SWCNT was achieved in successive steps. After spraying the dispersion of nanotubes for 2 seconds, the layer of SWCNT was dried, thoroughly washed with water and dried again. The process was repeated a certain number of times in different sets of electrodes obtaining electrodes with different layer thicknesses. The thickness was measured by ESEM (FEI Company, Inc.) and a mechanical profilometer yielding values of 10, 35 and 50 μ m, respectively.

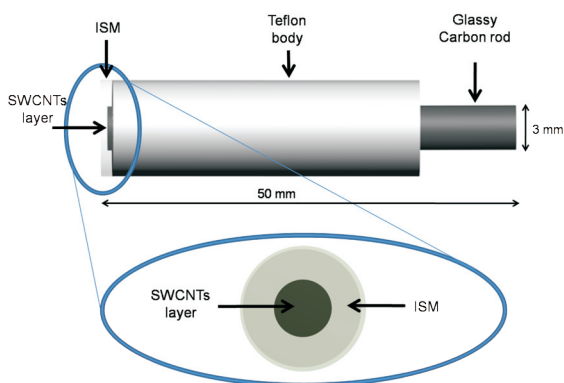


Figure 5.1 - Scheme of the solid-contact electrode with a layer of SWCNT.

Electrochemical measurements were performed by using a one-compartment, three electrodes electrochemical cell. The working electrode was GC/SWCNT (area 0.07 cm²) and the auxiliary electrode was a glassy carbon rod. The reference electrode was a Ag/AgCl/KCl (3 M) single junction electrode (Model 6.0733.100, Metrohm, Switzerland). All dc potentials (E_{dc}) are referred to this reference electrode. In some cases the cell solution was purged with argon or oxygen depending on the experiment and all measurements were performed at room temperature (23 ± 2 °C). All electrochemical measurements were made using an Autolab general purpose electrochemical system and Autolab frequency response analyzer system (AUT20.FRA2-AUTOLAB, Eco Chemie, B.V., The Netherlands).

The cyclic voltammograms (CV) were recorded in 0.1 M KCl solution. Three cycles in the potential range -0.5 V to 0.5 V at a scan rate of 0.1 V/s were performed in each case. The GC/SWCNT electrodes, immersed in aqueous KCl, NaCl or NaClO₄ solutions, were studied by electrochemical impedance spectroscopy (EIS) at E_{dc} in the range -0.2 to 0.2 V. The GC/SWCNT electrodes were equilibrated for at least 2 min at each E_{dc} before EIS was performed. The impedance spectra were recorded in a frequency range (100 kHz–10 mHz) wide enough to cover the processes of interest, by using a sinusoidal excitation signal (single sine) with an excitation amplitude (ΔE_{ac}) of 10 mV. The impedance spectra were then fitted to an equivalent electrical circuit by using the Autolab impedance analysis software.

5.2.5. Results and discussion

5.2.5.1. Characterization by cyclic voltammetry

Cyclic voltammograms in 0.1 M KCl solution were recorded with electrodes which have different thicknesses of the SWCNT layer as shown in **Figure 5.2**.

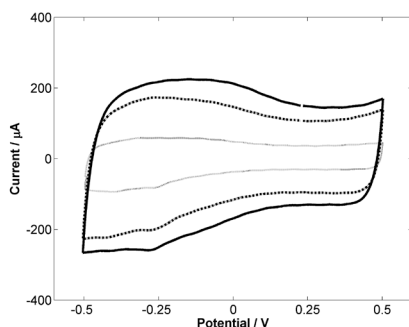


Figure 5.2 - Cyclic voltammograms for GC/SWCNT electrodes in 0.1 M KCl at different transducing layer thicknesses: 10 μm (tight dotted line), 35 μm (dashed line) and 50 μm (thick solid line). Potential scan rate = 0.1 V s^{-1} .

The general shapes of the cyclic voltammograms are similar in all cases. There are two regions that can be easily distinguished. One of them is related to the redox process (from -0.5 V to 0.1 V) and another is related to the capacitive process (from 0.1 V to 0.4 V). A reduction peak can be seen around -0.25 V that can be attributed to oxygen reduction at the SWCNT surface. The thicker the SWCNT layer, the higher the current recorded for each electrode.

The influence of O_2 on the cyclic voltammogram is shown in **Figure 5.3A** and **Figure 5.3B** where the measurements were obtained in the presence and absence of oxygen for SWCNT electrode and GC rod respectively. The oxygen reduction occurs in both electrodes and the reduction peak decreases when a stream of argon was bubbled into the solution. The oxygen reduction at CNT starts at a slightly more positive potential than for GC bare. Consequently, SWCNT displays a small catalytic effect on the reduction of oxygen.

On the other hand, the presence of oxygen does not modify substantially the current values in the range where the capacitive processes occur (from 0.1 V to 0.4 V). The majority of electrochemical impedance measurements were recorded in this potential range, including measurements under open circuit conditions.

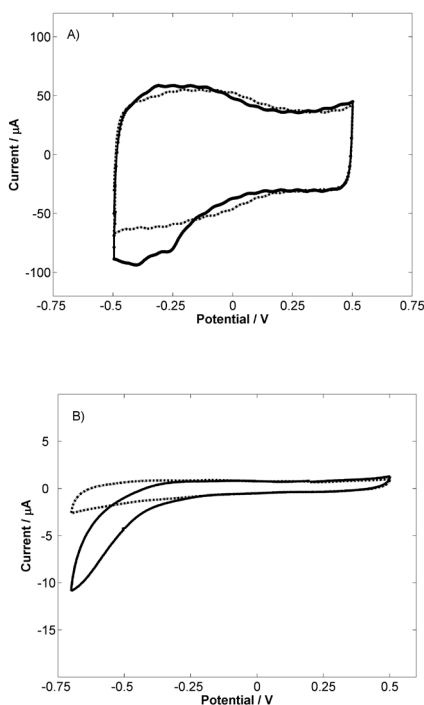


Figure 5.3 - (A) Cyclic voltammograms for SWCNT electrodes in 0.1 M KCl in presence of oxygen (thick solid line) and in the absence of oxygen (dotted line). SWCNT layer thickness = 10 μm . (B) Cyclic voltammogram of a bare GC rod in 0.1 M KCl in presence of oxygen (thin solid line) and in the absence of oxygen (dotted line). Potential scan rate = 0.1 V s^{-1} .

5.2.5.2. Characterization by electrochemical impedance spectroscopy

Typical impedance spectra (complex plane impedance plots) of the GC/SWCNT electrode in 0.1, 0.05 and 0.01 M KCl are shown in **Figure 5.4**. The impedance spectra are dominated by a 90° capacitive line, which extends down to low frequencies (0.3 Hz). At high frequencies, only a slight deviation from the capacitive line can be seen, indicating fast charge transfer at the GC/SWCNT and SWCNT/solution interfaces as well as fast charge transport in the SWCNT layer. As shown in **Figure 5.4**, the high frequency intersection with the Z' axis depends strongly on the electrolyte concentration and is consequently determined mainly by the solution resistance and not by the ohmic resistance of the SWCNT film. Impedance plots of GC/SWCNT electrodes recorded in 0.1 M NaCl and 0.1 M NaClO₄ solutions showed the same general shape as the impedance plot of the GC/SWCNT electrode in 0.1 M KCl.

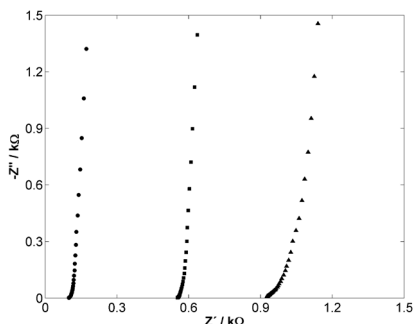


Figure 5.4 - Impedance plots of the GC/SWCNT electrode at different concentrations of supporting electrolyte (KCl): (●) 0.1 M; (■) 0.05 M; (▲) 0.01 M. SWCNT layer thickness = 10 μm . Frequency range = 0.3 Hz – 10 kHz. $E_{\text{dc}} = 0.2 \text{ V}$. $\Delta E_{\text{ac}} = 10 \text{ mV}$.

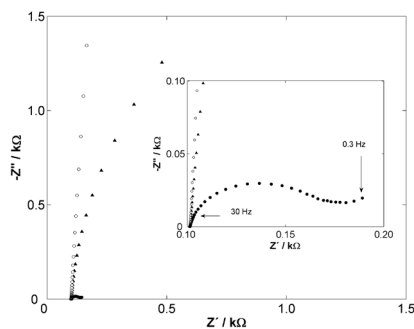


Figure 5.5 - Influence of E_{dc} on impedance plots of the GC/SWCNT electrode in 0.1 M KCl solution: (○) 0.2 V; (▲) 0 V; (■) -0.2 V. SWCNT layer thickness = 10 μm . Frequency range = 0.3 Hz – 10 kHz. $\Delta E_{\text{ac}} = 10 \text{ mV}$. A magnification of the spectra at high frequency values is represented in the inset.

Figure 5.5 shows impedance spectra recorded at three different dc potentials ($E_{\text{dc}} = -0.2, 0.0$ and 0.2 V) in presence of air. The variations in E_{dc} produce changes in the impedance spectra especially in the range from 30 Hz towards lower frequencies. A semicircle, indicating the presence of a charge-transfer process can be observed at negative potential ($E_{\text{dc}} = -0.2 \text{ V}$). This is in agreement with the reduction peak observed in the cyclic voltammograms. Therefore, the processes that occur at low frequencies are highly dependent on the E_{dc} in presence of oxygen. However, at high frequencies ($> 30 \text{ Hz}$) the impedance spectra is not modified by the applied E_{dc} even in presence of oxygen.

The influence of oxygen on the impedance spectra at open circuit potential was assessed by obtaining the spectra in absence and presence of argon bubbling through the solution (**Figure 5.6**). Both spectra shown in **Figure 5.6** have practically the same shape in the measured frequen-

cy range, showing that the presence of oxygen does not influence the signal obtained at open circuit potential. This is in accordance with the voltammograms shown in **Figure 5.3**. The discussion below is focused on the impedance response in the E_{dc} range where the oxygen-dependent redox process is not observed.

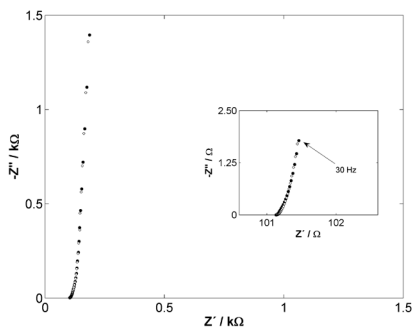


Figure 5.6 - Impedance plot of GC/SWCNT recorded at $E_{dc} = 0.2$ V in: (○) the absence of oxygen, (●) the presence of oxygen. SWCNT layer thickness = $10 \mu\text{m}$. Frequency range = 0.3 Hz – 10 kHz. $\Delta E_{dc} = 10$ mV.

It should be mentioned that there is a striking similarity between the impedance spectra of the GC/SWCNT films studied in this work and Pt/PEDOT films studied earlier under the same experimental conditions⁸. Both SWCNT and PEDOT show apparently similar capacitive behavior and very low overall resistance.

5.2.5.3. Equivalent circuit

Several equivalent electrical circuits were initially tested by non-linear least squares fitting of the experimental data. The best equivalent circuit is shown in **Figure 5.7**. The same equivalent circuit was successfully used earlier to describe the impedance spectra of Pt/PEDOT electrodes in aqueous solutions⁸. This equivalent circuit gives excellent fits from 0.3 Hz to 10 kHz. At low frequency, the vertical line that appears (**Figure 5.4–5.6**) corresponds to the low frequency bulk capacitance of the SWCNT film. The average error (χ^2) of the fits for 100 different impedance spectra of SWCNT films with different thicknesses and supporting electrolytes was around 10^{-4} . The equivalent circuit is composed of the solution resistance (R_s), the capacitance (C_d) and the ‘classical’ finite-length Warburg diffusion element (Z_D), all connected in series:

$$Z = R_s + j(\omega C_d)^{-1} + Z_D \quad (5.1)$$

The Z_D element is characterized by the diffusional time constant (τ_D), the diffusional pseudocapacitance (C_D) and the diffusion resistance ($R_D = \tau_D/C_D$), as described by¹⁶:

$$Z_D = (\tau_D/C_D) \coth(j\omega\tau_D)^{0.5}/(j\omega\tau_D)^{0.5} \quad (5.2)$$

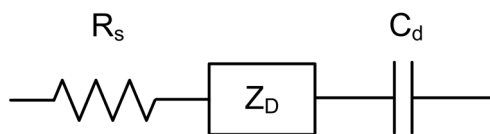


Figure 5.7 - Equivalent circuit. R_s = solution resistance, C_d = bulk capacitance, Z_D = finite-length Warburg diffusion element.

The mathematical expressions (5.1) and (5.2) explain correctly the form of the impedance spectra recorded. At the same time, each element of the expression can be assigned to a different part of the impedance plot. The impedance response of Z_D is equivalent to that of a finite-length open transmission line where the finite diffusion length causes the phase angle to shift from 45 to 90°¹⁶. The capacitance component C_d is necessary in the model to account for the deviation from an ideal 45° diffusion line at high and intermediate frequencies and it improves the quality of the fit significantly. From the point of view of the processes that occur in the electrode, each element of the equivalent circuit can be assigned to its corresponding event as well. The solution resistance (R_s) is related to the mobilities of the ions that are present in the solution. Both capacitance components C_d and C_D are related to the bulk capacitance, although the first one can be assigned to an electronic capacitance that would describe the interaction or transduction between the ions of the solution and the electrons of the SWCNT, while C_D is related to an ionic pseudocapacitance associated to the transport and diffusion of the ions from the solution into the SWCNT layer including diffusion in electrolyte-filled pores in the SWCNT layer.

5.2.5.4. Resistance

The value of the solution resistance R_s , obtained after the fitting process, is inversely proportional to the concentration of the supporting electrolyte, as could be expected (Table 5.1). R_s is independent of the thickness of the SWCNT film (Table 5.2). Experiments undertaken at the same experimental conditions but in different supporting electrolyte resulted in the following values for R_s : 101±3 Ω (0.1M KCl), 141±3 Ω (0.1M NaCl) and 151±4 Ω (0.1M NaClO₄), which correlate with the mobilities of the different ions. From the R_s values obtained at different thickness of the SWCNT layer, we cannot find any possible contribution from the ohmic resistance of the SWCNT film to R_s and therefore this resistance seems to be dominated by the resistance of the electrolyte solution.

[KCl]/M	R_s/Ω	τ_D/s	C_D / mF	R_D/Ω^a	$C_d/\mu\text{F}$
0.1	101	0.29	3.27	90	449
0.05	561	0.41	2.61	301	451
0.01	928	1.16	1.99	581	455

Table 5.1 - EIS results for the GC/SWCNT electrode (thickness = 10 μm) obtained by fitting the experimental data to the equivalent circuit shown in Figure 5.7 (Edc = 0.2 V). ^a $R_D = \tau_D / C_D$

Electrolyte / 0.1M	Thickness (μm)	R_s / Ω
KCl	10	101 \pm 3
KCl	35	102 \pm 4
KCl	50	99 \pm 2

Table 5.2 - EIS results for the GC/SWCNT electrode with different thicknesses obtained by fitting the experimental data to the model in **Figure 5.7** ($E_{dc} = 0.2 \text{ V}$).

The diffusional resistance (R_D) was found to be inversely proportional to the concentration of supporting electrolyte as well. The influence of the SWCNT thickness on R_D is shown in **Table 5.3**, where it can be seen that the resistance decreases when the thickness is increased using KCl as supporting electrolyte. However, when using the two other electrolytes (NaCl and NaClO_4) minimum values can be observed for the intermediate thickness of the SWCNT layer (35 μm). The trends are not so clear, but R_D seems to depend more on the cation than the anion.

Electrolyte / 0.1M	Thickness (μm)	τ_D / s	C_D / mF	R_D / Ω
KCl	10	0.29	3.27	90
KCl	35	0.31	1.97	77
KCl	50	0.26	3.04	71
NaCl	10	0.15	2.14	143
NaCl	35	0.20	1.82	113
NaCl	50	0.21	1.92	147
NaClO_4	10	0.22	2.20	115
NaClO_4	35	0.28	1.95	108
NaClO_4	50	0.34	2.03	169

Table 5.3 - Diffusional time constant (τ_D), diffusional pseudocapacitance (C_D) and diffusional resistance ($R_D = \tau_D / C_D$) for GC/SWCNT electrodes of different thickness in 0.1 M KCl, NaCl and NaClO_4 as supporting electrolyte. Data obtained by fitting experimental EIS data to the model in **Figure 5.7** ($E_{dc} = 0.2 \text{ V}$).

5.2.5.5. Capacitance

The electronic capacitance (C_d) increases with increasing thickness of the SWCNT film, independently of the electrolyte used in the solution, as shown in **Table 5.4**. Furthermore, these values are quite independent of the concentration of the supporting electrolyte (KCl), as shown in **Table 1**. These results allow inferring that C_d is related to the bulk properties of the SWCNT film. When comparing the magnitude of C_d of SWCNT and PEDOT of a given film thickness it can be concluded that the bulk charge density is about an order of magnitude lower for the SWCNT films used in this work than for electrosynthesized PEDOT ⁸.

In contrast to C_d , the diffusional pseudocapacitance (C_p) was found to increase with increasing concentration of the supporting electrolyte (Table 5.1) but C_p is only slightly influenced by the thickness of the film. The value of C_p is around one order of magnitude larger than C_d for the same film thickness. Therefore, C_p can be related to ion diffusion in electrolyte-filled pores in the SWCNT layer.

Electrolyte / 0.1M	Thickness (μm)	$C_d/\mu\text{F}$
KCl	10	449
KCl	35	2180
KCl	50	2964
NaCl	10	473
NaCl	35	2354
NaCl	50	4787
NaClO ₄	10	465
NaClO ₄	35	2245
NaClO ₄	50	4071

Table 5.4 - Capacitance of GC/SWCNT electrodes of different thicknesses in 0.1 M KCl, NaCl and NaClO₄ as supporting electrolyte obtained by fitting experimental EIS data ($E_{dc} = 0.2$ V) to the model in Figure 5.7.

5.2.5.6. Diffusion

The diffusional time constant (τ_D) is related to the diffusion coefficient (D) and the diffusion length (L) as follows: $\tau_D = L^2/D$ (5.3)

According to Eq. (5.3), τ_D should be proportional to L^2 if D is constant. Assuming a uniform film growth and film morphology, τ_D is therefore expected to be proportional to the square of the thickness of SWCNT. However, the EIS results (Table 5.1) show that τ_D is directly proportional (for NaClO₄ electrolyte) or even independent of the layer thickness of SWCNT (for KCl and NaCl electrolytes). This indicates that the diffusion length is not determined by the film thickness, as can be expected if the film is porous and contains a significant amount of supporting electrolyte. This is supported by the strong dependence of R_D and τ_D on the supporting electrolyte concentration (Table 5.1). Similar behavior was observed for PEDOT⁸. This electrochemical behavior of SWCNT could be explained by the spaghetti-like morphology of the carbon nanotube layer, resulting in a porous film.

5.2.5.7. Physical transduction mechanism

The physical transduction mechanism of the carbon nanotubes in solid-contact potentiometric electrodes has yet to be studied in detail. However, the comparison between the behavior of carbon nanotubes in ISE and in FET could provide some clues.

In CNTFET, the carbon nanotubes are located on the surface of the supporting substrate¹⁷. Therefore, they are in direct contact with the environment, similar to our configuration in ISE where our 'environment' is either the electrolyte solution or the ion-selective membrane. Moreover, CNTFET perform detection in a capacitive way, similar to the model established in CNT based ISE.

The sensing capacity of carbon nanotubes relies on the extreme sensitivity of the nanotube electrical properties to changes in local chemical environments. It has been reported that the solid-state gate of the CNTFET can be replaced by nearby molecules that modulate the carbon nanotube conductance^{18,19}. Therefore, although other effects may also be present (such as carrier mobility changes or Schottki barrier effects), electrostatic gating has been reported as the dominant and most reproducible mechanism²⁰. Electrostatic gating can be explained by the electronic characteristics of the nanotubes, which determines the sensitivity of the conductance on the surface charge²¹.

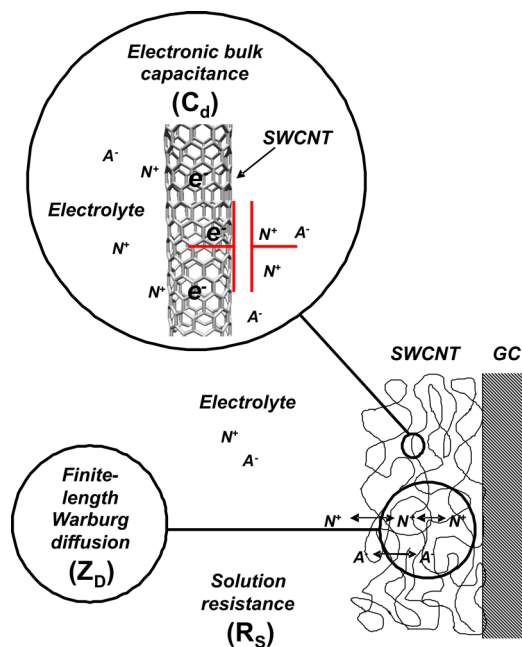


Figure 5.8 - Schematic description of the ion-to-electron transduction process of the GC/SWCNT/electrolyte system (corresponding to the equivalent circuit shown in **Figure 5.7**). N^+ = cation, A^- = anion, e^- = electron. Within the electronic bulk capacitance, it is depicted the asymmetric capacitor established between the SWCNT wall and the solution (that would be replaced by the ion-selective membrane in a solid-contact ISE).

Therefore, we could think of a mechanism in ISEs related to the one described by electrostatic gating: the presence of charged ions in the solution (in absence of polymeric membrane) or the ion-selective membrane, in close contact to the carbon nanotubes, could also modulate the carbon nanotube charge. In this way, the ion-to-electron transduction is possible when the charge of the CNT (electrons /holes in CNT) is modulated by an applied potential in presence of charge-compensating ions. The processes of charging/discharging would provide the capacitive coupling in CNT.

The transduction process that takes place at the GC/SWCNT/electrolyte system, considered in the equivalent circuit (Figure 5.7), is depicted schematically in Figure 5.8. At sufficiently low frequencies diffusion is not rate-limiting, and Figure 5.8 can be simplified to the electronic bulk capacitance section (in series with the solution resistance). In potentiometry we are measuring the potential at equilibrium (steady state), so we are in the region of very low (zero) frequency where the electronic bulk capacitance section is valid (if there are no parasitic side reactions).

5.2.6 Conclusions

The results obtained in this work show that the electrochemical properties of spray-deposited SWCNT films are strikingly similar to those of electrosynthesized PEDOT⁸. Both materials show very small resistance and a large bulk capacitance. In the case of SWCNT the origin of the bulk capacitance is expected to be the large double layer capacitance while in the case of PEDOT it is expected to be due to the faradaic process (redox capacitance) involving reversible oxidation (doping) of the conjugated polymer chains with simultaneous insertion/expulsion of charge-compensating ions. It can thus be postulated that in the case of fast ion and electron transfer and transport processes, both type of mechanisms give rise to similar capacitive behavior. Our results show that non-Faradaic (SWCNT) double-layer charging of a porous electrode (SWCNT) can give a very similar impedance response as Faradaic redox charging of an electroactive polymer film (PEDOT). Both materials can be described schematically as an asymmetric capacitor where one side is formed by electrons (holes) in the carbon nanotube wall or along the conjugated polymer chain and the other side is formed by cations (anions) in the solution (or in the ion-selective membrane when used as solid-contact in ISEs), as shown schematically in Figure 5.8.

Although the underlying mechanism in electroactive polymers and SWCNT is different, both types of materials can work as ion-to-electron transducers in SC-ISEs.

5.2.7. Acknowledgments

We thank the Spanish Ministry of Education and Science, MEC, for supporting the work through the project grants NAN2004-09306-C05-05 and CTQ2007-67570. GAC also acknowledges MEC for the doctoral fellowship AP2006-04171.

5.2.8 References

- (1) Bakker, E.; Pretsch, E. *Angewandte Chemie-International Edition*. **2007**, *46*, 5660-5668.
- (2) Pretsch, E. *Trac-Trends in Analytical Chemistry*. **2007**, *26*, 46-51.
- (3) Bobacka, J.; Ivaska, A.; Lewenstam, A. *Chemical Reviews*. **2008**, *108*, 329-351.
- (4) Cadogan, A.; Gao, Z. Q.; Lewenstam, A.; Ivaska, A.; Diamond, D. *Analytical Chemistry*. **1992**, *64*, 2496-2501.
- (5) Bobacka, J. *Analytical Chemistry*. **1999**, *71*, 4932-4937.
- (6) Michalska, A. *Analytical and Bioanalytical Chemistry*. **2006**, *384*, 391-406.
- (7) Bobacka, J. *Electroanalysis*. **2006**, *18*, 7-18.
- (8) Bobacka, J.; Lewenstam, A.; Ivaska, A. *Journal of Electroanalytical Chemistry*. **2000**, *489*, 17-27.
- (9) Vazquez, M.; Bobacka, J.; Ivaska, A.; Lewenstam, A. *Sensors and Actuators B-Chemical*. **2002**, *82*, 7-13.
- (10) Maksymiuk, K. *Electroanalysis*. **2006**, *18*, 1537-1551.
- (11) Sutter, J.; Pretsch, E. *Electroanalysis*. **2006**, *18*, 19-25.
- (12) Lai, C. Z.; Fierke, M. A.; Stein, A.; Buhlmann, P. *Anal. Chem*. **2007**, *79*, 4621-4626.
- (13) Crespo, G. A.; Macho, S.; Rius, F. X. *Analytical Chemistry*. **2008**, *80*, 1316-1322.
- (14) Lai, C. Z.; Joyer, M. M.; Fierke, M. A.; Petkovich, N. D.; Stein, A.; Buhlmann, P. *Journal of Solid State Electrochemistry*. **2009**, *13*, 123-128.
- (15) Furtado, C. A.; Kim, U. J.; Gutierrez, H. R.; Pan, L.; Dickey, E. C.; Eklund, P. C. *Journal of the American Chemical Society*. **2004**, *126*, 6095-6105.
- (16) MacDonald, J. R. *Impedance Spectroscopy*; Wiley, New York, 1987.
- (17) Gruner, G. *Analytical and Bioanalytical Chemistry*. **2006**, *384*, 322-335.
- (18) Kong, J.; Franklin, N. R.; Zhou, C. W.; Chapline, M. G.; Peng, S.; Cho, K. J.; Dai, H. J. *Science*. **2000**, *287*, 622-625.
- (19) Collins, P. G.; Bradley, K.; Ishigami, M.; Zettl, A. *Science*. **2000**, *287*, 1801-1804.
- (20) Heller, I.; Janssens, A. M.; Mannik, J.; Minot, E. D.; Lemay, S. G.; Dekker, C. *Nano Letters*. **2008**, *8*, 591-595.
- (21) Artyukhin, A. B.; Stadermann, M.; Friddle, R. W.; Stroeve, P.; Bakajin, O.; Noy, A. *Nano Letters*. **2006**, *6*, 2080-2085.

UNIVERSITAT ROVIRA I VIRGILI

SOLID CONTACT ION SELECTIVE ELECTRODES BASED ON CARBON NANOTUBES

Gastón Adrián Crespo Paravano

ISBN:978-84-693-6428-4/DL:T-1630-2010

UNIVERSITAT ROVIRA I VIRGILI

SOLID CONTACT ION SELECTIVE ELECTRODES BASED ON CARBON NANOTUBES

Gastón Adrián Crespo Paravano

ISBN:978-84-693-6428-4/DL:T-1630-2010



CHAPTER 6 APPLICATIONS

UNIVERSITAT ROVIRA I VIRGILI

SOLID CONTACT ION SELECTIVE ELECTRODES BASED ON CARBON NANOTUBES

Gastón Adrián Crespo Paravano

ISBN:978-84-693-6428-4/DL:T-1630-2010

6.1. Introduction

In the last two chapters, we have elucidated the transducing mechanism of the single wall carbon nanotubes in solid contact ion selective electrodes. The large capacitance generated in the interface between the membrane and the SWCNTs layer and the high contact surface shown by SWCNTs enable it to be used as transducer in SC-ISEs.

As previously mentioned in the introduction of the **Chapter 2**, SWCNTs display either semiconducting or metallic properties. In contrast, the MWCNTs show a strong metallic behavior. In Field Effect Transistors (FETs) the conducting properties of the CNTs play a considerable role in the transduction signal. Taking this evidence into account, the influence of the conducting character of the CNTs on the transducer capacity is evaluated in this chapter.

In a similar way, the functionalization of the CNTs with carboxylic groups provides CNTs with interesting operational characteristics, such as solubility in different media and reactivity towards further functionalization. However, the effect of this functionalization on the transducing capabilities of the potentiometric signal has not been considered so far. Therefore, the performance of both non-carboxylated SWCNTs and MWCNTs and low-carboxylated SWCNTs and MWCNTs is tested in SC-ISE. Section 6.2 and 6.3 show the electrochemical characterization and potentiometric behaviour of two SC-ISEs based on non-carboxylated CNTs. A selective membrane to proton and non-carboxylated SWCNTs were used in section 6.2, whereas a selective membrane to Choline (and derivates) and non-carboxylated SWCNTs were employed in section 6.3. In this latter section, we tested a new synthetic ionophore to determine choline. Octaamide cavitand is a selective supramolecular receptor to choline developed by Ballester's group. Therefore, a solid contact ion-selective electrode for choline and derivates is reported in 6.3.

Sections 6.4 and 6.5 shown some preliminary results related to applications of the SC-ISEs based on CNTs in actual settings. Although these studies are at the beginning stage at the moment, we considered to include them here to show the versatility and future possibilities of SC-ISEs based on CNTs. Our interest is to show the applicability of the SC-ISEs in very different fields so as to expand the use of this new analytical tool.

In section 6.4 prototypes of solid contact electrodes, adapted to support high pressures, these were tested up to 21 bar. Although, Ca^{+2} and pH electrodes were tested in the laboratory, only proton SC-ISEs were dipped in the lake and potentiometric measurements were recorded as a function of the depth of the aquatic column. Moreover, the influence the sunlight on the potentiometric signal transduced by two types of solid materials (POT and CNTs) is compared.

On-line monitoring of chemical processes has always been an interesting and complicated challenge. For this reason, in section 6.5, SC-ISEs based on CNTs are assayed in a preliminary way

to monitor a catalytic denitrification process. This process is useful to regenerate underground water samples containing high levels of nitrate. As a consequence, the performance analytical parameters of each sensor are evaluated both in batch and on-line modes. After these initial trials, the sensing system should be thoroughly tested and validated and applied to real underground water samples.

6.2. “Solid contact pH-selective electrode using multi-walled carbon nanotubes”

Analytical Bioanalytical Chemistry. 2009, 395, 2371-2376

Gastón A. Crespo, Derese Guga, Santiago Macho and F. Xavier Rius*

*Department of Analytical and Organic Chemistry, Rovira i Virgili University, 43007 Tarragona, Spain.

6.2.1. Abstract

Multi-walled carbon nanotubes (MWCNT) are shown to be efficient transducers of the ionic-to-electronic current. This enables the development of a new solid-contact pH selective electrode that is based on the deposition of a 35 μm thick layer of MWCNT between the acrylic ion selective membrane and the glassy carbon rod used as the electrical conductor. The ion-selective membrane was prepared by incorporating tridodecylamine as the ionophore, potassium tetrakis[3,5-bis(trifluoromethyl)phenyl]borate as the lipophilic additive in a polymerized methylmethacrylate and an n-butyl acrylate matrix. The potentiometric response shows Nernstian behaviour and a linear dynamic range between 2.89 and 9.90 pH values. The response time for this electrode was less than 10 s throughout the whole working range. The electrode shows a high selectivity towards interfering ions. Electrochemical impedance spectroscopy and chronopotentiometry techniques were used to characterise the electrochemical behaviour and the stability of the carbon nanotube-based ISE.

6.2.2. Keywords

Potentiometric ion-selective electrodes, solid-state sensors, pH, multi-walled carbon nanotubes.

6.2.3. Introduction

The expansion of “modern potentiometry” in recent years can be attributed mainly to the development of solid-contact ion-selective electrodes (SC-ISE), the synthesis of new ion selective membranes and ionophores and the attainment of very low detection limits along with significant selectivity coefficients [1]. Together, these developments have led to the technique being adopted in new analytical applications in many interesting fields [2]. The main advantages of potentiometry are its excellent performance parameters [3] and its simplicity which make this technique comparable, and in some cases better, than other analytical techniques that are more expensive or that require time-consuming preprocessing steps.

In particular, instrumental pH measurements are usually recorded with potentiometric electrodes. The standard pH glass electrode is the most popular sensor because of its high selectivity, reliability and wide dynamic pH range. However, pH-glass electrodes have several limitations, most notably their fragility [4]. Moreover we should also consider the drawbacks resulting from the presence of the internal reference solution. With this configuration the measurements always should always be performed in vertical position and some factors such as high pressure, temperature and small sample volumes can acquire relevance in some environmental, industrial and medical applications [5].

As it is well known, solid-contact electrodes display the inherent advantage with respect to classical electrodes of having removed the internal solution. In this sense, the conducting polymers family of solid transducers has been used from several years also to develop all-solid-estate pH electrodes showing excellent ion-to-electron transducing ability. However, some negative effects like light sensitivity, secondary undesired reactions and the presence of a water layer between the polymeric membrane and the solid-contact transducing polymer affect considerably the potentiometric signal.

In an attempt to overcome these disadvantages, we report here the development and characterization of the first pH potentiometric solid-contact electrode using a network of non-carboxylated multiwall carbon nanotubes (MWCNTs) as a transducer layer.

Recently, different carbon-based nanostructured materials such as three-dimensional macroporous carbon [6] and fullerenes [7] have been assayed as ion-to-electron transducers. Our group has shown that single wall carbon nanotubes (SWCNTs) can perform as solid-contact ion-to-electron transducers, providing additional advantages over electroactive polymers [8]. The high stability of the potential is due to the material's large double layer capacitance, which in turn is due to its a very large surface to volume ratio [9,10]. Additionally, carbon nanotubes display hydrophobicity, an important feature for preventing water layers forming between the ion-selective membrane and the transducing layer. Moreover, they are insensitive both to light and to species displaying redox behaviour that might induce side reactions.

MWCNTs display structural similarities to SWCNTs, although they are usually much larger in diameter due to the presence of the rolled over concentric graphene layers [11]. In contrast to SWCNT, where the electrical properties depend on their helicity and diameter, MWCNTs are mostly metallic and electronic conduction essentially occurs through the outer shell, although interactions with the inner shells may also influence their electronic properties [12].

In the present paper we report that MWCNTs can also act as effective transducers in solid state electrodes, behaving in a similar way to SWCNTs. Metallic nanotubes also transduce the signal in an efficient way in ISEs, in contrast to the alternative potentiometric sensors, field effect transistors, which need to be semiconducting. To illustrate this, we have developed a solid-state pH electrode using an acrylic ion selective membrane [13] and MWCNT as the solid transducer.

6.2.4. Experimental section

6.2.4.1 Chemicals

Methyl methacrylate (MMA), n-butyl acrylate (nBA), reagent grade benzene, dichloromethane, petroleum ether (80–100°C) and azobisisobutyronitrile initiator (AIBN) were purchased from Fluka. AIBN was recrystallised with warm methanol before use. Lithium acetate dehydrate, potassium, sodium, lithium, ammonium, calcium and magnesium chlorides (all analytical grade) were purchased from Fluka. The hydrogen ion ionophore (tri-n-dodecylamine, TDDA) and the lipophilic additive potassium tetrakis[3,5-bis(trifluoromethyl)-phenyl]borate were purchased from Sigma-Aldrich. Multi-wall nanotubes (MWNTs) with an outer diameter of 10–20 nm, a length of around 50 μm , a surface area of 400 m^2/g and more than 95% purity were obtained from Heji, Inc. All solutions were prepared using deionized water (18.2 $\text{M}\Omega\cdot\text{cm}$ specific resistance) obtained with a Milli-Q PLUS (Millipore Corporation).

Buffers solutions were prepared at constant ionic strength ($I=0.01\text{ M}$) for different pHs, their anion composition being: chloroacetate, $\text{pH}=2.89$; formate, $\text{pH}=4.16$; acetate, $\text{pH}=4.75$; phosphate, $\text{pH}=6.27$ and 7.55 ; borate, $\text{pH}=8.86$; carbonate, $\text{pH}=9.9$; butylamine, $\text{pH}=10.87$ and 11.54 . A universal buffer containing sodium borate, sodium acetate and sodium dihydrogen phosphate was prepared in 1 mM of each component. NaOH or HCl 0.1 M was added to fine-tune the pH of the universal buffer. All of these analytical grade reagents were obtained from Fluka as well.

6.2.4.2. Preparation of methacrylate/acrylate polymers

The procedure for synthesizing the matrix of methyl methacrylate (MMA) and n-butyl acrylate (nBA) was adopted from Heng and Hall [14]. The method uses free radicals to polymerize the solution. This was accomplished by adding 0.40 g of MMA, 5.54 g of nBA and 2.88 mg of AIBN to 3 mL of dry benzene to act as initiators. The MMA-nBA mixture was degassed with nitrogen for 15 minutes before being heated for 12 hours at 80 °C. The MMA-nBA copolymer was then

isolated by precipitation with petroleum ether and purified in the same solvent. The transparent and sticky matrix was dried for two days in vacuum before use and was characterized by RMN H (data not shown) to determine the ratio between each monomer in the final product (MB 1:10).

6.2.4.3. Development of the solid-contact pH ISE

The electrodes were developed in our laboratory. A glassy carbon (GC) rod (Sigradur®G, length 50 mm and diameter 3 mm) provided by HTW GmbH was introduced inside a Teflon body in order to provide both the electrode support and the electrical contact between the ion-selective electrode and the potentiometer (the active surface was around 7 mm²). The electrode was first polished using abrasive paper (Carbimet 600/P1200, Buehler) and subsequently treated using alumina of different grain-size (30, 5 and 1 μm Micropolish II, Buehler). A layer of MWCNTs was deposited by spraying an aqueous dispersion containing 10⁻² % wt. of the non-carboxylated MWCNTs and 1 % wt. of sodium dodecyl sulphate (SDS) onto the GC. Prior to the deposition, the dispersion was homogenized by tip-sonicator for 30 min (amplitude 60 %, cycle 0.5, Ultrascall-prozessor UP200S, Dr. Hielscher, Germany). The deposition was achieved in successive steps. After spraying the dispersion of MWCNTs for 2 seconds, the layer was dried, thoroughly washed with water and dried again. The process was repeated 35 times obtaining a thickness around 35 μm measured by ESEM.

6.2.4.4. Ion selective membrane preparation

The hydrogen ion selective membrane was made of 1.95 % in wt. ionophore (tri-n-dodecylamine, TDDA), 0.58 % in wt. KTpCIPB and 97.47 % in wt. self plasticized MMA-nBA polymeric matrix. 200.06 mg of the ion-selective membrane were dissolved in 2 mL dichloromethane. The mixture was mixed in vortex for 1 hour. Then 150 μL of the membrane cocktail was drop-casted onto the MWCNT layer that had been previously deposited onto the glassy carbon electrode.

The conditioning of the electrodes was fundamental to obtaining reliable and successful results. The electrodes were conditioned in pH=3 for 1 day and then in pH=12 for 2 days [3].

6.2.4.5. Instruments and EMF measurements

All electromotive forces (EMF) were measured at room temperature (23±2 °C) in stirred solutions and using a 16 channel high input impedance voltmeter (EMF16, Lawson's Labs, USA). A double-junction Ag/AgCl/ 3 M KCl reference electrode (type 6.0729.100, Methrom AG) containing a 1 M LiAcO electrolyte bridge was employed. Activity coefficients were calculated using the Debye–Huckel approximation and the potential measurements were corrected by using the Henderson equation to determine the liquid junction potential. The experimental pH values were recorded in parallel with a calibrated-glass pH electrode (pH meter GLP21, Crison).

6.2.4.6. Impedance spectra of MWCNT based hydrogen ion sensor

The measurements were taken under open circuit potential using one-compartment cell with three-electrodes. The working electrode was GC/MWCNT/ISM (area 0.07 cm²) and the auxiliary electrode was a glassy carbon rod. The reference electrode was an Ag | AgCl | KCl (3M) single junction (Model 6.0733.100, Metrohm). All measurements were taken at room temperature (23 ± 2 °C). All electrochemical measurements were made using an Autolab general purpose electrochemical system and an Autolab frequency response analyser system (AUT20.FRA2-AUTOLAB, Eco Chemie, B.V., The Netherlands). The impedance spectra were recorded within the frequency range from 10 kHz to 0.3 Hz and the amplitude for the sinusoidal excitation signal was 10 mV. Autolab impedance analysis software was used to fit the spectra to an equivalent electrical circuit that had previously been reported by our group [9] for electrodes with SWCNTs as the transducer.

6.2.4.7. Chronopotentiometric measurements

A constant current of a 1 nA and 5 nA was applied for 100 s followed by a reversed current of the same magnitude for the same time. The potentials were measured in a solution of pH=4.16 at 23 ± 2 °C. These measurements were recorded with a one-compartment, three-electrode cell in which the electrode under study was the working electrode. The reference electrode was Ag/AgCl/KCl (3 M), and the auxiliary electrode was a glassy carbon rod. All potentials measurements refer to this reference electrode.

GC/SWCNT electrodes were equilibrated for at least 2 min at each E_{dc} before EIS was performed. The impedance spectra were recorded in a frequency range (100 kHz–10 mHz) wide enough to cover the processes of interest, by using a sinusoidal excitation signal (single sine) with an excitation amplitude (ΔE_{ac}) of 10 mV. The impedance spectra were then fitted to an equivalent electrical circuit by using the Autolab impedance analysis software.

6.2.5. Results and discussion

Figure 6.2.1 displays the potentiometric EMF recorded at pH values ranging from 2.89 to 11.54 (while keeping the same ionic strength) using the MWCNTs-ISE. A Nernstian response was obtained for different electrodes, obtaining values of 58.8 ± 0.4 mV/unit of pH. The mean and standard deviation of the slope was evaluated using nine pH points of the calibration curve for three different electrodes in three different days. The linear dynamic range spans seven pH units from 2.89 to 9.90 (**Figure 6.2.1**).

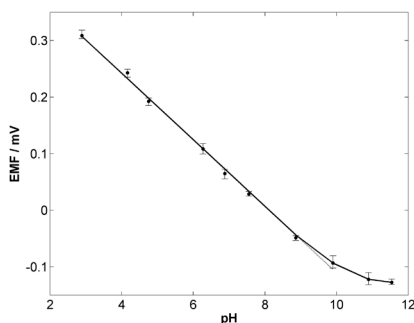


Figure 6.21 - Calibration curve for MWCNT pH sensors in different buffer solutions at constant ionic strength ($I=0.01$ M). Slope of 58.8 ± 0.4 mV/ pH unit. The error bars represent the standard deviation at each point of the calibration curve for three different electrodes in three different days.

The response time ($t_{95\%}$) of the electrode has been calculated following the IUPAC criteria [15] and using the calibration curve with successive additions of 0.1 M HCl so as to decrease the pH in the solution from 11 to 3 (Figure 6.22). The value obtained for the whole range of pH is shorter than 10 s.

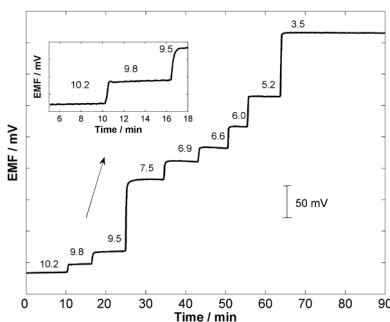


Figure 6.22 - Response time ($t_{95\%}$) derived from EMF responses of the MWCNT pH sensor over time for increasing pH values in the test solution.

The selectivity coefficients ($\log K_{ij}^{pot}$) for the MWCNT-based pH ISE were calculated using the Fixed Interference Method [16]. The most common cations in aqueous solutions such as Li^+ , Na^+ , K^+ , NH_4^+ , Ca^{+2} and Mg^{+2} were tested. The EMF were measured in the presence of 0.1 M concentration of each secondary ion. For all cases, Nernstian responses were obtained with a high degree of linearity over the reported pH range. Table 6.2.1 lists the logarithmic selectivity coefficients, which show that the ion-selective membrane of the electrode makes it very highly selective towards the secondary ions tested, findings which agree with previously reported results [17].

Interference (M)	Slope (mV/dec)	Selectivity ($\log K_{ij}^{\text{pot}}$)
K^+	-60.01	-7.86
NH_4^+	-59.2	-8.90
Li^+	-59.5	-8.90
Na^+	-59.8	-8.90
Ca^{+2}	-29.2	-8.36
Mg^{+2}	-29.8	-9.40

Table 6.21 - Potentiometric selectivity coefficients ($\log K_{ij}^{\text{pot}}$) determined for the MWCNT-based pH electrode incorporating the ionophore tridodecylamine to the methacrylic-acrylic polymeric membrane. The FIM method was employed, using 0.1 M concentrations of the secondary ion in all cases.

Figure 6.23A shows the complex impedance plot for GC/MWCNT where the spectrum is dominated by a 90° capacitive line which extends down to low frequencies (0.3 Hz). At high frequencies, only a slight deviation from the capacitive line can be observed, indicating a fast transduction across the MWCNT film / electrolyte solution. The value for the double layer capacitance obtained after the fitting was $100 \mu\text{F}$. The impedance plot shape agrees with previous spectra reported for carboxylated SWCNTs [9].

Impedance measurement of the GC/MWCNT/Membrane was also recorded and is shown in **Figure 6.23B**. This type of spectrum shows the behaviour of the membrane in the electrode. At high frequencies the signal is mainly dominated by the resistance and the geometric capacitance in parallel with the membrane, as is shown by the small semicircle between 0.1-10 kHz. On the other hand, there is a diffusional component (45° line) at low frequencies which is related to diffusion of the analyte from the solution into the ISM.

Reversal chronopotentiometry has been applied to evaluate the stability of the electrode developed according to Bobacka (**Figure 6.2.4**) [18]. The potential jump is related to the total resistance (R). The total resistance calculated for the electrodes developed at two levels of current ($I = 1$ and 5 nA) was around $R = 13 \text{ M}\Omega$. From the same experimental plots, the stability of the potentials can be derived from the ratio $\Delta E/\Delta t$. The resulting values were $\Delta E/\Delta t = 40 \mu\text{V/s}$ and $140 \mu\text{V/s}$ for 1 nA and 5 nA respectively. As expected, the value obtained for low frequency capacitances is quite similar for both currents and is near to $30 \mu\text{F}$, thus indicating a potentiometric drift of 0.1 mV/h when the flow current in the system is around 10^{-12} A . These results closely agree with the stability parameters obtained in the potentiometric experiments.

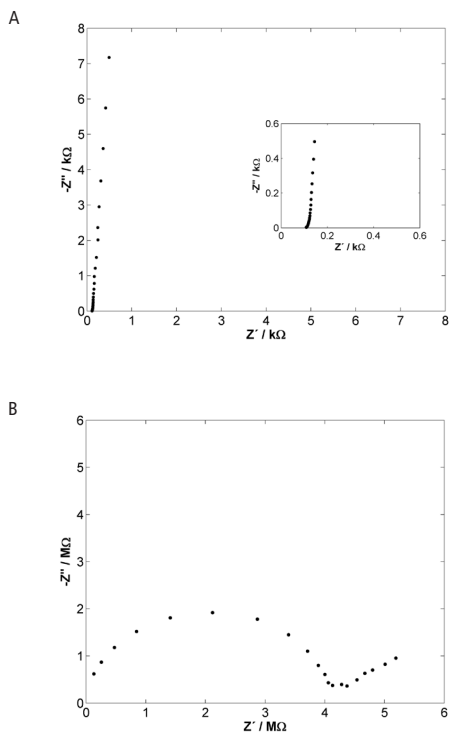


Figure 6.23 - Experimental data obtained from Electrochemical Impedance spectrum analysis (EIS). **A)** Impedance plot of GC/MWCNT recorded at $E_{dc}=0.2$ V, range 0.3 Hz – 10 kHz. $\Delta E_{ac}=10$ mV in pH=4.16. Inset: range 3 Hz-10 kHz. Fitting values, $C_{dl}=100$ μ F. **B)** Electrochemical Impedance plot of GC/MWCNT/ISM recorded at $E_{dc}=0.2$ V, range 0.01 Hz – 100 kHz. $\Delta E_{ac}=10$ mV in pH=4.16.

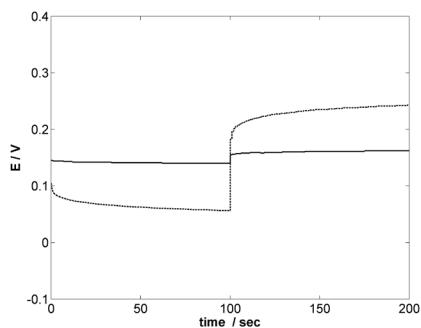


Figure 6.24 - Chronopotentiometric results for MWCNTs sensor at pH=4.16. Solid line: applied current -1 nA for 100 s and 1 nA for 100 s. Dotted line : applied current -5 nA for 100 s and 5 nA for 100 s.

Finally, we used the potentiometric water layer test [19] to assess the stability of the MWCNTs-ISE by studying the presence and possible influence of an aqueous solution film at the interface between the ISM and the MWCNTs. The experiment was done in three steps (Figure 6.2.5). Firstly, the EMF was recorded for 1 hour in HCl 10^{-3} M, H^+ being the primary analyte. Secondly, the solution was changed to KCl 10^{-3} M (interference) and the potential was recorded for 3 hours. Finally, the electrode was submerged again in the initial solution for 24 hours. The absence of a positive slope in the second step suggests that no undesirable water film was formed between the solid internal contact and the sensing membrane. The highly hydrophobic character of the MWCNT network could be the main reason for the absent or reduced water layer. In addition, the intermediate term stability was calculated with the data generated in the third step of the test. The value obtained corresponds to $0.5 \text{ mV}\cdot\text{h}^{-1}$ for 16 hours.

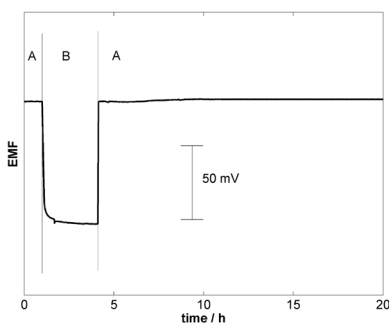


Figure 6.2.5 – Water layer test for MWCNT pH sensor. The measurements were recorded in 10^{-3} M HCl (A) and in 10^{-3} M KCl at pH = 5 (B).

6.2.6. Conclusions

Results show that an MWCNT network placed between the self plasticized polymeric membrane and the glassy carbon rod is able to efficiently transduce the ionic into electronic current. We have not found a noticeable difference between the transducing behaviour of single-walled and multi-walled carbon nanotubes. Since the main parameter governing the transduction process is attributed to the double layer capacitance, it is logical that no significant differences appear between semiconducting and metallic carbon nanotubes, unlike in field effect transistors. The MWCNT-based solid-contact pH electrode displays a Nernstian response with a linear pH range from 2.89 to 9.90. The electrode displays considerable stability, with response times shorter than 10 s. The new pH-sensor can successfully discriminate the most common interfering ions present in the usual water samples. Moreover, the absence of an aqueous layer, which is probably due to the hydrophobic character of MWCNTs, increased the stability of the electrodes.

The development of solid-contact ion-selective electrodes based on carbon nanotubes enables this type of sensor to be miniaturized, a process that has already started in our laboratory.

6.2.7. Acknowledgments

This work was supported by the Spanish MICINN, through the project grants NAN2004-09306-C05-05 and CTQ2006-7-67570/BQU. G.A.C. also acknowledges MICINN for the doctoral fellowship AP2006-04171 and D.G acknowledges the economic support provided by the Universitat Rovira i Virgili.

6.2.8. References

- [1] Bakker, E. and E. Pretsch, *Modern Potentiometry*. Angewandte Chemie-International Edition, 2007. 46(30) 5660-5668.
- [2] Bobacka, J., A. Ivaska, and A. Lewenstam, Potentiometric ion sensors. *Chemical Reviews*, 2008. 108(2) 329-351.
- [3] Chumbimuni-Torres, K.Y., N. Rubinova, A. Radu, L.T. Kubota, and E. Bakker, Solid contact potentiometric sensors for trace level measurements. *Analytical Chemistry*, 2006. 78(4) 1318-1322.
- [4] Michalska, A., A. Hulanicki, and A. Lewenstam, All-solid-state hydrogen ion-selective electrode based on a conducting poly(pyrrole) solid contact. *Analyst*, 1994. 119(11) 2417-2420.
- [5] Lindner, E. and R.E. Gyurcsanyi, Quality control criteria for solid-contact, solvent polymeric membrane ion-selective electrodes. *Journal of Solid State Electrochemistry*, 2009. 13(1) 51-68.
- [6] Lai, C.Z., M.M. Joyer, M.A. Fierke, N.D. Petkovich, A. Stein, and P. Buhlmann, Subnanomolar detection limit application of ion-selective electrodes with three-dimensionally ordered macroporous (3DOM) carbon solid contacts. *Journal of Solid State Electrochemistry*, 2009. 13(1) 123-128.
- [7] Fouskaki, M. and N. Chaniotakis, Fullerene-based electrochemical buffer layer for ion-selective electrodes. *Analyst*, 2008. 133(8) 1072-1075.
- [8] Crespo, G.A., S. Macho, and F.X. Rius, Ion-selective electrodes using carbon nanotubes as ion-to-electron transducers. *Analytical Chemistry*, 2008. 80(4) 1316-1322.
- [9] Crespo, G.A., S. Macho, J. Bobacka, and F.X. Rius, Transduction Mechanism of Carbon Nanotubes in Solid-Contact Ion-Selective Electrodes. *Analytical Chemistry*, 2009. 81(2) 676-681.
- [10] Lai, C.Z., M.A. Fierke, A. Stein, and P. Buhlmann, Ion-Selective Electrodes with Three-Dimensionally Ordered Macroporous Carbon as the Solid Contact. *Anal. Chem.*, 2007. 79(12) 4621-4626.
- [11] Dai, H.J., Carbon nanotubes: opportunities and challenges. *Surface Science*, 2002. 500(1-3) 218-241.
- [12] Monthieux, M., P. Serp, E. Flahaut, M. Razafinimanana, C. Laurent, A. Peigney, W. Bacsá, and J.-M. Broto, Introduction to Carbon Nanotubes, in *Springer Handbook of Nanotechnology*. 2007 43-112.
- [13] Heng, L.Y., L.H. Chern, and M. Ahmad, A hydrogen ion-selective sensor based on non-plasticised methacrylic-acrylic membranes. *Sensors*, 2002. 2(8) 339-346.
- [14] Heng, L.Y. and E.A.H. Hall, Methacrylic-acrylic polymers in ion-selective membranes: achieving the right polymer recipe. *Analytica Chimica Acta*, 2000. 403(1-2) 77-89.
- [15] Buck, R.P. and E. Lindner, Recommendations for nomenclature of ion selective electrodes - (IUPAC Recommendations 1994). *Pure and Applied Chemistry*, 1994. 66(12) 2527-2536.
- [16] Bakker, E., E. Pretsch, and P. Buhlmann, Selectivity of potentiometric ion sensors. *Analytical Chemistry*, 2000. 72(6) 1127-1133.
- [17] Piao, M.H., J.H. Yoon, J. Gerok, and Y.B. Shim, Characterization of all solid state hydrogen ion selective electrode based on PVC-SR hybrid membranes. *Sensors*, 2003. 3(6) 192-201.

- [18] Bobacka, J., Potential stability of all-solid-state ion-selective electrodes using conducting polymers as ion-to-electron transducers. *Analytical Chemistry*, 1999. 71(21) 4932-4937.
- [19] Fibbioli, M., W.E. Morf, M. Badertscher, N.F. de Rooij, and E. Pretsch, Potential drifts of solid-contacted ion-selective electrodes due to zero-current ion fluxes through the sensor membrane. *Electroanalysis*, 2000. 12(16) 1286-1292.

6.3. “Determination of choline and derivatives with a solid-contact ion-selective electrode based on octaamide cavitand and carbon nanotubes”

Biosensors and Bioelectronics 2009, 25, 344–349.

Jordi Ampurdanés ^a, Gastón A. Crespo ^a, Alicia Maroto^a,
M. Angeles Sarmentero ^c, Pablo Ballester ^{b,c*} and F. Xavier Rius ^{a*}

^a Department of Analytical and Organic Chemistry. University of Rovira i Virgili Marcel·lí Domingo, s/n. 43007. Tarragona, Spain.

^b Institute of Chemical Research of Catalonia (ICIQ) Av. Països Catalans, 16 43007 Tarragona, Spain.

^c Catalan Institution for Research and Advanced Studies (ICREA). Pg. Lluís Companys 23, 08010 Barcelona (Spain).

6.3.1. Abstract

A new solid-contact ion-selective electrode has been developed for determining choline and derivatives in aqueous solutions. The backbone of this new potentiometric sensor is the conjunction of the cavitand receptor, as the molecular recognition element, and a network of non-carboxylated single-walled carbon nanotubes, acting as a solid transducer material. The octaamide cavitand, a synthetic receptor that is highly selective for biologically important trimethyl alkylammonium cations such as choline, acetylcholine or carnitine, makes the selective determination of these compounds possible for the first time. The guest–host interaction takes place in the acrylate ion-selective membrane of the solid-contact electrode. The sensor was characterized by electrochemical impedance spectroscopy and environmental scanning electron microscopy. The new electrode displays a nearly Nernstian slope (57.3 ± 1.0 mV/decade) and very stable behaviour ($\Delta E/\Delta t = 224 \mu\text{V h}^{-1}$) throughout the dynamic range (10^{-5} to 10^{-1} M). The limit of detection of $10^{-6.4}$ M and the high selectivities obtained will enable choline and derivatives to be determined in biological samples. Finally, the stability of the electrical potential of the new solid-contact electrode was examined by performing current-reversal chronopotentiometry and the influence of the interfacial water film was evaluated by the potentiometric water layer test.

6.3.2. Keywords

Solid-contact sensor; Single-walled carbon nanotubes; Choline; Octaamide cavitand; Ion-selective electrode.

6.3.3. Introduction

In recent years, a new generation of potentiometric solid-contact ion-selective electrodes (SC-ISE) (Bobacka et al. 2008) have achieved high selectivities and very low limits of detection (LOD) (Chumbimuni-Torres et al. 2006), which makes them comparable to other more costly analysis techniques. Solid-contact electrodes are regarded as the potentiometric sensors of the future since they can be miniaturized and fabricated using the well-known thick- and thin-film technologies (Pretsch 2007). Very recently, different carbon-based nanostructured material such as three-dimensionally ordered macroporous carbon (Lai et al. 2008) and fullerenes (Fouskaki and Chaniotakis 2008) have been used as solid-contact transducers in ISE (Bakker and Pretsch 2007). Our group has also reported on the performance of single-walled carbon nanotubes (SWCNTs) as solid transducers that provide additional advantages over electroactive polymers, which have commonly been used as ion-to-electron transducers to date. SWCNTs exhibit excellent long-term potential stability, hydrophobicity and insensitivity to light and to species displaying redox characteristics such as oxygen, which might induce side reactions that could interfere with the electromotive force (EMF) generated (Crespo et al. 2008) and (Crespo et al. 2009). Although ISEs have been widely used, the species detected are generally very hydrophilic ions such as inorganic cations and anions, or small organic ions related principally to pesticides or drugs (Bakker et al. 1997). Therefore, the development of a potentiometric solid contact sensor to detect specific molecules that play a role in the metabolic process is still a challenge. This sensor could be very useful in clinical analysis.

The ionophore plays a central role in the detection system of ISE. The octaamide cavitand (Ballester and Sarmentero 2006) and (Ballester et al. 2002), a synthetic receptor highly selective for biologically important trimethyl alkylammonium cations (i.e., choline, acetylcholine, and carnitine), allows the selective binding of these compounds. The guest–host interaction takes place in the acrylate polymeric matrix, which constitutes the ion-selective membrane (ISM) of the solid-contact electrode. Cation- π attractive interactions between the positive charge of the guest and the electron-rich aromatic surfaces of the synthetic host result in the formation of complexes with high kinetic and thermodynamic stability. The positive charge of choline (2-hydroxyethyl-trimethylammonium) and the roughly spherical shape of its trimethylammonium group constitutes a perfect fit to the negative aromatic surfaces and concave cavity provided by the octaamide cavitand. (Figure 6.3.1)

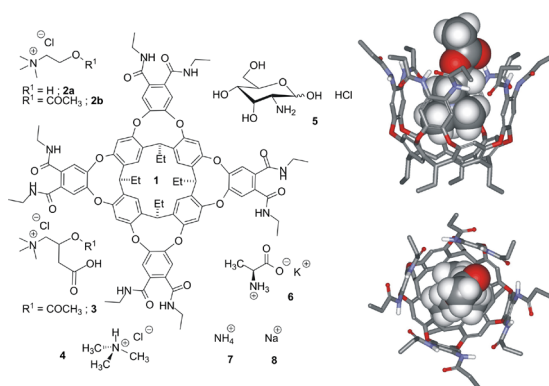


Figure 6.3.1 - Molecular structures of the octaamide cavitand 1 and the ions tested in this study (2a: choline, 2b: acetylcholine, 3: carnitine, 4: trimethylamine, 5: l-alanine, 6: ammonium, 7: ammonium, 8: sodium). Side and top views of the octaamide cavitand–acetylcholine complex.

Because choline and its derivatives, i.e., acetyl choline, carnitine and choline phospholipids are linked to many important biological processes, they constitute relevant targets for molecular recognition and sensing. Choline is an essential nutrient (Zeisel 2006), (Zeisel 2000) and (Zeisel and Blusztajn 1994) acetyl choline is an important excitatory neurotransmitter (Leitinger and Simmons 2000) carnitine is involved in the metabolism of lipids (Fujii et al. 2008), and choline-containing phospholipids are responsible for important properties of the cell wall (Conde-Alvarez et al. 2006).

The well-established methodologies for choline detection (Barkhimer et al. 2008) employing radio-enzymatic and chemiluminescent assays (Adamczyk et al. 2006), chromatographic (Holm et al. 2003), (Gamache et al. 2007) and (Zhang et al. 2007) and amperometric (Mitchell 2004) techniques pose several drawbacks, mainly related to the sample pre-processing steps. The extraction and derivatization of the target analytes or immobilization of the reactants, among other processes, are tedious and costly. The pre-processing stages are also difficult to miniaturize and may contribute to the contamination of the sample due to excessive manipulation.

In an attempt to overcome these disadvantages, here we report the development and characterization of the first potentiometric solid-contact electrode for the straightforward quantitative determination of choline and derivatives using a specifically designed synthetic receptor, the octaamide cavitand entrapped in an acrylic matrix, as ionophore and a network of non-carboxylated SWCNTs as a transducer layer.

6.3.4. Experimental

6.3.4.1. Chemical reagents and material

Methyl methacrylate (MMA), n-butyl acrylate (nBA), reagent grade benzene (C_6H_6), dichloromethane (CH_2Cl_2), tetrahydrofuran (C_4H_8O), petroleum ether (80–100 °C) and azobisisobutyronitrile initiator (AIBN) were purchased from Fluka. AIBN was recrystallised with warm methanol (CH_3OH) before use. Analytical grade chloride salt of acetylcholine ($C_7H_{16}NO_2Cl$ or $AChOCl$), d-(+)-glucosamine hydrochloride ($C_6H_{13}NO_5 \cdot HCl$), trimethylamine hydrochloride ($C_3H_9N \cdot HCl$), l-alanine hydrochloride ($C_3H_7NO_2 \cdot HCl$), ammonium chloride (NH_4Cl), sodium chloride ($NaCl$) were also obtained from Fluka. Analytical grade choline chloride ($C_5H_{14}NOCl$ or $ChOCl$), acetyl-l-carnitine ($C_9H_{17}NO_4$), sodium dodecyl sulphate (SDS), used as a surfactant in the SWCNTs dispersions, were provided by Sigma. Octaamide cavitand (ionophore, $C_{84}H_{88}N_8O_{16}$, MW: 1465.6), choline tetrakis (4-chlorophenyl)borate ($C_{29}H_{30}BCl_4NO$) and acetylcholine tetrakis (4-chlorophenyl)borate ($C_{31}H_{32}BCl_4NO_2$) were synthesized and provided by P. Ballester's group (Institute of Chemical Research of Catalonia, ICIQ, Spain). Non-carboxylated SWCNTs with 95% purity were purchased from Carboxex Inc. All solutions were prepared using deionised water (18.2 M Ω cm specific resistance) obtained with a Milli-Q PLUS (Millipore Corporation, Bedford, MA, USA).

6.3.4.2. Preparation of the electrode

The electrodes were fabricated in our laboratory (Figure 6.3.2). A glassy carbon (GC) rod (length 50 mm and diameter 3 mm) provided by *Sigradur*[®]G was inserted into a Teflon body to act as the electrode support as well as the electrical contact between the ion-selective electrode and the potentiometer (the active surface was approximately 7 mm²). The electrode was polished using a sheet of abrasive paper (Buehler Carbimet 600/P1200) and subsequently treated using alumina of different grain sizes (30, 5 and 1 μ m Buehler Micropolish II, USA). SWCNTs were deposited by spraying (Crespo et al. 2008) an aqueous dispersion containing 10⁻² wt.% of the non-carboxylated SWCNTs and 1% wt. of sodium dodecyl sulphate (SDS), thereby coating the GC with a layer of SWCNTs. Before deposit, the dispersion was homogenized using a tip-sonicator for 30 min (amplitude 60%, cycle 0.5, Ultrashallprozessor UP200S, Dr. Hielscher). The SWCNTs were deposited in successive steps. The dispersion of SWCNTs was sprayed for 2 s; the layer of SWCNTs was then dried, thoroughly washed with water, and dried again. The process was repeated 35 times resulting in a thickness of approximately 30 μ m.

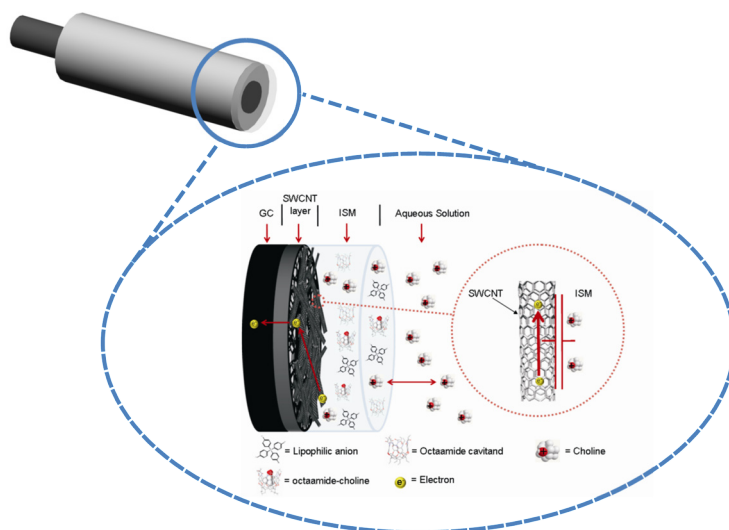


Figure 6.3.2 - Schematic representation of the various parts of the solid-contact ion-selective electrode developed. In the larger zoom, the membrane components can be observed. The smaller zoom shows the representation of the transduction process (ion-to-electron) due to the intrinsic large capacitance of the interface SWCNT-membrane.

6.3.4.3. Ion-selective membrane synthesis and deposition

The ion-selective membrane is formed by an acrylic matrix with the required amount of the octaamide cavitand (ionophore) and lipophilic anion (ChO^+ -tetrakis) according to the reported procedures (Michalska et al. 2004) and (Lai et al. 2008). A total of 200 mg of cocktail was used (96.5% acrylic membrane, 3% ionophore and 0.5% lipophilic anion). The polymeric acrylic matrix (MMA-nBA, ratio 1:10) was synthesized from methyl meta (MMA) and nBA monomers using the procedure described by (Heng and Hall 2000). Acrylic membranes without plasticizers have lower diffusion coefficient than others like PVC-plasticizer membrane improving some performance parameters such as LOD and lifetime of the sensor. 100 μL of the cocktail-membrane was deposited onto the electrode by drop casting. The electrode was maintained under dry ambient conditions for one day. The thickness of the membrane was measured by environmental scanning electron microscopy being around 100 μm . It was subsequently conditioned in the appropriate solution depending on the measurement performed.

6.3.4.4. Conditioning of the electrode

Conditioning of the electrodes is a fundamental step in obtaining reliable and successful results. The electrodes were conditioned in a 10^{-3} M for one day and subsequently in 10^{-9} M of the primary ion for two days (Chumbimuni-Torres et al. 2006). However, specific types of condition-

ing described in the text were applied depending on the measurement taken. Finally, before the water layer test the electrodes were conditioned overnight in 10^{-2} M choline chloride (ChOCl).

6.3.5. Electrochemical measurements

6.3.5.1. Potentiometric measurements

All electromotive forces (EMF) were measured at room temperature (23 ± 2 °C) in stirred solutions using a Lawson's multichannel (16 channels). A double-junction Ag/AgCl/3 M KCl reference electrode (type 6.0729.100, Methrom AG) containing a 1 M LiAcO electrolyte bridge was employed. Activity coefficients were calculated by the Debye–Huckel approximation and the potential measurements were corrected using the Henderson equation for the liquid junction potential determination. The calibration curves for choline were determined by consecutive additions of different concentrations and the limit of detection (LOD) of the electrodes was calculated using the dilution method recommended by IUPAC (Lindner and Umezawa 2008) using a 846 dosing unit interface device (Metrohm, Switzerland). The experiments were performed in a one-compartment cell in which the three working electrodes were measured simultaneously.

The potentiometric selectivity coefficients ($\log K_{ij}^{\text{pot}}$) for several secondary ions were obtained by the separated solution method (SSM) (Bakker et al. 2000). These secondary ions, corresponding to analytes present in blood samples, were chosen in order (i) to demonstrate the compatibility of the ionophore against choline and derivatives (acetylcholine), (ii) to observe the influence in the selectivity of molecules displaying a higher hydrophilicity such as acetyl-L-carnitine, trimethylamine, alanine and glucosamine, and (iii) to evaluate the selectivity against small cations such as Na^+ and NH_4^+ .

The long-term stability of the electrodes was evaluated by recording the potentiometric signal for $10^{-3.6}$ M of chloride choline over a long period. Three additions of 10^{-6} , $10^{-4.6}$ and $10^{-3.6}$ M were performed to achieve the final activity from the initial conditions in which the electrode was conditioned (10^{-9} M).

6.3.5.2. Chronopotentiometric measurements

A constant current of a 1 nA was applied for 60 s followed by a reversed current of the same magnitude for the same amount of time. The potentials were measured in a solution of 0.1 M choline chloride (ChOCl) at room temperature (23 ± 2 °C). These measurements were recorded by using a one-compartment, three-electrode cell to which the electrode under study was acting as the working electrode. The reference electrode was Ag/AgCl/KCl (3 M), and the auxiliary electrode was a glassy carbon rod. All potential measurements refer to this reference electrode.

6.3.5.3. Impedance measurements

Electrochemical measurements were performed by using a one-compartment, three-electrodes electrochemical cell. The working electrode was GC/SWCNT/ISM (area 0.07 cm²) and the auxiliary electrode was a glassy carbon rod. The reference electrode was a Ag|AgCl|KCl (3 M) single junction (Model 6.0733.100, Metrohm). All measurements were performed at room temperature (23 ± 2 °C). All electrochemical measurements were made using an Autolab general purpose electrochemical system and Autolab frequency response analyser system (AUT20.FRA2-AUTOLAB, Eco Chemie, B.V., The Netherlands). The impedance spectra were recorded in a frequency range (10 kHz to 0.3 Hz) and were then fitted to an equivalent electrical circuit, previously reported by our group (Crespo et al. 2009) for electrodes with SWCNTs as transducers, using the Autolab impedance analysis software.

6.3.5.4. Water layer test

In order to demonstrate that there was no thin aqueous layer between the polymeric membrane and the SWCNTs network that would introduce long-term potential instabilities, the well-known water layer test (Fibbioli et al. 2000) was performed. The measurement was taken using a 0.1 M choline chloride solution in the first and third steps of the test, and a 0.1 M ammonium chloride solution as an interference solution in the second step.

6.3.6. Results and discussion

Figure 6.3.2 shows the three main sections of the developed electrode: the ISM, the SWCNTs layer and the glassy carbon as the electronic conducting substrate. The acrylate polymeric membrane (Heng and Hall 2000), containing the octaamide cavitand (ionophore) and choline tetrakis(4-chlorophenyl)borate as the lipophilic anion in contact with the test solution allows the primary ion choline to be distributed between the two immiscible phases. Because equilibrium is established quickly, a boundary potential is generated at the aqueous/organic interface which depends on the logarithmic activity of the choline ion in the aqueous solution (Bakker and Pretsch 2007). The layer of SWCNTs functions as a transducer providing a high degree of stability in the potentiometric signal, converting the ionic current in the polymeric membrane to the electronic current that flows through the glassy carbon conducting rod (**Figure 6.3.2**).

6.3.6.1. Potentiometric measurements

Figure 6.3.3 illustrates the EMF signal recorded after successive additions of the choline ion to the test solution. It can be observed that the signal has stable behaviour, with no perturbations or random noise after each addition. In each case, when the concentration increases the response time decreases. As can be observed in the insets of **Figure 6.3.3**, at intermediate values of total

concentration of choline, such as $10^{-3.5}$ M, the time response ($t_{90\%}$) was less than 1 min, while at the lowest concentration values the time response was around 10 min.

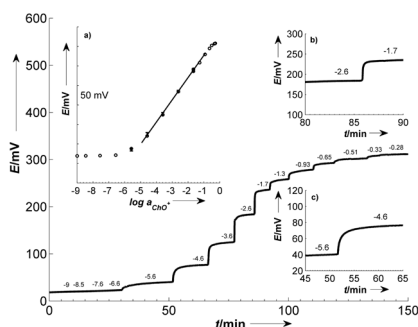


Figure 6.3.3 - Time response and short-term stability of the signal for the solid-contact ion-selective electrode upon additions of increasing amounts of choline to the test solution. Inset (a), electromotive force (EMF) signal dependence on $\log a_{\text{ChO}^+}$. The error bars correspond to the range values obtained for three electrodes. Slope = 57.3 ± 1.0 mV/decade and four logarithmic units of dynamic range. Insets (b) and (c) show the response time profile at two levels of concentration of ChO^+ $10^{-1.7}$ and $10^{-4.6}$ respectively.

The previous data were used to obtain the calibration plot (**Figure 6.3.3, inset a**). A Nernstian response is obtained with a sensitivity value of 57.3 mV/decade with a standard deviation of 1.0 mV/decade for three different electrodes. In addition, to evaluate the repeatability of the E° potential along time, calibration curves for choline have been recorded at different days ($N = 15$). The mean E° value (308 ± 20 mV) expressed with its corresponding standard deviation. The dynamic range has a length of approximately four logarithmic units.

The potentiometric limit of detection (LOD), which was defined as the cross section of the two linear segments of the response function and calculated using the dilution method recommended by IUPAC (Lindner and Umezawa 2008), is $10^{-6.4}$ M (figure not shown). The medium-term potentiometric stability was evaluated by recording the EMF value for a solution containing $10^{-3.6}$ M of choline chloride (**Figure 6.3.4**). A very small drift of ($224 \mu\text{V h}^{-1}$) was observed for 20 h (**Figure 6.3.4b**). This low value demonstrates that the electrode has very stable behaviour in medium-term conditions. The electrodes were used for at least three months and obtained practically the same values for slope, time of response and drift.

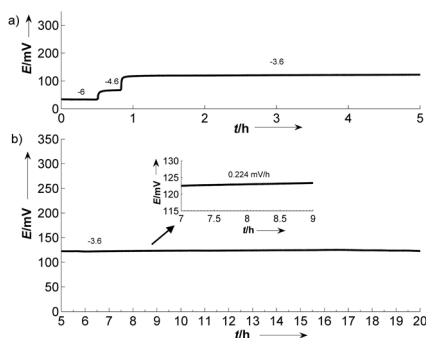


Figure 6.3.4 - Stability of the electrode response over 20 h. The value of the drift was 224 $\mu\text{V/h}$. (a) Three consecutive additions were performed to reach a final activity of $10^{-3.6}$ M of choline chloride. (b) Signal recorded from 5 to 20 h without changes in the concentration of the analyte.

The potentiometric selectivity coefficients ($\log K_{ij}^{\text{pot}}$ being i = primary analyte and j = secondary ion in **Figure 6.3.1**) of the choline electrode are mainly determined by two factors: (a) the ion-exchange ability of the polymeric membrane ($\log K_{ij}$) and (b) the molecular recognition properties of the entrapped cavitand receptor related to the stability constant values of the complexes (β , and β_j) (Bakker and Pretsch 2007). The values of the selectivity coefficients observed for acetylcholine ($K_{2a-2b} = 0.0 \pm 0.1$), acetyl-L-carnitine ($K_{2a-3} = -1.2 \pm 0.2$) and trimethylamine ($K_{2a-4} = -1.0 \pm 0.1$) are in good agreement with the fact that all of them have the same quaternary ammonium group and their complexes with the cavitand display stability constant on the same order of magnitude as those corresponding to the choline-cavitand complex. The slight selectivity displayed towards acetyl-L-carnitine and trimethylamine are due to the larger hydrophilic character of these molecules, in comparison with choline or acetylcholine. In the case of ammonium ($K_{2a-7} = -2.3 \pm 0.1$) and sodium ($K_{2a-8} = -2.2 \pm 0.2$), the lack of interactions CH- π and the high energy required for desolvation hinder the interaction between these cations and the cavitand, explaining the larger selectivity coefficient found. The largest values for the selectivity coefficient were obtained to glucosamine $K_{2a-5} = -3.3 \pm 0.3$ and L-alanine $K_{2a-6} = -3.5 \pm 0.2$, which displays no size or shape complementarity with the receptor and they are more hydrophilic than any other organic molecule tested.

6.3.6.2. Chronopotentiometric measurements

Reversal chronopotentiometry was used to evaluate the electrical capacity of the solid contact and the potential stability of the electrode developed. The potential jump is related to the total resistance (R), according to Ohm's law, $R = E/I$. The total resistance estimated for the electrodes developed was $R = 15.7 \text{ M}\Omega$ ($I = 1 \text{ nA}$) (figure not shown). From the same experimental plots,

the short-term stability of the potentials can be derived from the ratio $\Delta E/\Delta t$. Following the fundamental capacitor equation, $I = C \cdot dE/dt$. The value obtained for the capacitance (C) was $9.1 \mu\text{F}$ ($I = 1 \text{ nA}$) and the resulting value for the potential drift was $\Delta E/\Delta t = 130 \mu\text{V/s}$.

6.3.6.3. Impedance measurements

Figure 6.3.5a shows the complex impedance plot for GC/SWCNT where the spectrum is dominated by a 90° capacitive line, which extends down to low frequencies (0.3 Hz). At high frequencies, only a slight deviation from the capacitive line can be observed, indicating a fast transduction across the SWCNTs film/electrolyte solution. The value obtained for C_{dl} ($100 \mu\text{F}$) is similar to other values reported for carboxylated SWCNTs (Crespo et al. 2008) and . The impedance measurement of the GC/SWCNT/Membrane was also recorded and it is shown in **Figure 6.3.5b**. In this type of spectrum the behaviour of the membrane in the electrode can be observed. At high frequencies the signal is mainly dominated by the resistance and geometric capacitance in parallel of the membrane. Therefore, the small semicircle between 0.1 and 10 kHz can be observed. On the other hand, at low frequencies a diffusional component appears (45° line) related to the diffusion of the analyte from the solution into the ISM.

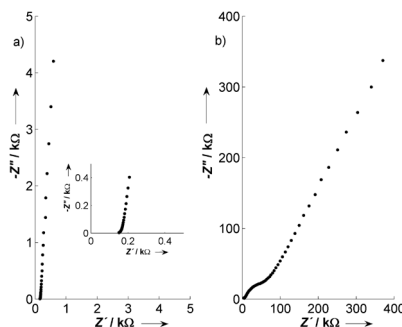


Figure 6.3.5 - Experimental data obtained from Electrochemical Impedance Spectroscopy (EIS) analysis. (a) Complex impedance plot of GC/SWCNT recorded at $E_{dc} = 0.2 \text{ V}$, range 0.3 Hz to 10 kHz. $\Delta E_{ac} = 10 \text{ mV}$ in 0.1 M ChOCl . Thickness of $30 \mu\text{m}$. Inset: Range 3 Hz to 10 kHz. Fitting values, $R_s = 151 \Omega$; $C_d = 100 \mu\text{F}$. (b) Complex impedance plot of GC/SWCNT/ISM recorded at $E_{dc} = 0.2 \text{ V}$, range 0.01 Hz to 100 kHz. $\Delta E_{ac} = 10 \text{ mV}$ in 0.1 M ChOCl . The thickness of the membrane was around $100 \mu\text{m}$.

6.3.6.4. Water layer test

The results of the potentiometric water layer test can be observed in **Figure 6.3.6**. Initially, the signal was recorded in a 0.1 M choline chloride solution for 1.5 h and a near to zero positive drift was observed, indicating that the primary ion is not accumulated in the water layer. After changing the sample from the primary ion to the interfering ammonium ion (0.1 M for 3.5 h) the final

equilibrium is reached immediately, appearing a reduced positive potential drift, which indicates that ChO^+ is hardly replaced by NH_4^+ in the water film formed between the ion-selective membrane and the SWCNTs layer. The equilibrium is again reached fast when the interfering solution was finally replaced by the initial 0.1 M ChOCl solution, appearing a slight negative drift that is stabilized in a few minutes. These results indicate that only a reduced or inexistent water layer is formed in our electrode. These results are consistent with those found previously (Crespo et al. 2008) in which the hydrophobic character of the SWCNTs was assigned as the main reason for the absence of the water layer. Moreover, this hydrophobic character is reinforced in the present work in which we used non-carboxylated carbon nanotubes.

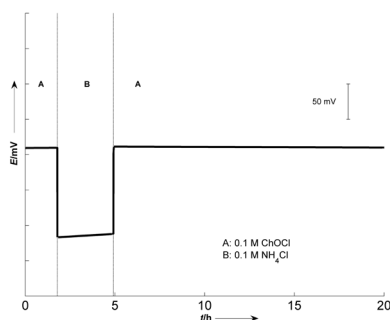


Figure 6.3.6 - Water layer test for the SC-ISE for choline. The measurements were recorded in 0.1 M ChOCl (A) and in 0.1 M NH_4Cl (B).

Among the numerous methods that have been developed to detect choline and derivatives, those based on the separation of the target from the sample matrix, such as gas chromatography, capillary electrophoresis or HPLC, clearly reach the highest sensitivities and lowest detection limits. However, they often require derivatization or preconcentration preprocessing steps and use costly detection systems based, for instance, on fluorescence laser-based systems or mass spectrometry (Barkhimer et al. 2008). On another hand, electrochemical detection methods are much more accessible although their use is not straightforward since choline and derivatives are not inherently electroactive species. Mitchell developed an amperometric sensor containing multienzyme layers immobilized with bovine serum albumin by cross-linking with glutaraldehyde (Mitchell 2004). This author reported detection limits in the range of 0.4 μM , response times shorter than 1 s and appropriate selectivity relative to the most common analytes present in biological samples. Miniaturized coated-wire ion-selective electrodes in conjunction with capillary electrophoresis have been recently reported (Kappes et al. 2000). The sensing mechanism employed in this latter case is not based on the recognition ability of the ionophore but

on the electrostatic attraction between bulky ionic pairs. These authors reported comparable performance parameters to those reported in the present paper except for selectivity. It is well known that the selectivity is compromised in these systems based on ion-exchange mechanisms, although in the Kappes' report this feature is irrelevant due to the on-line coupling with the capillary electrophoresis system.

6.3.7. Conclusions

In summary, a new solid-contact ion-selective electrode to determine choline and derivatives in aqueous solutions has been developed based on the host-guest interaction of the octaamide cavitand in the hydrophobic environment of the polymeric membrane. We have taken advantage of this supramolecular interaction, only studied in non-aqueous solvents to date, to determine choline in aqueous solutions. The limit of detection obtained could allow the determination of choline in biological samples as blood (Zeisel 2000) and (Adamczyk et al. 2006). The non-carboxylated single-walled carbon nanotubes, used for the first time as solid transducer, exhibit a similar behaviour to the carboxylated nanotubes. Finally, the solid nature of the transducer will allow the easier miniaturization of the electrode.

6.3.8. Acknowledgments

We thank the Spanish Ministry of Science and Innovation, MICINN, for supporting the work through the project grants CTQ2007-67570/BQU, NAN2004-09306-C05-05 and CTQ2008-00222/BQU. J.A. would also like to thank URV for providing his fellowship. G.A.C acknowledges MEC for the doctoral fellowship AP2006-04171.

6.3.9. References

- Adamczyk, M., Brashear, R.J., Mattingly, P.G., Tsatsos, P.H., 2006. *Anal. Chim. Acta* 579(1), 61-67.
- Bakker, E., Buhlmann, P., Pretsch, E., 1997. *Chem. Rev.* 97(8), 3083-3132.
- Bakker, E., Pretsch, E., 2007. *Angew. Chem. Int. Ed.* 46(30), 5660-5668.
- Bakker, E., Pretsch, E., Buhlmann, P., 2000. *Anal. Chem.* 72(6), 1127-1133.
- Ballester, P., Sarmentero, M.A., 2006. *Org. Lett.* 8(16), 3477-3480.
- Ballester, P., Shivanyuk, A., Far, A.R., Rebek, J., 2002. *J. Am. Chem. Soc.* 124(47), 14014-14016.
- Barkhimer, T.V., Kirchoff, J.R., Hudson, R.A., Messer Jr, W.S., Viranga Tillekeratne, L.M., 2008. *Anal. Bioanal. Chem.* 392(4), 651-662.
- Bobacka, J., Ivaska, A., Lewenstam, A., 2008. *Chem. Rev.* 108(2), 329-351.
- Conde-Alvarez, R., Grilla, M.J., Salcedo, S.P., de Miguel, M.J., Fugier, E., Gorvel, J.P., Moriyon, I., Iriarte, M., 2006. *Cell. Microbiol.* 8(8), 1322-1335.
- Crespo, G.A., Macho, S., Bobacka, J., Rius, F.X., 2009. *Anal. Chem.* 81(2), 676-681.
- Crespo, G.A., Macho, S., Rius, F.X., 2008. *Anal. Chem.* 80(4), 1316-1322.
- Chumbimuni-Torres, K.Y., Rubinova, N., Radu, A., Kubota, L.T., Bakker, E., 2006. *Anal. Chem.* 78(4), 1318-1322.
- Fibbioli, M., Morf, W.E., Badertscher, M., de Rooij, N.F., Pretsch, E., 2000. *Electroanalysis* 12(16), 1286-1292.
- Fouskaki, M., Chaniotakis, N., 2008. *Analyst* 133(8), 1072-1075.
- Fujii, H., Ishiguro, Y., Uchida, E., Yamamoto, S., 2008. *Nutr. Immunol.* 8(2), 92-98.
- Gamache, P., Zhang, Q., Himmelfarb, J., 2007. *Clin. Chem.* 53(6), A20-A20.
- Heng, L.Y., Hall, E.A.H., 2000. *Anal. Chim. Acta* 403(1-2), 77-89.
- Holm, P.I., Ueland, P.M., Kvalheim, G., Lien, E.A., 2003. *Clin. Chem.* 49(2), 286-294.
- Kappes, T., Schnierle, P., Hauser, P.C., 2000. *Electrophoresis* 21(7), 1390-1394.
- Lai, C.Z., Joyer, M.M., Fierke, M.A., Petkovich, N.D., Stein, A., Buhlmann, P., 2008. *J. Solid State Electrochem.* 13(1), 123-128.
- Leitinger, G., Simmons, P.J., 2000. *J. Comp. Neurol.* 416(3), 345-355.
- Lindner, E., Umezawa, Y., 2008. *Pure Appl. Chem.* 80(1), 85-104.
- Michalska, A.J., Appaih-Kusi, C., Heng, L.Y., Walkiewicz, S., Hall, E.A.H., 2004. *Anal. Chem.* 76(7), 2031-2039.
- Mitchell, K.M., 2004. *Anal. Chem.* 76(4), 1098-1106.

- Pretsch, E., 2007. Trends Anal.Chem. 26(1), 46-51.
- Zeisel, S.H., 2000. Nutrition 16(7-8), 669-671.
- Zeisel, S.H., 2006. Annu. Rev. Nutr. 26, 229-250.
- Zeisel, S.H., Blusztajn, J.K., 1994. Annu. Rev. Nutr. 14, 269-296.
- Zhang, J.J., Zhu, Y., 2007. J. Chromatogr. A 1170, 114-117.

6.4. Robust potentiometric sensors to determine ionic gradients in aquatic environments

Mathias Kirf ^a, Gastón A. Crespo ^b, F. Xavier Rius ^b and Bernhard Wehrli ^{a*}

^a Swiss Federal Institute of Aquatic Science & Technology (EAWAG)

Surface Water - Research and Management. Dept. of Environmental Sciences,
ETH Zürich. Seestrasse 79, 6047 Kastanienbaum, Switzerland.

^b Department of Analytical and Organic Chemistry.

Universitat Rovira i Virgili, Marcel·lí Domingo s/n., 43007 Tarragona, Spain.

6.4.1. Introduction

Chemical gradients in the aquatic environment are abundant. The biosphere is inhomogeneous from the physicochemical point of view, and patchiness is a constant feature of all ecological systems [1]. Gradients are the result of the physical separation of sources and sinks and build up on different scales. Fluxes along these gradients may control the supply of a limiting resource, determine the activity of e.g. consuming biota, and lead in general to dynamic steady states [2].

Interfaces between two abiotically distinct habitats may be established where two limiting resources are supplied from different directions. Therefore, interfaces are zones of special interest, as they are often the locus where biogeochemical cycles most visibly take place. Microorganisms, as engines of biogeochemical cycles may accumulate at the interception and enforce opposing gradients. Metabolic rates may be so high that the limiting resources hardly overlap [3].

Given known gradients (concentration profiles) and transport regimes, fluxes at such interfaces are relatively easily accessible through Fick's laws of diffusion or simple models of one-dimensional turbulent diffusion. Production or consumption rates of bulk or individual sources and sinks are quantifiable, expanding insight at different scales [2, 4].

Therefore, knowledge of the shape of concentration profiles at the biogeochemistry interface is extremely important to research many unknown processes. But, from the analytical point of view, the detailed study of gradients in the aquatic environment is a hard challenge which has not yet been exhaustively explored. Here, *in-situ* techniques preferred rather than the classical

approach based on sample collection, storage, transport and analysis in the laboratory. The recording of dense and large datasets to account for natural spatial and temporal variations is facilitated. No sample handling or storage is required, eliminating sample alteration or contamination. Combined with real-time data-interpretation, in-situ measuring techniques enable the precise analysis at specific points and further analysis in a reduced monitoring time [5].

On the other hand, *in-situ* measurements of ionic gradients in engineered or natural aquatic environments thrive since the development the of ion-selective membrane based potentiometric electrodes (ISEs) [5]. Potentiometric ion selective microsensors/microelectrodes with internal solution (IS-ISEs) are still typical research tools used to study microbial processes in aquatic environments, as their high resolution resolves steep gradients usually associated with microbial processes [6]. However, the well-known limitations of these kinds of sensors related to the presence of internal liquid have been described [7]. Several years ago a systematic limitation of IS-ISEs was eliminated, yielding robust sensors with an unmatched low detection limit and signal stability. The inner electrolyte of classical ISEs was replaced with new solid state ion-to-electron transducers. This eliminated the outward transmembrane flux of primary ions at low sample activities [8, 9]. Along with new calibration protocols, the “classical detection limit” of liquid ISEs from around 10^{-6} M was improved by more than 3 orders of magnitude reaching 10^{-9} M values [10, 11]. In combination with the elimination of membrane-plasticizers, these new solid-contact SC-ISEs offer better signal stability, less drift and faster response times than the classical PVC-based devices. Slightly better selectivities and better reproducibility of the individual sensor response are to be expected [12]. In the same way, larger stability and longer life-time are achieved. In addition, the storage of the electrodes in dry conditions can be a great advantage. Crespo and coworkers [13, 14] introduced carbon-nanotubes (CNTs) as solid-contact material for ISEs. The chemical inert properties of CNTs demonstrated a better behaviour than other materials, with special regard to light-sensitivity and potential-stability [15]. Here we explore the potential of one of the most promising solid-contact techniques for applications in aquatic environments. Specifically, we develop and apply in an underwater environment (i.e. in pressure higher than atmospheric conditions) CNTs-based ion-selective electrodes for Ca^{2+} and pH. Moreover, the influence of sunlight on the potentiometric signal transduced by the conducting polymer POT is compared to the one transduced by CNTs.

6.4.2. Experimental section

6.4.2.1. Development of waterproof electrodes

The electrodes were developed following the design of Crespo et.al [14] with modifications to ensure the waterproofing and resistance to high to pressure changes between 1 and 25 bar. (Figure 6.4.1).

A glassy carbon (GC) rod with polished surface (length 50 mm and diameter 3 mm, Sigradur G) was pressed into a Teflon tube (length =80 mm, outer diameter = 6 mm, inner diameter = 3 mm). The inner backside of the tube was threaded, and a single gold connector fitted with an o-ring, to prevent any pressure-leakage into the sealed connector unit, was also used. The internal contact between connector and rod was provided by a drop of silver varnish (EPO-TEK H20E, EPOTEX®).

Watertight, pressure-resistant and exchangeable/replaceable connection of the electrode to the coaxial cable of the electrometer was achieved by screwing the female connector into a Teflon tube (50 mm length, 15 mm outer diameter, 6.6 mm inner diameter) fitted with a radial mounted o-ring (8.5 diameter, 1.5 mm gauge). The female connector was soldered to a coaxial cable and the tube was backfilled with high resistance poly-urethane. This setup was pressure tested for 21 bar.

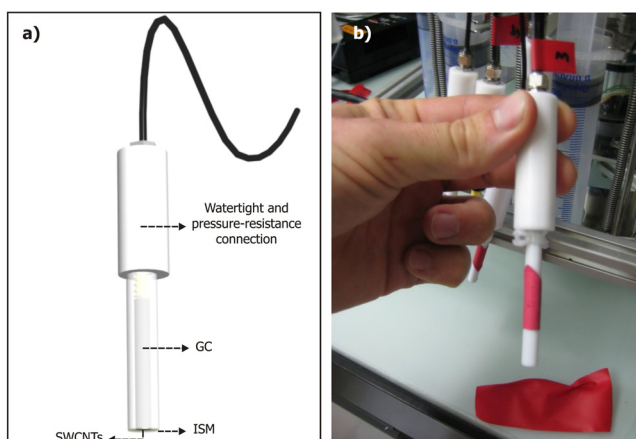


Figure 6.4.1 – a) Scheme of solid contact ion selective electrode based on SWCNTs. This electrode was carefully developed showing watertight and pressure-resistance properties. b) Photograph of the real SC-ISEs with the column pressure compensation.

The GC-surface was sprayed with single wall carbon nanotubes (SWCNTs) previously purified [13]. Two different acrylic ion selective membranes were prepared: i) Calcium membrane: 15 mmol/kg of ionophore IV for calcium, 5 mmol/kg of KTFPB, 20 mmol/kg of ETH500 and 96 mg of the acrylic matrix (nBA-MMA). ii) pH membrane: 30 mmol/kg of ionophore II (4-Nonadecylpyridine) for proton, 7.6 mmol/kg of KTFPB, 15 mmol/kg of ETH500 and 96 mg of the acrylic matrix (nBA-MMA). 1 mL of dichloromethane was used to dissolve the reagents and 1 hour of vigorous agitation was needed to obtain homogeneous cocktails. After that, membranes were deposited on the GC-SWCNTs layer by drop casting and posteriorly dried at room temperature over night. The conditioning methodology was always the same, trying to obtain the best performance pa-

rameters. Primary analyte in two ranges of concentrations were used: 10^{-3} M for 24 hours and 10^{-9} M for 48 hours in stirring solutions. Moreover, GC-electrodes with polythiophene (POT) as transducer were used in order to compare light sensitivity.

6.4.2.2. Potentiometric measures

Lawson multichannel potentiometers, both with common and high input resistances ($10^{13}\Omega$ and $10^{15}\Omega$) were used to record electromotive forces (EMF). A double-junction Ag/AgCl/KCl (3 M) reference electrode (type 6.0729.100, Methrom AG) containing a 0.1-1 M LiAcO electrolyte bridge was used. Potential values were corrected for liquid-junction potentials according to the Henderson equation. Activity coefficients were calculated by the Debye–Hückel approximation.

In situ measurements were obtained using a custom built Profiling Ion selective Analyzer (PIA) (Figure 6.4.2). PIA integrates an embedded computer (Z-Brain, Schmid Engineering Systems AG), an amplifier (custom-made picoamperemeter with an input-resistance $\geq 10^{15}\Omega$), solid contact ion selective electrodes, auxiliary sensors (pressure, conductivity and oxygen) and a syringe-based water sampler. Profiles were recorded in-situ by slowly lowering the instrument through the water column. The data was transferred online to an external computer on board (Figure 6.4.3). Measurements were recorded in Vierwaldstätter Lake (Lucerne, Switzerland).

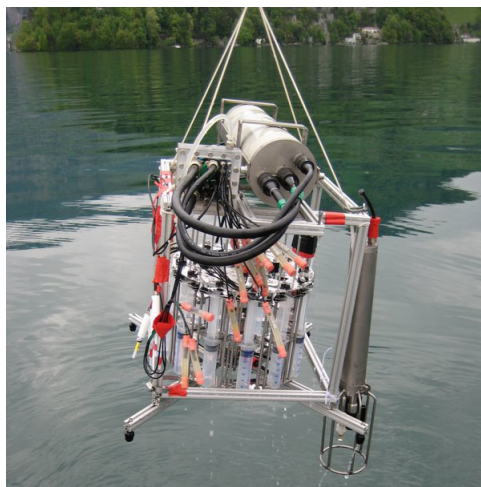


Figure 6.4.2 – Photograph of the Profiling Ion selective Analyzer (PIA). Several sensors can be observed hanging from PIA, within them, the SC-ISEs (bottom-left-part).

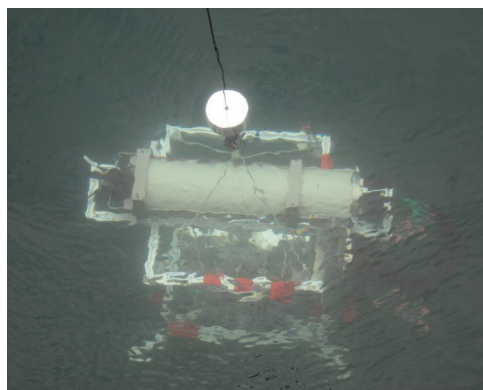


Figure 6.4.3 – Photograph of PIA submerging in the depths of the lake. This device has been submerged up to 150 meters supporting a high pressure.

6.4.3. Results and discussion

6.4.3.1. Calibration of the electrodes

This section shows the calibration curve and the analytical parameters for calcium and pH solid contact electrodes tested in the laboratory. **Figure 6.4.4a** shows the EMF versus time for different Ca^{2+} activities using the calcium electrode and the successive additions procedure. The sensor starts responding at changes of concentration between 10^{-9} and 10^{-8} M. Therefore, the LOD according to the IUPAC recommendations is near to 10^{-8} M. Another relevant performance parameter is response time (t_{90}). It is defined as the required time to reach 90% of stable signal after the change of the concentration sample. Response time (t_{90}) for calcium sensor is 30 seconds irrespective of the calcium ion concentration. **Figure 6.4.4b** shows the calibration curve displaying a linear range from 10^{-8} M to 10^{-3} M.

Figure 6.4.4c shows the EMF versus time for different pH values and **Figure 6.4.4d** the calibration of the pH sensor. The linear range spans 4.5 logarithmic units and the time of response (t_{90}) is 40 seconds along the whole linear range. Long term stability was checked by two sensors being $150 \mu\text{V}\cdot\text{h}^{-1}$ (Calcium sensor, 10^{-3} M of Ca^{2+} for 24 hours), and $350 \mu\text{V}\cdot\text{h}^{-1}$ (pH sensor, $\text{pH}=3$ M for 24 hours).

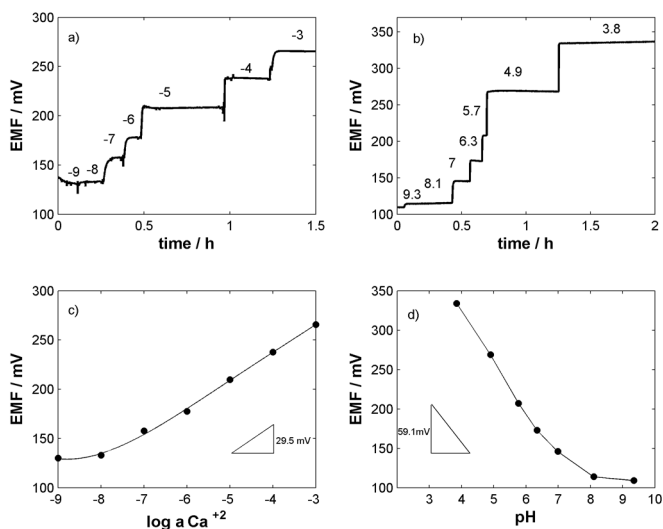


Figure 6.4.4 –Analytical performance parameters for watertight and pressure-resistance SC-ISEs tested on the laboratory.

a) EMF vs. time at different activities of calcium in logarithmic units. **b)** EMF vs. time at different pH in logarithmic units. **c)** Calibration curve of calcium SC-ISE. **d)** Calibration curve of pH-SC-ISEs.

6.4.3.2. Light sensitivity test

Carbon nanotubes are light insensitive nanostructured materials under normal laboratory conditions. **Figure 6.4.5** shows the comparison of the potentiometric signal for two identical solid contact electrodes containing respectively, CNTs and POT as transducers.

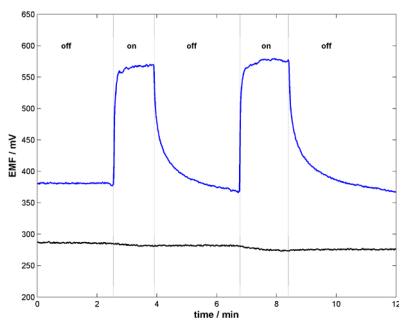


Figure 6.4.5 – The effect of the artificial-light on two different transducers is shown. A light bulb (100 W) is placed near to the potentiometric cell (RE is coated with aluminum foil). A bulb is switched "on" and "off" respectively as shown in the figure. Both signals correspond to SC-ISEs for calcium ions. Blue line signal: POT as transducer; black line signal: SWCNTs as transducer. The potentiometric signals are recorded in a 10^{-3} M of $CaCl_2$.

The signal recorded for the POT electrode shows a large shift when the electrode is exposed to strong visible light (light bulb, 100 W). While the CNTs-based electrode shows only a slight deviation on the baseline. In a similar way to other applications, light sensitivity is of major concern in aquatic research due to the translucent properties of water and the effect of light-intensity and spectrum to the different depths.

6.4.3.3. *In-situ* measurements

In-situ measurements using both CNT-based and POT-based pH-selective sensors have been performed on a preliminary basis. **Figure 6.4.6** shows a profile of the recorded potential as a function of the depth of the lake using POT-based pH selective electrode. Strong drift in the signal during the measurement is observed. In fact, near to the surface up to -10 m, the drift is sharply negative ($3 \text{ mV}\cdot\text{m}^{-1}$). Then, a positive drift from -10 m to -30 m around $1 \text{ mV}\cdot\text{m}^{-1}$ is observed. Finally, a large step around -50 m followed the stable signal from -50 m to -70 m is achieved. The first potential decrement (0-10m) could be correlated to the effect of sunlight on the POT layer as described above. The signal could not be attributed to changes in the pH, although non-*in-situ* pH measurements display a shift of 0.25 units, (**Figure 6.4.6**) due to the fact that the potentiometric signal must decrease when the pH increases. Most likely, the second part of the graph (10-30m) could be correlated to a shift on the pH, although the large fluctuation at 50 m cannot be yet explained. With these preliminary results, the strong affect of the sunlight on the potentiometric signal in the first 30 meters, deems POT not suitable for this applications.

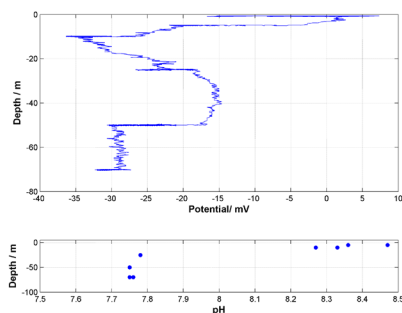


Figure 6.4.6—Potentiometric signal profile as a function of depth for a pH-SC-ISEs based on POT as transducer is represented. This profile is recorded by PIA device submerged in the lake. In the bottom figure, several water samples are acquired at different depths and measured in the surface with a commercial IS-ISEs and SC-ISEs. Posteriorly, a calibration curve is plotted with these values.

In strong contrast, **Figure 6.4.7** shows the signal of the CNT-based sensors. Whereas random noise is presented as well, there is not a strong drift like in the POT sensor. The figure also displays the random noise, taking into account that the units of the abscissa axis have been largely modified with respect to the previous figure. Moreover, no signal increase is observed in the vicinity of the lake-surface; instead, the sensors follow the shift in pH to slightly higher values.

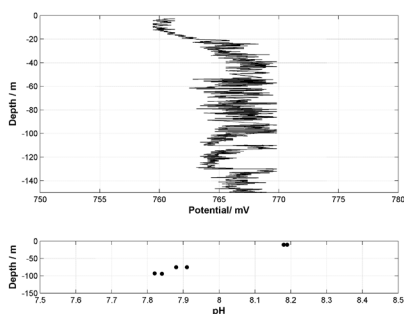


Figure 6.4.7 – Similar to figure 6.4.6, although in this case pH-SC-ISEs based on SWCNTs as transducer is employed.

Both pH results as function of the depth in **Figure 6.4.6** and **Figure 6.4.7** are in agreement with the biological processes involved at the different levels. Within the photosynthetic active zone near to the surface, where suspended algae consume dissolved CO_2 increasing values of pHs are expected.

6.4.4. Conclusions

Solid contact ion selective electrodes based on carbon nanotubes are a promising sensor-technology for aquatic research field. In fact, the major problem of other transducer elements, namely the high sensitivity to sunlight has been overcome due to the properties of the inert carbon nanotubes towards light. Moreover, CNTs-based electrodes tested in the laboratory display similar performance parameters as one of the best macro solid contact electrodes reported until now [11]. More in-situ measurements are currently being performed for other analytes such as potassium and nitrate.

Miniaturization of CNTs-based electrodes is now being developed in our research group. These new devices are especially interesting in this field because they will enable the precise determination of ionic interchange in specific solid-liquid interfaces such as those between plants and soils in the aquatic media. Microscale measurements will profit from a high spatial resolution recorded in a short response time. Finally, the shelf-life of the electrodes should improve due to their ability to be stored in dry storage conditions.

6.4.5. Acknowledgments

M.K.K. acknowledges Christian Dinkel for support with the amplification-electronics and during the general development of the Profiling Ion Analyzer PIA.

G.A.C. also acknowledges MICINN for the doctoral fellowship AP2006-04171. The authors thank Professor Ernö Pretsch for his recommendations and encouraging discussions.

6.4.6. References

- [1] Brune, A., P. Frenzel, and H. Cypionka, *Life at the oxic-anoxic interface: microbial activities and adaptations*. Fems Microbiology Reviews, 2000. 24(5) 691-710.
- [2] Jorgensen, B.B. and N.P. Revsbech, *Diffusive boundary-layers and the oxygen-uptake of sediments and detritus*. Limnology and Oceanography, 1985. 30(1) 111-122.
- [3] Murray, J.W., L.A. Codispoti, and G.E. Friederich, *Oxidation-reduction environments - the suboxic zone in the black-sea, in Aquatic Chemistry - Interfacial and Interspecies Processes*, C.P. Huang, C.R. Omelia, and J.J. Morgan, Editors. 1995. 157-176.
- [4] Kuypers, M.M.M., A.O. Sliemers, G. Lavik, M. Schmid, B.B. Jorgensen, J.G. Kuenen, J.S.S. Damste, M. Strous, and M.S.M. Jetten, *Anaerobic ammonium oxidation by anammox bacteria in the Black Sea*. Nature, 2003. 422(6932) 608-611.
- [5] Buffle, J. and G. Horvai, *In situ monitoring of aquatic systems : chemical analysis and speciation. IUPAC series on analytical and physical chemistry of environmental systems*. 2000: Chichester, J. Wiley.
- [6] Debeer, D., J.C. Vandenhevel, and S.P.P. Ottengraf, *Microelectrode measurements of the activity distribution in nitrifying bacterial aggregates*. Applied and Environmental Microbiology, 1993. 59(2) 573-579.
- [7] Lindner, E. and R.E. Gyurcsanyi, *Quality control criteria for solid-contact, solvent polymeric membrane ion-selective electrodes*. Journal of Solid State Electrochemistry, 2009. 13(1) 51-68.
- [8] Sokalski, T., A. Ceresa, T. Zwickl, and E. Pretsch, *Large improvement of the lower detection limit of ion-selective polymer membrane electrodes*. Journal of the American Chemical Society, 1997. 119(46) 11347-11348.
- [9] Mathison, S. and E. Bakker, *Effect of transmembrane electrolyte diffusion on the detection limit of carrier-based potentiometric ion sensors*. Analytical Chemistry, 1998. 70(2) 303-309.
- [10] Bakker, E. and E. Pretsch, *Potentiometric sensors for trace-level analysis (vol 24, pg 199, 2005)*. Trac-Trends in Analytical Chemistry, 2005. 24(5) 459-459.
- [11] Chumbimuni-Torres, K.Y., N. Rubinova, A. Radu, L.T. Kubota, and E. Bakker, *Solid contact potentiometric sensors for trace level measurements*. Analytical Chemistry, 2006. 78(4) 1318-1322.
- [12] Sutter, J., A. Radu, S. Peper, E. Bakker, and E. Pretsch, *Solid-contact polymeric membrane electrodes with detection limits in the subnanomolar range*. Analytica Chimica Acta, 2004. 523(1) 53-59.
- [13] Crespo, G.A., S. Macho, and F.X. Rius, *Ion-selective electrodes using carbon nanotubes as ion-to-electron transducers*. Analytical Chemistry, 2008. 80(4) 1316-1322.
- [14] Crespo, G.A., S. Macho, J. Bobacka, and F.X. Rius, *Transduction Mechanism of Carbon Nanotubes in Solid-Contact Ion-Selective Electrodes*. Analytical Chemistry, 2009. 81(2) 676-681.
- [15] Lindfors, T., *Light sensitivity and potential stability of electrically conducting polymers commonly used in solid contact ion-selective electrodes*. Journal of Solid State Electrochemistry, 2009. 13(1) 77-89.

6.5. Potentiometric sensors for the *on-line* monitoring of a catalytic denitrification process

Collaboration with Dr. Noelia Barrabés and Prof. Didier Tichit from the Equipe Matériaux Avancés pour la Catalyse et la Santé(MACS), Institut Charles Gerhardt - UMR 5253 (CNRS/ENSCM/UM2/UM1) of Montpellier (France).

6.5.1. Introduction

Wastewater treatment has become a social, technological and economical necessity. Diffuse pollution of water resources from agricultural sources is a major environmental issue. The extensive use of chemical fertilizers and improper treatment of waste water from industry has led to an increase in nitrate concentration on the ground and surface of the water [1]. Nitrate anions compounds are proven to be harmful to the mammalian organisms. Inside the organism the nitrate anion is transformed into ammonium. Nitrite being an intermediate of the reaction, due to the partial reduction that took place. Nitrite is a causing agent of blue baby syndrome and it is also a precursor to the carcinogenic nitrous amines [2].

As a consequence, the legal limits imposed within the EU are 50, 0.1 and 0.5 mg.L⁻¹ for NO₃⁻, NO₂⁻ and NH₄⁺, respectively [2].

Many physicochemical and biological processes have been developed for removing nitrate from contaminated water [3], although they are hardly cost-effective or even detrimental due to potential side-effects on water quality. The main drawback of the physicochemical treatments such as reverse osmosis, electro dialysis and ion exchange resins, is that the procedure consists of the separation and concentration of the pollutant [3]. Therefore, the resulting brine has to be treated afterwards.

As is well known, biological treatment is highly effective for the removal of nitrates. Despite their success and cost effectiveness, biodegradation processes are inherently slow and do not allow high degrees of removal. The sludge formed during biological treatment has to be disposed of either by landfilling or by burning. The cost of these disposal methods should be accounted for. In addition, sludge disposal may pose environmental problems.

On the other hand, catalytic denitrification is emerging as one of the most promising and flexible techniques for an efficient solution to the problem. In this process, nitrate ions are reduced using hydrogen over bimetallic catalyst. The reaction follows a consecutive reaction scheme in which nitrite is an intermediate, while nitrogen and ammonium are the final products [4]. The main advantages of the catalytic reduction of nitrate is that the reaction is performed in mild

conditions (room temperature and atmospheric pressure) [5] [6] and subproducts are not obtained. In fact catalytic denitrification leads to nitrogen gas and clean water, if the conversion is complete.

The most accepted general reaction mechanism for the nitrate reduction is that proposed by Epron et al. [7]. It is assumed that the promoting metal is responsible for the nitrate reduction by a redox reaction leading to the intermediate nitrite. This intermediate is further reduced on the noble metal surface to nitrogen or undesired ammonium. In addition, the noble metal regenerates the oxidized form of the non noble metal by the hydrogen chemisorbed leading to the metallic promoter metal and avoiding the deactivation of the catalyst (Figure 6.5.1).

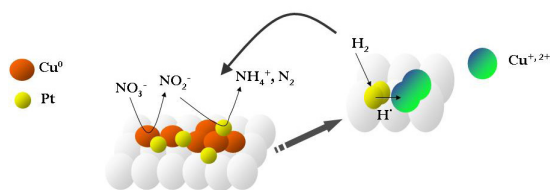


Figure 6.5.1 – Scheme of general mechanism reaction for a model catalyst as PtCu/Al₂O₃. Orange spheres (Cu⁰), yellow spheres (Pt⁰), green spheres (Cu⁺²) and grey spheres (Al₂O₃, support).

The noble metal itself does not present activity to nitrate reduction, although it is effective in the nitrite elimination. However, when noble metal (Pt or Pd) is supported on oxides with redox properties such as CeO₂, TiO₂ or SnO₂, these catalysts are active in the nitrate reduction. In this case, it is proposed that the nitrate is reduced to nitrite in the oxygen vacancies of the oxide support surface. Whereas the noble metal plays the same role in the reaction, the reduction of nitrite to the products, and, the regeneration of the catalysts by the chemisorb hydrogen.

The reaction has been developed for treatment of groundwater resources to supply drinking water quality to the population. In this way, compact, continually working, inexpensive and fast systems are required.

In contrast to the reaction part, the detection of subproducts and products play an important role in the processes. Usually, liquid chromatography (for NO₃⁻ and NO₂⁻) and ultraviolet spectroscopy (for NH₄⁺) are the most common techniques used to analyze the final concentrations at the exit of the reactor [5]. These traditional procedures required the pretreatment of large sample volumes (at least 10 mL) that should be previously filtered and stored before the chemi-

cal analysis. Moreover, nitrate, nitrite and ammonium can not be quantified at the same time as the analysis. Therefore, the analysis time takes longer than one day to obtain the concentration profiles resulting from the catalytic process using the same catalyst.

On-line monitoring of the reaction is an attractive possibility to overcome the drawbacks of the classical analysis methodology. By *on-line* monitoring the activities of the nitrate ions and its subproducts after the catalytic process we may know the extent of the reaction. Furthermore, catalyst properties and mechanism's can be studied in detail. In fact, problems related to the reaction can be solved immediately.

Inner solution commercial (IS-ISEs) have been not implemented to monitor catalytic denitrification processes at least in laboratory scales. The current of hydrogen to reduce the catalyst flowing, and the overpressure generated on the system could damage the ion selective membrane. In addition, the commercial IS-ISEs are not easy-handle, especially due to their large size. It would be difficult to adapt them to the small flow-cell.

Therefore, we developed an *on-line* potentiometric detection system integrated with solid contact ion selective electrodes based on carbon nanotubes for monitoring the catalytic denitrification processes. The high stability of these sensors [8], due to the presence of an inert carbon nanotubes layer, enables the recording of measurements for a long time in the presence of a hydrogen current through the detection system. In addition, this simple, robust and inexpensive detection system is made accessible for many industrial applications, where the *on-line* monitoring is needed.

6.5.2. Experimental section

6.5.2.1. Manufacturing of the sensors

A glassy carbon (GC) rod with polished surface (length 50 mm and diameter 3 mm, Sigradur G) was pressed into a PVC tube (length =80 mm, outer diameter = 6 mm, inner diameter = 3 mm). The inner backside of the tube was threaded, and a single gold connector fitted with an o-ring, to prevent any pressure-leakage into the sealed connector unit, was also used. The internal contact between connector and rod was provided by a drop of silver varnish (EPO-TEK H20E, EPOTEX®). The GC-surface was sprayed with single wall carbon nanotubes (SWCNTs) previously purified [9].

6.5.2.2. Membrane cocktail preparation

Three different acrylic ion selective membranes were prepared: i) Ammonium membrane: 15 mmol/kg of ionophore III, 7.5 mmol/kg of TDMACl, 20 mmol/kg of ETH500 and 96 mg of the acrylic matrix (nBA-MMA). ii) Nitrate membrane: 10 mmol/kg of ionophore III, 5 mmol/kg of TDMACl and 96 mg of the acrylic matrix (nBA-MMA). iii) Nitrite: 10 mmol/kg of ionophore I, 5 mmol/

kg of TDMACl, 20 mmol/kg of ETH500 and 96 mg of the acrylic matrix (nBA-MMA) [10]. 1 mL of dichloromethane was used to dissolve the reagents and 1 hour of vigorous agitation was needed to obtain homogeneous cocktails. After that, membranes were deposited on the GC-SWCNTs layer by drop casting and posteriorly dried at room temperature over night. The conditioning process was accomplished in two steps: i) 24 hours at 10^{-3} M of primary and ii) 24-48 hours at 10^{-9} M of primary ion, in order to obtain the best performance analytical parameters [11].

6.5.2.3. Reagents

Catalyst preparation (Pt/Ceria) is described in [12]. Platinum salt (H_2PtCl_6) dissolved in water was impregnated on the CeO_2 . After that, the sample was dried overnight and then calcined in order to remove the remaining precursor salts. Sodium nitrate salt from Sigma-Aldrich was used to prepare the feed solution and the standards. Nitrite and ammonium standards were prepared from sodium nitrite acquired from Prolabo and ammonium nitrate from ACROS. All of the reagents used are analytical grade.

6.5.2.4. Instrumentation

The catalytic reduction of nitrate was performed in a fixed-bed reactor system (Figure 6.5.2). The liquid feed solution with $130 \text{ mg}\cdot\text{L}^{-1}$ of nitrate was prepared by dissolving $NaNO_3$ in Milli Q water and introduced to the reactor by a positive displacement pump (HP) at $1 \text{ mL}\cdot\text{min}^{-1}$. The hydrogen flow was adjusted by a mass flow controller at $3 \text{ mL}/\text{min}$. The tubular reactor, 15 cm long and $\frac{1}{2}$ " outer diameter, was placed in an oven coupled with a temperature control system. The reactor was filled with 200 mg of catalyst. Double junction agar reference electrode (3M KCl/1M LiAcO) was used.

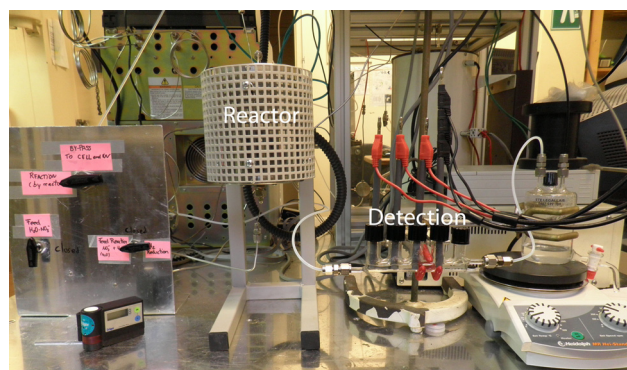


Figure 6.5.2 – The reactor where the catalytic reaction is accomplished, converting nitrate into nitrite, ammonium and nitrogen is shown. Products of the reaction are directed to the flow-cell detection where the SC-ISEs are placed. The flow-cell is hermetically close to avoid lack of hydrogen.

The resulting liquid flow containing nitrate, nitrite, ammonium and nitrogen was directed towards the measurement cell where the solid-state electrodes were placed (nitrite, nitrate, ammonium and reference electrodes), as observed in **Figure 6.5.3**.

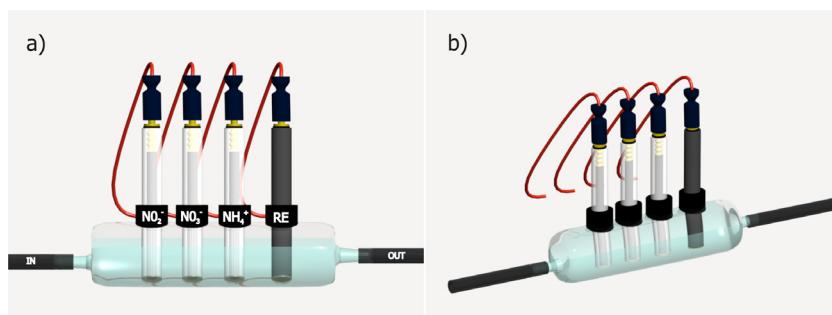


Figure 6.5.3 – The flow-cell contained the three working SC-ISEs and the reference electrode (RE) is displayed.

6.5.3. Results and discussion

6.5.3.1. Flow calibration of the electrodes

Nitrate, nitrite and ammonium solid contact electrodes were calibrated separately using the same volumetric flow rate as used for the measurement of the products of the catalytic process. Additionally, in order to compare the results, calibrations were also performed in batch conditions.

Figure 6.5.4, 6.5.5 and 6.5.6 show the *on-line* EMF recording as a function of the time and the molar concentration of NO₃⁻, NO₂⁻ and NH₄⁺ respectively. These calibration curves were recorded by successive additions methodology.

The calibration curve for the nitrate electrode was obtained by employed three concentration standards distributed from 10⁻⁴ to 10⁻³ M of NO₃⁻ (6.2 - 62 mg.L⁻¹ NO₃⁻). Similarly, the calibration curve for the nitrite electrode was obtained using three standards from 10⁻⁵ to 10⁻³ M of NO₂⁻ (0.46 - 46 mg.L⁻¹ of NO₂⁻) and; for the ammonium electrode standards from 10⁻⁶ to 10⁻³ M of NH₄⁺ (0.018 - 18 mg.L⁻¹ of NH₄⁺) were attained. All the electrodes developed exhibit either a small sub Nernstian or Nernstian response in the working ranged tested (**inset Figure 6.5.4, 6.5.5 and 6.5.6**). The response time of the system is around at 3 minutes for all electrodes in the flow cell. These response times of the system are conditioned by the volume of the flow-cell (~3mL) and the flow rate. Therefore, the flow rate is 1 mL/min and the volume of the flow-cell is 3mL, therefore, in 3 minutes the signal reached the stationary state for a constant concentration.

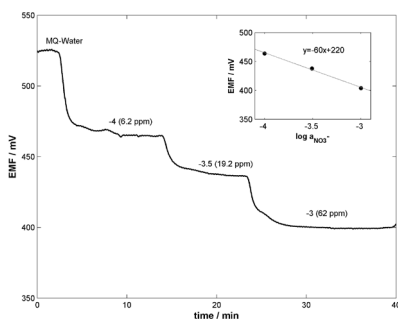


Figure 6.5.4 – EMF vs. time at three concentrations of NO_3^- in *on-line* conditions (flow rate: 1 mL/min). Inset plot shows the calibration curve for NO_3^- SC-ISE with its corresponding sensitivity (60 mV/dec).

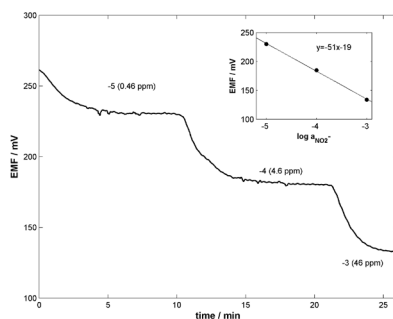


Figure 6.5.5 – EMF vs. time at four concentrations of NO_2^- in *on-line* conditions (flow rate: 1 mL/min). Inset plot shows the calibration curve for NO_2^- SC-ISE with its corresponding sensitivity (51 mV/dec).

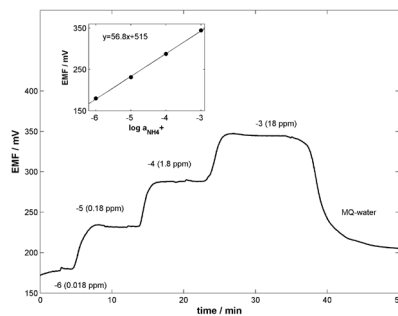


Figure 6.5.6 – EMF vs. time at three concentrations of NH_4^+ in *on-line* conditions (flow rate: 1 mL/min). Inset plot shows the calibration curve for NH_4^+ SC-ISE with its corresponding sensitivity (56.8 mV/dec).

On the other hand, taking into account that the sensing mechanism of the ion selective electrodes is really fast and reversible, having maximum value response time of between 30-60 seconds. For this reason, calibrations in batch conditions for three electrodes were accomplished in order to determine the performance analytical parameters, such as, the limit of detection, sensitivity and especially the response time. (Appx 4, Figure 1,2,3 and, Table 1).

The potentiometric selectivities were evaluated for each sensor in the range of concentrations that we expected to have as a result of the catalytic reaction. We considered including the selectivity experiment and the obtained results in Appendix 4, because selectivity of the SC-ISEs is not one of the main objectives of this work (Appx 4, Figure 4).

6.5.3.2. Control of a catalytic reaction

The catalytic reduction of nitrates reaction was performed using Pt/CeO₂ catalyst without previous reduction treatment, in order to observe the behavior of the catalyst in this hypothetical case. Figure 6.5.7 shows the potentiometric signal for the three sensors during the reaction time. The signal recorded until the peak, i.e, from 0 min to 20 min corresponds to the feed solution of the reactor (130 mg.mL⁻¹ of NO₃⁻). At 19 min the dual valve is switched and the feed solution starts to pass throughout the reactor that contains the catalyst. After 3 min non-converted nitrate and the products of the reaction arrive at the measurement cell. A peak tailing, either positive or negative depending on the sensor, appears at around 28 minutes. The signals recover the baseline values around at 100 minutes into the reaction. Figure 6.5.8 shows a zoom of the Figure 6.5.7 in the reaction zone. Taking into account that ISEs for anions and cations show a negative and positive sign sensitivity respectively, Figure 6.5.8 can be described as: nitrate signal presents a positive transient peak, i.e., decrease of the nitrate concentration, related to the conversion of nitrate into nitrite and ammonium. In the same way, a positive peak for ammonium indicates an increase of the ammonium concentration in the system. Finally, a negative transient for nitrite points out an increase of the nitrite concentration.

Furthermore, these results can be interpreted from the catalytic point of view, where the catalyst shows a maximum of nitrate conversion at 25 min. After that, the deactivation of the catalyst accompanied with a decrease of nitrate conversion is observed. Moreover, these results are in agreement with the unsuitable pre-treatment reduction of the catalyst. Catalysts in the oxidized form show a short time activity in terms of nitrate conversion (peak at 25 min, Figure 6.5.7), due to the fact the active centers of the catalyst cannot be regenerated.

The most relevant data of this catalyst are found between 25 and 35 minutes, where the maximum conversion is reached. By using common analytical techniques, it would be difficult to record these data due to the complexity of the samples acquired every 10 minutes or less for 24 hours.

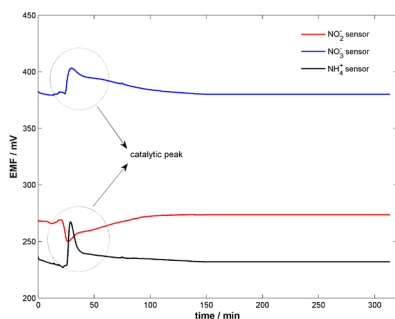


Figure 6.5.7 – On-line monitoring of a denitrification process in the same flow conditions as previously mentioned (Pt/CeO₂ catalyst is used). Three potentiometric signals vs. time are recorded at the same time: blue line signal for NO₃⁻ electrode; red line signal for NO₂⁻ electrode and black line signal for NH₄⁺ electrode. The catalytic peak where the catalyst displays the maximum conversion rate is indicated.

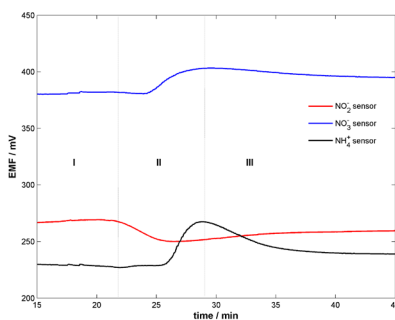


Figure 6.5.8 – Zoom of Figure 6.5.7 in maximum activity shown for the catalyst. Three regions are inserted in the graph indicating different processes. **I)** Baseline of 130 mg.L⁻¹ of NO₃⁻ (feed solution). **II)** Activity zone. The catalyst starts to convert NO₃⁻ reaching the maximum conversion rate. **III)** Deactivation of the catalyst.

Following the calibration curves derived previously (**Figure 6.5.4, 6.5.5 and 6.5.6**), an estimation of the concentration in ppm (mg.L⁻¹) at different times of reaction for each sensor can be obtained. For instance, at 28.4 min the maximum nitrate conversion is 54% with a 96% of nitrogen selectivity, whereas at 90 min the catalyst is completely deactivated showing 1 % of nitrate conversion (**Appx 4, equations 1-4**).

6.5.4. Conclusions

Solid contact ion selective electrodes based on CNTs have been implemented to monitor catalytic processes that have an importance from the point of view of processing environmental samples. The hydrogen current and the overpressure into the system have not influenced the quality of the potentiometric signal.

The performance parameters shown for these SC-ISEs enables the monitoring of this catalytic process in terms of lower limit of detection, sensitivity, stability and linear range. Although, the response time of the system is large (3 min) for a flow system, the catalyst used in this analysis was chosen as the worst case. In other words, without pre-treatment the catalyst is rapidly deactivated showing changes in concentration in short intervals of time. However, in real applications, the catalyst would never display this behaviour, showing a slight deactivation in long intervals of time. For instance, this catalyst (Pt/CeO₂) with an efficient pre-treatment was tested for one week showing the same nitrate rate conversion [5].

These electrodes have not been yet fully characterized in this preliminary work, especially their analytical performance with real samples where the amount and identity of interferences are unknown. In the same way, the incorporation of microelectrodes in order to reduce the volume of the flow cell would be an improvement so as to reduce the long response time observed.

6.5.5. References

- [1] Centi, G. and S. Perathoner, *Remediation of water contamination using catalytic technologies*. Applied Catalysis B-Environmental, 2003. 41(1-2) 15-29.
- [2] Kapoor, A. and T. Viraraghavan, *Nitrate removal from drinking water - Review*. Journal of Environmental Engineering-Asce, 1997. 123(4) 371-380.
- [3] Lecloux, A.J., *Chemical, biological and physical constrains in catalytic reduction processes for purification of drinking water*. Catalysis Today, 1999. 53(1) 23-34.
- [4] Vorlop, K.D. and T. Tacke, *1st Steps Towards Noble-Metal Catalyzed Removal of Nitrate and Nitrite from Drinking-Water*. Chemie Ingenieur Technik, 1989. 61(10) 836-837.
- [5] Barrabes, N., J. Just, A. Dafinov, F. Medina, J.L.G. Fierro, J.E. Sueiras, P. Salagre, and Y. Cesteros, *Catalytic reduction of nitrate on Pt-Cu and Pd-Cu on active carbon using continuous reactor - The effect of copper nanoparticles*. Applied Catalysis B-Environmental, 2006. 62(1-2) 77-85.
- [6] Warn, J., I. Turunen, T. Salmi, and T. Maunula, *Kinetics of nitrate reduction in monolith reactor*. Chemical Engineering Science, 1994. 49(24, Part 2) 5763-5773.
- [7] Epron, F., F. Gauthard, C. Pineda, and J. Barbier, *Catalytic reduction of nitrate and nitrite on Pt-Cu/Al₂O₃ catalysts in aqueous solution: Role of the interaction between copper and platinum in the reaction*. Journal of Catalysis, 2001. 198(2) 309-318.
- [8] Crespo, G.A., S. Macho, J. Bobacka, and F.X. Rius, *Transduction Mechanism of Carbon Nanotubes in Solid-Contact Ion-Selective Electrodes*. Analytical Chemistry, 2009. 81(2) 676-681.
- [9] Crespo, G.A., S. Macho, and F.X. Rius, *Ion-selective electrodes using carbon nanotubes as ion-to-electron transducers*. Analytical Chemistry, 2008. 80(4) 1316-1322.
- [10] Heng, L.Y. and E.A.H. Hall, *Producing "self-plasticizing" ion-selective membranes*. Analytical Chemistry, 2000. 72(1) 42-51.
- [11] Chumbimuni-Torres, K.Y., N. Rubinova, A. Radu, L.T. Kubota, and E. Bakker, *Solid contact potentiometric sensors for trace level measurements*. Analytical Chemistry, 2006. 78(4) 1318-1322.
- [12] Barrabés, N., A. Dafinov, F. Medina, and J.E. Sueiras, *Catalytic reduction of nitrates using Pt/CeO₂ catalysts in a continuous reactor*. Catalysis Today, 2010. 149(3-4) 341-347.

UNIVERSITAT ROVIRA I VIRGILI

SOLID CONTACT ION SELECTIVE ELECTRODES BASED ON CARBON NANOTUBES

Gastón Adrián Crespo Paravano

ISBN:978-84-693-6428-4/DL:T-1630-2010

UNIVERSITAT ROVIRA I VIRGILI

SOLID CONTACT ION SELECTIVE ELECTRODES BASED ON CARBON NANOTUBES

Gastón Adrián Crespo Paravano

ISBN:978-84-693-6428-4/DL:T-1630-2010



CHAPTER 7 MINIATURIZATION

UNIVERSITAT ROVIRA I VIRGILI

SOLID CONTACT ION SELECTIVE ELECTRODES BASED ON CARBON NANOTUBES

Gastón Adrián Crespo Paravano

ISBN:978-84-693-6428-4/DL:T-1630-2010

7.1. Introduction

To satisfy the need for faster analytical information, multitarget and/or multisample determinations would be highly desirable in potentiometry. The possibility of developing multianalyte electrodes would add substantial value to their already attractive characteristics: very high sensitivities and selectivities, affordable cost, simplicity of use and portability. Miniaturization is a prerequisite in the development of multielectrodes. However, unlike FETs, ISEs have only been miniaturized in a robust way very recently [1]. Although very small needle-type ISEs employing internal reference electrodes/solution have been used for several years, their construction is delicate and they suffer from the lack of physical robustness. Solid state ISEs, which eliminate the internal solution and introduce solid transducers, represented a new wave of potentiometric electrodes. Conducting polymers appeared to be promising transducers, able to convert ionic current into electronic current using the redox properties of these materials. However, these electroactive polymers have several drawbacks, of which are previously mentioned in **Chapter 2**. Perhaps one of the strongest limitations is that conducting polymers are sensitive to light [2]. The difference in energy between the valence and conducting bands of most of these compounds matches the visible-near UV wavelengths of daylight, which is clearly a serious instrumental problem.

In this chapter we introduce the miniaturization of ISEs using carbon nanotubes, a nanostructured material that overcomes the problems shown by electroactive polymers.

- [1] Anastasova-Ivanova, S., U. Mattinen, A. Radu, J. Bobacka, A. Lewenstam, J. Migdalski, M. Danielewski, and D. Diamond, *Development of miniature all-solid-state potentiometric sensing system*. Sensors and Actuators B: Chemical, 2010. 146(1) 199-205.
- [2] Lindfors, T., *Light sensitivity and potential stability of electrically conducting polymers commonly used in solid contact ion-selective electrodes*. Journal of Solid State Electrochemistry, 2009. 13(1) 77-89.

7.2. “Nanometric solid-contact ion-selective electrodes using carbon nanotubes as transducers”. In preparation

Gastón A. Crespo ^a, Robert E. Gyurcsányi ^b, Geza Nagy ^c Santiago Macho ^a and F. Xavier Rius ^a

^a Department of Analytical and Organic Chemistry, Rovira i Virgili University, 43007 Tarragona, Spain.

^b Department of Inorganic and Analytical Chemistry, Budapest University of Technology and Economics, Szt. Gellert ter 4, H-1111 Budapest, Hungary.

^c University of Pecs, Department of General and Physical Chemistry, Pecs, Ifjusag utja 6, Hungary.

7.2.1. Abstract

Multiwall carbon nanotubes are fundamental components of the developed solid contact nano-pipette electrodes. Multiwall carbon nanotubes are used as efficient transducers able to convert ionic current to electronic current. We have used the innovative flash electrophoretic technique to attach multiwall carbon nanotubes onto tiny metallic surfaces, optimizing the process and avoiding the use of any dispersant or surfactant that might interfere with the signal. The resulting solid contact nano-electrode has around 200 nm of sensor area. In fact, they will be able to penetrate cells and tissues.

The potentiometric response shows Nernstian behavior and a linear dynamic range between $10^{-6.5}$ and 10^{-2} M. A stable long-term signal is obtained around a few mV per hour. Although these nanoelectrodes are developed for sporadic measurements, we demonstrate that they can also be used to monitor long term processes due to the stability of the response.

Finally, an enriching discussion about theoretical and practical potentiometric limitations at nano-scale is included.

7.2.2. Introduction

Currently, miniaturization is a clear trend in many research fields. It is a desirable prerequisite for the portability of instruments. However, in electrochemistry, it has been used from more than fifty years mainly for medical and physiological purpose [1]. Although, the concept

of miniaturization is sometimes a little confusing due to the fact that it can refer to a reduction in size of just a few millimeters or, up to a few nanometers. In this report it will be used as a process for achieving potentiometric electrodes in which the active area is in the nanometer range taking advantage of the well-known technology employed in the previous chapters to develop macro electrodes.

Potentiometric microelectrodes (μ ISEs) or potentiometric micropipettes with internal cation or anion exchanger solutions with suitable selectivity emerged at the beginning of 1970 for intracellular measurements of potassium and chloride [2, 3]. Following the same idea, other micro potentiometric devices were developed with sensing/detection purposes in several well established analytical techniques such as chromatography [4] or capillary electrophoresis [5], and the new scanning electrochemical microscopy (SECM) [6, 7]. On the other hand, inherent disadvantages of microelectrodes made with inner filling solutions have been reported [8]. Some of these disadvantages include, the drying out of the inner solution, the impossibility to work with high pressure or temperature and contamination of the sample due to the transmembrane fluxes as well as the tedious, and many times unsuccessful, microelectrode construction.

In this way, the development of solid contact microelectrodes (SC- μ ISE) principally is motivated by the miniaturization process and their practical applications. It must be taken into account that an efficient transducer element must be used to obtain a stable potentiometric signal and suitable analytical parameters, otherwise the well known coated wire electrodes (CWE) are achieved [9]. Transducer elements based on only Faradaic process such as poly-pyrrole poly-thiophene derivatives and hydrogel Ag/AgCl have been used until now. However, in the last decade only a few articles were reported using solid contact methodology at the micro or nano scale [10-13]. The incorporation of nanostructured materials as solid-contact transducers represented a breakthrough in the field. The implementation of three dimensional nanostructured carbon monoliths, 3DOM [14], fullerenes [15], carbon nanotubes [16] and other nanostructured materials, as ion to electron transducers confer to the ion-selective electrodes high robustness degree with respect to light sensitivity, undesirable redox side reactions and the presence of a water layer. As it was demonstrated by our group single wall and multiwall carbon nanotubes, transducer layers show a large low frequency capacitance involved in the stabilization of potentiometric signal as well as in the transduction mechanism [17]. Furthermore, the large interfacial area between the carbon nanotubes layer and the polymeric membrane of the ISE provides a non-polarizable interface able to convert the potential generated in the membrane surface into an electronic signal [17, 18].

Among the different types of nanostructured material, carbon nanotubes are very versatile, displaying interesting electronic properties that depend on their widely different structural conformations [19]. Nevertheless, the deposition of the carbon nanotubes with or without surfactants, on different reduced area surfaces was always a challenge. Taking advantage of the acid

chemical functionalization, carboxylic groups can be generated on the surface of the tubes conferring to them an ionic character. The ionized nanotubes can migrate under the influence of a DC field [20], enabling their deposition onto conducting surfaces. In addition, covalent or non covalent functionalization of the carbon nanotubes with synthetic receptors open up in this way new avenues in the potentiometric field.

In this report, the first nano-potentiometric electrode or nanopipette based on multiwall carbon nanotubes as transducer is reported. Electrophoretic deposition process (EDP) was tested and used to deposit homogenous layers of multiwall carbon nanotubes on the distal ends of different wires. In this way, we expect to overcome the drawbacks and the instabilities shown for the conventional micropipettes using internal filling solutions. Moreover, potentiometry is forced here towards its intrinsic limits from the point of view of both the proper interchange current on the phase boundary and of the electrode and the electronic devices used.

7.2.3. Experimental section

7.2.3.1. Reagents and materials

Selectophore grade N,N-dicyclohexyl-N',N'-dioctadecyl-diglycolic diamide (ETH 5234), potassium tetrakis[3,5-bis(trifluoromethyl)phenyl]borate (KTFPB), 2-nitrophenyloctylether (o-NPOE). All chemicals used for the preparation of the solutions were of analytical grade and were obtained from Sigma-Aldrich. All solutions were prepared using deionized water (18 M Ω cm specific resistance), obtained with a Milli-Q PLUS (Millipore Corporation, Bedford, MA). Twenty-five micrometer diameter platinum wires were purchased from Goodfellow (Cambridge, UK). Quartz capillaries were provided from Sutter Instrument (Novato, USA). Multi-wall nanotubes (MW-CNTs) with 95 % purity (outer diameter of 10–20 nm, a length of around 50 μ m) were obtained from Heji, Inc.

7.2.3.2. Electrode construction

Quartz capillaries with internal filament (Internal Diameter 0.7 mm and Outer Diameter 1 mm, length 100 mm, Sutter Instruments) were used in the fabrication of nanoelectrodes. A Sutter 2000 puller machine was employed to make the nano-pipettes. The puller machine has different options that enable us to obtain several sharp ends with lengths and diameters of the pipettes depending on some basic parameters such as puller force-time and temperature of the laser. These parameters were optimized in two program lines obtaining nanopipettes with 2 mm of sharpening and around 200 nm of diameter (First line: 575 3 35 145 75; second line: 425 0 15 128 200). **Figure 7.1a**, **7.1b** and **7.1c** show the characterization of the tip by scanning electron microscopy after gold metallization (10 nm) deposited by sputtering.

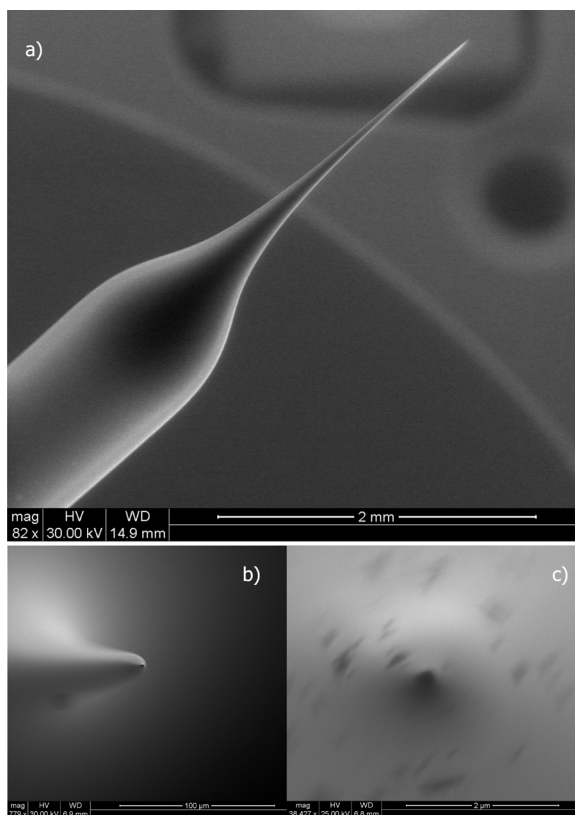


Figure 7.1 – SEM image: **a)** Tip of the nano-pipette after gold metallization. The sharpened length is around 2 mm. **b)** Zoom of the image a) at the tip of the nano-pipette. The black dot corresponds to the hole where the membrane will be placed. **c)** The nano-hole. The measured diameter is around 200 nm.

7.2.3.3. Silanization

The electrodes were placed horizontally inside the bottom part of the glass Petri dish, held with temperature resistance glue. The Petri dish was placed in an oven at 120 °C for 1 hour to eliminate any possible traces of water attached to the glass. After this stage, 50 μL of tri-N-butylchlorosilane were introduced inside the Petri dish and it was covered again.

The electrodes were exposed to chlorosilane concentrated vapours for 5 min, subsequently the cover was removed, and the electrodes were left in the oven at 120 °C for 6 h [21].

The silanization process involves the transformation from a hydrophilic to a hydrophobic surface with the addition of trimethylsilane or other alkylsilane groups. Consequently, the silanization was done to overcome two annoying disadvantages that occur when we are working with

quartz or glass nanopipettes. One of them, it is to avoid the penetration of water from the aqueous solution to the membrane through the quartz wall that in contact with the membrane. The second is to facilitate the filling of the nanopipette with the hydrophobic cocktail, otherwise it is almost impossible for the cocktail to reach the ultra-small tip of the nanopipette.

7.2.3.4. Carbon Nanotubes dispersion

Multiwall carbon nanotubes (MWCNTs) suspension was prepared using a concentrated HNO_3 and H_2SO_4 solution (1:3 volume ratio). 0.1 g of MWCNTs was refluxed in 4 mL of the acidic mixture at 120 °C for 30 minutes. After cooling, the oxidized MWCNTs were rinsed with distilled water to neutral pH, with a yield around 50 wt.% [22]. 0.075 g of the functionalized MWCNTs were dispersed in 10 ml of milli Q water. The MWCNTs suspension was ultrasonicated in an ultrasonic bath (J.P.Selecta Ultrasonics, Spain) for 15 min and centrifuged (3000 rpm for 15 min) producing a well dispersed and stable MWCNT suspension prior to each deposition. The MWCNTs dispersion was characterized by TEM.

7.2.3.5. Carbon Nanotubes deposition

Electrophoretic deposition was carried out under a range of conditions, including variations of DC field (voltages of up to 20 V), deposition time and the separation of the working and counter electrodes in order to find optimal conditions. All EPD experiments were performed at room temperature. The distal ends of the counter and the working electrodes were placed facing each other at the required distance (1 cm) in the suspension and a constant DC voltage applied to the dispersion of MWCNTs using a power supply (Isotech IPS 1810H, Hong Kong) (Figure 7.2).

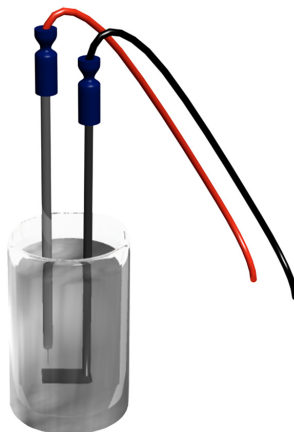


Figure 7.2 – Scheme of the electrophoretic deposition of MWCNTs onto the platinum wire (25 μm of diameter). The migration of MWCNTs is achieved by applying a flash DC potential. MWCNTs are displaced to the positive pole and attaching onto the Pt surface.

The optimal configuration consisted of applying 20 V for 30-40 seconds to the platinum working electrode (25 μm). We tested several conducting wires such as tungsten, steel, gold, carbon fiber and platinum. Platinum, used as the conducting wire proved best in terms of providing a uniform coating on the surface of the MWCNTs. Subsequently, the coated electrode was carefully removed from the EPD cell to minimise any loss of carbon nanotubes. The platinum wire was dried in air at room temperature for 1 h, and stored using the same conditions.

7.2.3.6. Membrane preparation

The composition is based on 2.52 mg of calcium ionophore IV (63.9 mmol/Kg), 1.40 mg potassium tetrakis[3,5-bis-(trifluoromethyl)phenyl]- borate (KTFPB) (50% mmol) and 45.32 mg of 2-nitrophenyloctylether (o-NPOE) [23]. In order to avoid the high resistance of the nano-electrode, PVC was not incorporated in the cocktail.

7.2.3.7. Electrode assembly

The nanopipette was backfilled up with the cocktail using a common syringe adapted with a special tube on the tip (0.5 mm diameter). After this, the electrode was held vertically (upside-down) in a support overnight to try to minimize the formation of bubbles.

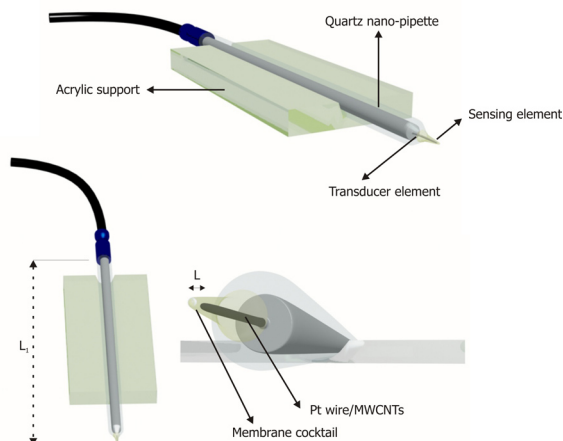


Figure 7.3 – Scheme of the nano-electrode shown in three different perspectives. Platinum wire coated with MWCNTs is inserted into the membrane cocktail. L represents the distance between the Pt wire/MWCNTs and the top of the tip in contact with the aqueous solution (200-500 μm). L_1 is the length of nano-pipette (5 mm).

When the membrane is successfully placed on the tip of the nanopipette, the narrow platinum wire with carbon nanotubes is carefully introduced into the cocktail up to the restricted limit caused by the angle-shape of the pipette. It is important to achieve reproducible devices in terms of distance between the top part of the tip and the CNTs-wire. Small variations in the distance

are reflected in the total resistance of the electrode (**Figure 7.3**). The longitude range estimated with the optical microscope, was between 200-500 μm . As the last step, the wire was fixed to the same support mentioned above by an adhesive in order to avoid electrical noise in the contacts.

7.2.3.8. Electrochemical measurements

7.2.3.8.1. Potentiometric measurements

All electromotive forces (EMF) were performed in a Faraday cage at room temperature in stirred solutions using a high impedance input ($10^{15}\Omega$) Lawson's multichannel (16 channels). A double-junction Ag/AgCl/3 M KCl reference electrode (type 6.0729.100, Methrom AG) containing a 0.01 M LiAcO electrolyte bridge was employed. Activity coefficients were calculated by the Debye-Hückel approximation and the potential measurements were corrected using the Henderson equation for liquid junction potential determination. Electrodes were initially conditioned for 12 hours in 10^{-3} M CaCl_2 and later on for 24 hours in 10^{-8} .

7.2.3.8.2. Impedance measurements

Electrochemical measurements were performed by using a one-compartment, three electrodes electrochemical cell. The working electrode was the nanopipette and the auxiliary electrode was a glassy carbon rod. The reference electrode was an Ag|AgCl|KCl (3 M) single junction (Model 6.0733.100, Metrohm). All measurements were performed at room temperature (23 ± 2 °C). All electrochemical measurements were made using an Autolab general purpose electrochemical system and an Autolab frequency response analyser system (AUT20.FRA2-AUTOLAB, Eco Chemie, B.V., The Netherlands). The impedance spectra were recorded in a frequency range (100 kHz to 0.01 Hz).

7.2.3.8.3. Resistance measurements

Resistance measurements were performed in a Faraday cage at room temperature in unstirred solutions with a Keithley 6514 electrometer in resistance mode. This device is able to record resistance values up to 200 G Ω . Two electrodes were employed, the nanopipette and the platinum electrode.

7.2.4. Results and discussion

Taking advantage of the hydrophilic character of functionalized carbon nanotubes, stable water dispersions without using any kind of surfactant are obtained when they are highly carboxylated. In fact, the ionic character acquired as a result of the chemical functionalization, is needed to produce the migration of MWCNTs when a DC flash voltage is applied between two electrodes.

As can be seen in SEM image (**Figure 7.4**), MWCNTs are distributed uniformly on the surface forming the typical "spaghetti" like layer. It is important to note that after the deposition and dry-

ing of the wire, carbon nanotubes are not easily removed by chemical or mechanical treatment, conferring robustness to the system.

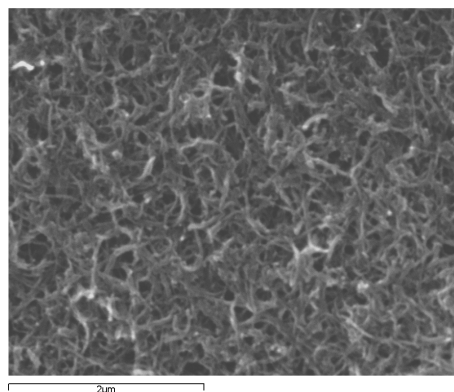


Figure 7.4 – MWCNTs layer deposited onto the Pt substrate displaying its uniform distribution as shown by the SEM image.

In the same way, the MWCNTs dispersion prepared in 7.2.3.4 was characterized by TEM. The strong acid purification cut the MWCNTs reducing their lengths by least in one magnitude order. **Figure 7.5** displays a TEM image where the MWCNTs can be observed. The lengths of several individual MWCNTs were measured inside the marked zone. The lengths are quite variable from 50 to 500 nm. In some cases, MWCNTs displaying 1 μm of length were found.

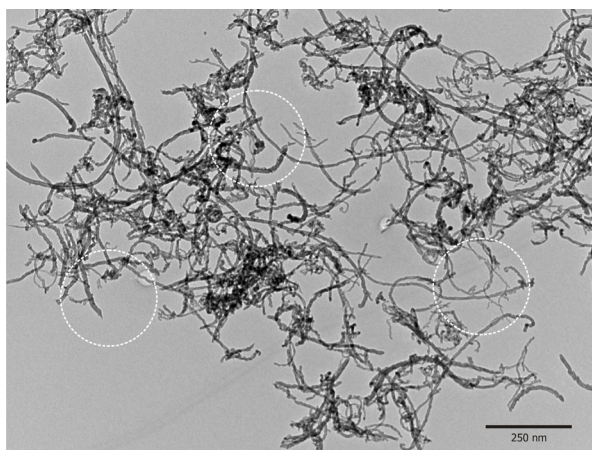


Figure 7.5 – TEM image of carboxylated MWCNTs dispersion prepared in water. The lengths of some MWCNTs were measured around the marked zone (dotted-line circle) ranging from 50 to 500 nm.

The factors involved in the deposition process were optimized starting from the same initial conditions proposed in Boccacini's report [20]. In this way, we found out that Pt is one of the best substrates due to its high stability properties and the easiness to deposit MWCNTs on it. For the platinum wire, applying 20 V several times during time intervals between 10 s to 120 s, the optimal deposition time is between 30 and 40 seconds. During shorter time periods, the coating was not complete and patches of substrate appeared. During longer periods, the thickness increased in a non-uniform way showing accumulations, elevations and depressions of MWCNTs. In fact, they seem to accumulate in a fluffy way, losing the robust properties. In the range from 5 to 20 V, there are negligible differences in terms of layer aspect although the higher the voltage applied the shorter the deposition time. Other types of metals such as gold or copper were also analyzed. However, inhomogeneous layers were obtained with these types of supports. Possibly the dissolution of these metals occurring at these voltage-current values is what makes the proper deposition of nanotubes difficult. Titanium wire shows a black color after the EDP, however MWCNTs were not observed on the examined surface under microscope inspection. It is highly probable that some Ti oxides can be formed, making the attachment of MWCNTs on the surface difficult. Inexpensive carbon fiber was also used as substrate obtaining very similar results to the ones obtained with platinum. Nevertheless, the fragility of the carbon fiber is an important drawback for nanoelectrode development.

Figure 7.6 shows the potentiometric response obtained at different concentrations of calcium as well as the calibration curve. The sensitivity follows Nernstian behavior for divalent cations. In the same figure, it can be observed that the limit of detection (LOD) is around $10^{-6.5}$ M. We expected to reach a very low LOD using this special cocktail because the concentration of ionophore inside the membrane is larger than the values used in traditional membranes.

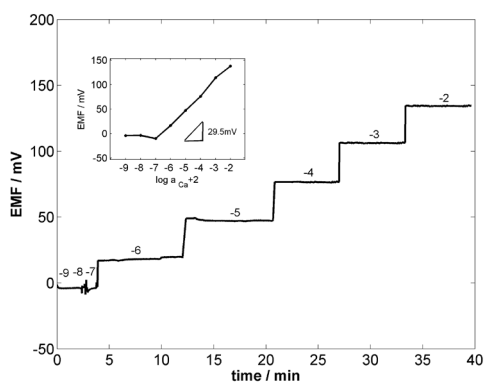


Figure 7.6 – The recorded EMF as function of the time for different activities of calcium. The plot in the inset shows the calibration curve for the developed calcium nano-electrode.

Other performance parameters of the solid contact nano-pipette developed with the incorporation of functionalized multiwall carbon nanotubes were evaluated, parameters such as, the long term stability. These electrodes show similar drift values (around a few $0.1 \text{ mV}\cdot\text{h}^{-1}$) [24] to other macroelectrodes using MWCNTs as a transducer. In fact a coated wire electrode without MWCNTs was developed in the same conditions showing a considerable associated drift. Selectivity was evaluated for Na^+ , K^+ , Li^+ , NH_4^+ and Mg^{+2} by SSM method [25] showing similar results as the ones obtained by Sundorf [23].

On another hand, it is well-known that one of the major problems concerning the development of ultra-small sensors is the large total resistance and the low exchange current density between the aqueous solution/membrane interface (10 nm). Nowadays, the commercial potentiometers have high-input impedance around $10^{15} \Omega$ or even higher, therefore, it is possible to work with resistances around $10^{11} \Omega$ ($10^{-2} \%$ precision in the voltage reader) and current values around 1 fA ($10^{-20} \text{ mol electron/s}$ or 10^4 electron/s) [26]. However, the lack of efficient exchange-current density can generate the polarization of the electrode. In an efficient transducer the exchange-current density must be higher than the measuring current. If the standard exchange current, which is of the order of $10^{-2} \text{ A}\cdot\text{cm}^{-2}$ and the measuring current it is only 1 fA, then the polarization process would occur when the surface area is smaller than 10^{-10} cm^2 and the sample activity is smaller than 10^{-6} M . Our developed nano-electrode has comparable dimensions. For this reason, a high amount of ionophore was incorporated into the membrane. An increase of exchange current should be achieved though the limit of detection does not reach values down to $10^{-6.5}$.

Additionally, a small parasitic current due to any external power can generate undesired noisy fluctuations in the recorded potential. Therefore, the measurements have to be performed inside a grounded Faraday cage and coaxial cables with their respective ground connection must be used.

Resistance values of nano-pipettes containing the same membrane cocktail and filled up with internal electrolyte (KCl 0.1 M) were evaluated and compared with our electrodes. As we expected, the nanopipette filled with the membrane cocktail shows higher resistance around $35 \pm 5 \text{ G}\Omega$ than the nanopipette filled with internal electrolyte displaying a resistance between 0.5-1 G Ω . On the other hand, MWCNTs nanopipettes could not be characterized by EIS due to poor resolution at these G Ω levels. Therefore, the high resistance values were recorded using a Keithley electrometer. The stabilization time of the signal using these devices is not short, due to the large RC factor.

7.2.5. Conclusions

We have developed for the first time a solid contact nano-electrode based on MWCNTs. The electrode shows suitable performance parameters that enable its application to samples where size is the largest restriction.

We have shown that MWCNTs can act efficiently as a transducer layer at the nano-scale improving some parameters previously reported for micropipette electrodes with internal solution.

On another hand, we report a simple-way to deposit MWCNTs on reduced and irregular surface areas like the distal ends of micro-metallic-wires. This deposition technique enables a further covalent functionalization of the deposited MWCNTs, attaching several organic functions as well as supramolecular receptors to the carboxylic groups generated in the initial treatment with strong acids.

Potentiometric technique was forced to its limits due to the ultra-small sensor area (10^{-10} cm²) and the high resistance (35 G Ω). Finally, these electrodes could be used to test samples having very reduced volumes, such as the physiological conditions inside the cells, where the estimation of calcium ions at these levels (10^{-6} M) is very relevant.

7.2.6. Acknowledgments

This work was supported by the Spanish MICINN, through the project grants NAN2004-09306-C05-05 and CTQ2006-7-67570/BQU. G.A.C. also acknowledges MICINN for the doctoral fellowship AP2006-04171. The authors thank Professor Ernő Pretsch for his recommendations and encouraging discussions.

7.2.7. References

- [1] Caldwell, P.C., *Studies on the internal pH of large muscle and nerve fibres*. Journal of Physiology-London, 1958. 142(1) 22-62.
- [2] Cornwall, M.C., D.F. Peterson, D.L. Kunze, J.L. Walker, and A.M. Brown, *Intracellular potassium and chloride activities measured with liquid ion exchanger microelectrodes*. Brain Research, 1970. 23(3) 433-436.
- [3] Khuri, R.N., S.K. Agulian, and J.J. Hajjar, *Measurement of intracellular potassium with liquid ion-exchange microelectrodes*. Journal of Applied Physiology, 1972. 32(3) 419-8.
- [4] Manz, A. and W. Simon, *Picoliter cell-volume potentiometric detector for open-tubular column LC*. Journal of Chromatographic Science, 1983. 21(7) 326-330.
- [5] Nann, A. and E. Pretsch, *Potentiometric detection of anions separated by capillary electrophoresis using an ion-selective microelectrode*. Journal of Chromatography A, 1994. 676(2) 437-442.
- [6] Wei, C., A.J. Bard, G. Nagy, and K. Toth, *Scanning electrochemical microscopy .28. ion-selective neutral carrier-based microelectrode potentiometry*. Analytical Chemistry, 1995. 67(8) 1346-1356.
- [7] Toth, K., G. Nagy, C. Wei, and A.J. Bard, *Novel application of potentiometric microelectrodes - scanning potentiometric microscopy*. Electroanalysis, 1995. 7(9) 801-810.
- [8] Lindfors, T., *Light sensitivity and potential stability of electrically conducting polymers commonly used in solid contact ion-selective electrodes*. Journal of Solid State Electrochemistry, 2009. 13(1) 77-89.
- [9] Bobacka, J., A. Ivaska, and A. Lewenstam, *Potentiometric ion sensors*. Chemical Reviews, 2008. 108(2) 329-351.

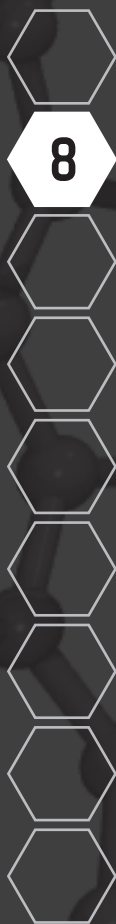
- [10] Gyurcsanyi, R.E., A.S. Nyback, K. Toth, G. Nagy, and A. Ivaska, *Novel polypyrrole based all-solid-state potassium-selective microelectrodes*. *Analyst*, 1998. 123(6) 1339-1344.
- [11] Lamaka, S.V., M.G. Taryba, M.L. Zheludkevich, and M.G.S. Ferreira, *Novel Solid-Contact Ion-Selective Microelectrodes for Localized Potentiometric Measurements*. *Electroanalysis*, 2009. 21(22) 2447-2453.
- [12] Gyetvai, G., S. Sundblom, L. Nagy, A. Ivaska, and G. Nagy, *Solid contact micropipette ion selective electrode for potentiometric SECM*. *Electroanalysis*, 2007. 19(10) 1116-1122.
- [13] Shim, J.H., J. Kim, G.S. Cha, H. Nam, R.J. White, H.S. White, and R.B. Brown, *Glass nanopore-based ion-selective electrodes*. *Analytical Chemistry*, 2007. 79(10) 3568-3574.
- [14] Lai, C.Z., M.A. Fierke, A. Stein, and P. Buhlmann, *Ion-Selective Electrodes with Three-Dimensionally Ordered Macroporous Carbon as the Solid Contact*. *Anal. Chem.*, 2007. 79(12) 4621-4626.
- [15] Fouskaki, M. and N. Chaniotakis, *Fullerene-based electrochemical buffer layer for ion-selective electrodes*. *Analyst*, 2008. 133(8) 1072-1075.
- [16] Crespo, G.A., S. Macho, and F.X. Rius, *Ion-selective electrodes using carbon nanotubes as ion-to-electron transducers*. *Analytical Chemistry*, 2008. 80(4) 1316-1322.
- [17] Crespo, G.A., S. Macho, J. Bobacka, and F.X. Rius, *Transduction Mechanism of Carbon Nanotubes in Solid-Contact Ion-Selective Electrodes*. *Analytical Chemistry*, 2009. 81(2) 676-681.
- [18] Fierke, M.A., C.Z. Lai, P. Buhlmann, and A. Stein, *Effects of Architecture and Surface Chemistry of Three-Dimensionally Ordered Macroporous Carbon Solid Contacts on Performance of Ion-Selective Electrodes*. *Analytical Chemistry*, 2010. 82(2) 680-688.
- [19] Dai, H.J., *Carbon nanotubes: Synthesis, integration, and properties*. *Accounts of Chemical Research*, 2002. 35(12) 1035-1044.
- [20] Cho, J., K. Konopka, K. Rozniatowski, E. Garcia-Lecina, M.S.P. Shaffer, and A.R. Boccacini, *Characterisation of carbon nanotube films deposited by electrophoretic deposition*. *Carbon*, 2009. 47(1) 58-67.
- [21] Tripathi, S., N. Morgunov, and E.L. Boulpaep, *Sub-micron tip breakage and silanization control improve ion-selective microelectrodes*. *American Journal of Physiology*, 1985. 249(5) C514-C521.
- [22] Boccacini, A.R., J. Cho, J.A. Roether, B.J.C. Thomas, E.J. Minay, and M.S.P. Shaffer, *Electrophoretic deposition of carbon nanotubes*. *Carbon*, 2006. 44(15) 3149-3160.
- [23] Sundfors, F., R. Bereczki, J. Bobacka, K. Toth, A. Ivaska, and R.E. Gyurcsanyi, *Microcavity based solid-contact ion-selective microelectrodes*. *Electroanalysis*, 2006. 18(13-14) 1372-1378.
- [24] Crespo, G.A., D. Guga, S. Macho, and F.X. Rius, *Solid-contact pH-selective electrode using multi-walled carbon nanotubes*. *Analytical and Bioanalytical Chemistry*, 2009. 395(7) 2371-2376.
- [25] Bakker, E., *Determination of improved selectivity coefficients of polymer membrane ion-selective electrodes by conditioning with a discriminated ion*. *Journal of the Electrochemical Society*, 1996. 143(4) L83-L85.
- [26] Morf, W., D. Ammann, and W. Slmon, *New horizons in the development of Ca²⁺-selective microelectrode: can single ions be determined?*. 1st Bioelectroanalytical Symposium, 1986 309.

UNIVERSITAT ROVIRA I VIRGILI

SOLID CONTACT ION SELECTIVE ELECTRODES BASED ON CARBON NANOTUBES

Gastón Adrián Crespo Paravano

ISBN:978-84-693-6428-4/DL:T-1630-2010



CHAPTER 8 CONCLUSIONS

UNIVERSITAT ROVIRA I VIRGILI

SOLID CONTACT ION SELECTIVE ELECTRODES BASED ON CARBON NANOTUBES

Gastón Adrián Crespo Paravano

ISBN:978-84-693-6428-4/DL:T-1630-2010

8.1. Conclusions

The main conclusion of this thesis is that a layer of **carbon nanotubes** (CNTs) can effectively act as an ion-to-electron transducer in solid contact ion selective electrodes (SC-ISEs). For the first time, we have demonstrated that this nanostructured material is not only a successful transducer but also displays several advantages over the previous materials used in solid-contact electrodes.

This general conclusion can be detailed in a series of specific conclusions:

Potentiometric results demonstrated that a layer of single wall carbon nanotubes deposited onto a non-conducting substrate (PVC) first and onto a conducting substrate later is able to transduce an ionic current into electronic current in SC-ISEs.

The transduction mechanism in SC-ISEs based on CNTs is elucidated by means of electrochemical techniques such as electrochemical impedance spectroscopy and cyclic voltammetry. The transduction mechanism proposed for a layer of CNTs perfectly fits the experimental results and it is in agreement with CNTs structure and properties. The high surface area to volume ratio and the intrinsic electronic characteristics of the CNTs are the reason for the high double layer capacitance appearing in the electrode, which is responsible of the stabilization of the potentiometric signal transduced.

Both single wall and multiwall carbon nanotubes, with different purification processes, are suitable materials to act as efficient transducers in SC-ISEs. The semiconducting, semi metallic or metallic properties of the CNTs do not affect the transduction event in potentiometric SC-ISEs, in contrast to other devices such as CNT field effect transistors, where the semiconducting character is a strong requirement.

The incorporation of a new synthetic ionophore into the polymeric ion selective membrane offers the opportunity to recognise choline and derivatives. The conjunction of two complementary technologies such as the use of non-carboxylated SWCNTs as transducers and synthetic receptors as new ionophores, generate an attractive SC-ISE capable to detect choline and derivatives.

The new solid contact electrodes offer the possibility to detect chemical species with interesting operational performance characteristics such as easy handling, rapidness, sensitivity, selectivity, low cost or the possibility to measure *in-situ* and under pressure conditions. In this way, the developed solid-contact electrodes contribute to several trends in modern chemical analysis. As examples of the above mentioned properties, the developed SC-ISEs based on CNTs have been applied to an environmental application and to monitor on-line a catalytic process, showing unique capabilities only achieved nowadays using non-portable very expensive instrumental techniques.

The main advantages of CNTs as components of the transducer layer in solid contact ion selective electrodes can be detailed as:

1. Insensitiveness to light and gases.
2. Large long term stability.
3. Insensitiveness to redox secondary reactions.
4. Lipophilicity.
5. Possibilities of miniaturization.

The possibility to miniaturize the SC-ISEs based on carbon nanotubes has been achieved in the last part of this thesis. The complexity of the development of micro or nano SC-ISEs is reflected in the literature where only a slight growing tendency of this topic is observed. As a proof of concept a nanometric (200 nm of diameter) solid contact ion selective electrode using CNTs as transducer is developed. The most important point is that CNTs play an important role in the transduction process at the nanometric scale. Nonetheless, at 10^{-10} cm² of active area, potentiometry is forced here towards its intrinsic limits from the point of view of both the proper interchange current across the phase boundary of the electrode and the electronic devices used. The analytical performance parameters of the nanometric electrode should be further optimised for the proper use of the electrodes in measurements with real samples such as calcium gradients in cells or tissues.

8.2. Future prospects

It has been recently demonstrated that CNTs can be incorporated in the polymeric matrix of ISEs improving the stability obtained with coated wire electrodes [1,2]. The suitable covalent or not covalent functionalization of CNTs with selective receptors will probably enable the incorporation of charged ionophores, avoiding the leaching out from the ion selective membrane.

SC-ISEs based on CNTs will be a promising technology to implement in applied fields such as biology or environmental sciences, where the actual analytical tools are unsuitable to trace down some processes.

Full-miniaturization of the SC-ISEs based on CNTs in the modes of needle-type electrodes using nano-pipettes or with planar electrodes will be an important challenge for the next future. Efforts will have to be put also in the development of reference electrodes and the suitable detection systems. This research will have a clear impact into areas such as clinical analysis, where the rapid quantification of ions or small molecules is essential in routine diagnostics.

8.3 References

- [1] Zhu, J., Y. Qin, and Y. Zhang, *Preparation of all solid-state potentiometric ion sensors with polymer-CNT composites*. *Electrochemistry Communications*, 2009. 11(8) 1684-1687.
- [2] Zhu, J., X. Li, Y. Qin, and Y. Zhang, *Single-Piece Solid-Contact Ion-Selective Electrodes with Polymer Carbon Nanotube Composites*. *Sensors and Actuators B: Chemical*, 2010. doi:10.1016/j.snb.2010.04.041.

UNIVERSITAT ROVIRA I VIRGILI

SOLID CONTACT ION SELECTIVE ELECTRODES BASED ON CARBON NANOTUBES

Gastón Adrián Crespo Paravano

ISBN:978-84-693-6428-4/DL:T-1630-2010



APPENDICES



UNIVERSITAT ROVIRA I VIRGILI

SOLID CONTACT ION SELECTIVE ELECTRODES BASED ON CARBON NANOTUBES

Gastón Adrián Crespo Paravano

ISBN:978-84-693-6428-4/DL:T-1630-2010

Appendix 1. Glossary

β_{iL}, β_i : formation constant between ligand and i ion

β_{jL}, β_j : formation constant between ligand and j ion

$c_{i(org)}, c_i$: activity coefficient of ion i in organic phase

$c_{j(org)}, c_j$: activity coefficient of ion j in organic phase

ΔE_{ac} : amplitude of the alternate current (Volts)

$\Delta G_r^{0,w \rightarrow m}$: standard free energy transition of ion i from water (aqueous) to membrane phase

Δx : thickness of diffusional layer in the aqueous phase

$n_{i(org)}^\circ$: standard chemical potential of ion i in aqueous phase [J mol⁻¹]

$n_{i(aq)}^\circ$: standard chemical potential of ion i in organic phase [J mol⁻¹]

μ ISEs: ion selective microelectrodes

τ_D : diffusional time constant (s⁻¹)

Ω : resistance unit (Ohm)

$a_i(I)$: activity of ion i in a pure phase of I

$a_{i(aq)}$: activity of ion i in aqueous phase

$a_{i(org)}$: activity of ion i in organic phase

$a_j(J)$: activity of ion j in a pure phase of J

AChOCl: acetylcholine chloride

AIBN: azobisisobutyronitrile initiator

a_K^{+} : activity of potassium in the sample

aq: aqueous phase

C_b : bulk capacitance

C_D : diffusional pseudocapacitance

C_d : electronic capacitance

C_{dl} : double layer capacitance

ChO⁺: choline ion

ChOCl: choline chloride

c_i : phase boundary concentration of i (mol L⁻¹)

$c_{i(aq)}, c_{i,bulk}$: concentration of ion i in aqueous phase (mol L⁻¹)

$c_{i(org)}$: concentration of ion i in organic phase (mol L⁻¹)

$c_{j(aq)}$: concentration of ion j in aqueous phase (mol L⁻¹)

$c_{j(org)}$: concentration of ion j in organic phase (mol L⁻¹)

CNTFET: carbon nanotubes field effect transistor

CNTs: carbon nanotubes

COOH: carboxyl function

CV: cyclic voltammetry

CWE: coated wire electrode

D: diffusion coefficient (cm² s⁻¹)

DC: direct current

DMA: decylmethacrylate

DMF: dimethylformamide

DOS: bis(2-ethylhexyl sebacate)

E_{const} : constant term of the potential equation

$E_{D,ref}$: liquid junction potential of the reference electrode

$E_{D'}$: the diffusional potential inside the membrane

E_{dc} : direct current potential

EDP: electrophoretic deposition

EIS: electrochemical impedance spectroscopy

E_M : membrane potential

EMF: electromotive force

E_i^o : standard potential of ion i

E_j^o : standard potential of ion j

E_{PB} : phase boundary potential between membrane/inner solution or inner solid contact with membrane

$E_{PB'}$: phase boundary potential between the membrane/sample

ESEM: scanning electron microscopy

ETH 1907: 4-Nonadecylpyridine (proton ionophore II)

ETH 500: Tetrakis(4-chlorophenyl)borate tetradodecylammonium salt

ETH 5234: calcium ionophore (IV)

F: Faraday constant (96485 C mol⁻¹)

fA: femtoampere (10⁻¹² Amperes)

GΩ: gigaohm (10⁹ Ohms)

GC: glassy carbon rod

Hz: frequency unit (Hertz)

I: current unit (Ampere)

i, *I*: primary ion

[IL]: concentration of complex inside the membrane

ISEs: Ion Selective Electrodes

IS-ISEs: internal solution ion selective electrodes

ISM: ion selective membrane

IUPAC: international union of pure and applied chemistry

j: interference ion

k_i : "single ion distribution coefficient of cation *i*"

K_{ij} : exchange equilibrium constant of ions *i* and *j* for aqueous and membrane phases.

k_j : "single ion distribution coefficient of cation *j*"

K_{ij}^{pot} : potentiometric selectivity coefficient of ion *i* and *j*

KTFPB: Potassium tetrakis[3,5-bis(trifluoromethyl)phenyl]borate

KTpCIPB: Potassium tetrakis[*p*-chlorophenyl]borate

L: diffusion length (cm)

L: Ligand or ionophore

LDL: lower detection limit

LOD: limit of detection

L_T : total ligand concentration (mol L⁻¹)

MMA: methylmethacrylate

mSWNTs: metallic single wall carbon nanotubes

MWCNTs: multiwall carbon nanotubes

N^- : anion with negative charge

N^+ : cation with positive charge

nA: nanoampere (10⁻⁹ Amperes)

NaTFPB: sodium tetrakis[3,5-bis(trifluoromethyl)-phenyl]borate

NaTPB: Sodium tetraphenylborate

n-BA: n-butyl acrylate

n_i : charge of the ion *i*

n_j : charge of the ion *j*

- o-NPOE*: *o*-nitrophenyl octyl ether
org: organic phase
PBP: phase boundary potential
 p_c : partition coefficient
PEDOT: poly(3,4-ethylenedioxythiophene)
PIA: profiling ion selective analyzer
POT: poly(3 -octylthiophene)
Pt: platinum wire
PVC: Poly(vinyl chloride)
R: cation exchanger
R: molar gas constant ($8.314 \text{ J K}^{-1} \text{ mol}^{-1}$)
R⁻: anion exchanger
 R_{ct} : charge-transfer resistance
 R_D : diffusion resistance
 R_e : electronic resistance
RMN: resonance magnetic nuclear
rpm: revolutions per minute
 R_s : solution resistance
 R_T : total ion-exchanger concentration (mol L^{-1})
s: constant ($59.2 \text{ mV}/n$)
SC- μ ISE: solid contact ion selective microelectrodes
SC-ISE: ion-selective electrodes with internal solid-contact
SDS: sodium dodecylsulfate
SEM: scanning electron microscopy
SSM: separated solution method
sSWNTs: semiconducting single wall carbon nanotubes
SWCNT: single-walled carbon nanotubes
SWCNTs: single wall carbon nanotubes
T: absolute temperature (K)
 $t_{90\%}$: response time
 $t_{95\%}$: response time

TDDA: tri-n-dodecylamine

TDMACl: tridodecylmethylammonium chloride

TEM: transmission electron microscopy

TGA: termogravimetric analysis

ULD: upper limit of detection

V: voltage unit (Volt)

Z: impedance

Z_D : "classical" finite-length Warburg diffusion element

Z_W : Warburg diffusion impedance

3DOM: three dimensional ordered macroporous

UNIVERSITAT ROVIRA I VIRGILI

SOLID CONTACT ION SELECTIVE ELECTRODES BASED ON CARBON NANOTUBES

Gastón Adrián Crespo Paravano

ISBN:978-84-693-6428-4/DL:T-1630-2010

Appendix 2. Equations

Complementary information of the **Chapter 2**.

Equation (2.19), (2.20) and (2.21) are in relation with (2.4) and (2.5)

$$\Delta G_{ir}^{0,w \rightarrow m} = \mu_{i(org)}^0 - \mu_{i(aq)}^0 = nFE_i^0 = RT \ln k_i \quad (2.19) \quad [22]$$

$$E_{PB} = \frac{RT}{n_i F} \ln k_i + \frac{RT}{n_i F} \ln \frac{a_{i(aq)}}{a_{i(org)}} \quad (2.20)$$

$$E_{PB} = \frac{RT}{n_i F} \ln \frac{k_i a_{i(aq)}}{a_{i(org)}} \quad s = \ln 10 \cdot \frac{RT}{F} \quad (2.21)$$

Equation (2.22) and (2.23) correspond to the deduction of (2.6). In equation (2.22) the charge balance between the concentration of the primary ion (I^+) and the total lipophilic ion sites (R_T) in the organic phase is shown.

$$(I^+)_{(org)} = R_T \quad \text{and} \quad a_{i(org)} = (I^+)_{(org)} \gamma_{i(org)} \quad (2.22)$$

$$E_{PB} = \frac{s}{n_i} \log \frac{k_i}{a_{i(org)}} + \frac{s}{n_i} \log a_{i(aq)} \quad \text{being a new} \quad E_i^0 = \frac{s}{n_i} \log \frac{n_i k_i}{R_T \gamma_{i(org)}} \quad (2.23)$$

Equation (2.24), (2.25), (2.26) and (2.27) correspond to the deduction of (2.7). Equation 2.24 shows the charge balance for the organic phase including the free primary ion concentration (I^+), the complex (ionophore-primary ion) concentration (IL^+) and the total lipophilic ion sites (R_T). Equation 2.25 displays the expression corresponding to the formation constant. Using (2.24) and (2.25), (2.26) and (2.27) are obtained.

$$(I^+)_{org} + (IL^+)_{org} = R_T \quad \text{and} \quad (L)_{org} + (IL^+)_{org} = L_T \quad (2.24)$$

$$\beta_{iL} = \frac{(IL^+)_{org}}{(I^+)_{org} (L)_{org}} \quad (2.25)$$

$$(I^+)_{org} = c_{i(org)} = \frac{R_T}{n \beta_{iL} (L_T - R_T / n)} \quad (2.26)$$

$$E_{PB} = E_i^0 + \frac{s}{n_i} \log a_{i(aq)} = \frac{s}{n_i} \log \frac{n_i k_i \beta_{iL} \left(L_T - \frac{R_T}{n} \right)}{\gamma_{i(org)} R_T} + \frac{s}{n_i} \log a_{i(aq)} \quad (2.27)$$

Selectivity equations without ionophore

$$K_{ij}^{pot} = \frac{a_i(I)}{a_j(J)^{n_i/n_j}} \quad (2.28)$$

$$a_i(I) = e^{\frac{n_i F}{RT}(E_i - E_i^0)} \quad \text{and} \quad a_j(J) = e^{\frac{n_j F}{RT}(E_j - E_j^0)} \quad \text{choosing } E_j = E_i \quad (2.29) \quad (2.30)$$

$$K_{ij}^{pot} = \frac{e^{\frac{n_i F}{RT}(E_i - E_i^0)}}{\left(e^{\frac{n_j F}{RT}(E_j - E_j^0)} \right)^{n_i/n_j}} = e^{\frac{n_i F}{RT}(E_j^0 - E_i^0)} \quad (2.31)$$

$$a_{i(org)} = \gamma_{i(org)} R_T \quad \text{and} \quad a_{j(org)} = \gamma_{j(org)} R_T \quad (2.32)$$

Inserting (2.23) and (2.32) for the primary ion and interference in (2.31), equation (2.33) is obtained:

$$K_{ij}^{pot} = 10^{\frac{n_i}{s}(E_j^0 - E_i^0)} = 10^{\frac{n_i}{s} \left(\frac{s \log \frac{k_j}{a_{j(org)}} - s \log \frac{k_i}{a_{i(org)}}}{n_j} \right)} = \frac{\gamma_i R_T}{k_i n_i} \left(\frac{k_j n_j}{\gamma_j R_T} \right)^{n_i/n_j} \quad (2.33)$$

Selectivity equations with ionophore

$$a_{i(org)} = \frac{\gamma_i R_T}{n_i \beta_{iL} (L_T - R_T / n_i)} \quad \text{and} \quad a_{j(org)} = \frac{\gamma_j R_T}{n_j \beta_{jL} (L_T - R_T / n_j)} \quad (2.34) \quad (2.35)$$

Inserting (2.23), (2.34) and (2.35) for the primary ion and interference in (2.31), equation (2.36) is obtained:

$$K_{ij}^{pot} = 10^{\frac{n_i}{s}(E_j^0 - E_i^0)} = \frac{\gamma_i R_T}{n_i \beta_{iL} k_i (L_T - R_T / n_i)} \left(\frac{n_j \beta_{jL} k_j (L_T - R_T / n_j)}{\gamma_j R_T} \right)^{n_i/n_j} \quad (2.36)$$

Nicolski-Eisenman-Bakker formalism,

This equation gives the phase boundary potential when the influence of the interference is small [27].

$$E = E_1^0 + \frac{RT}{n_i F} \ln \left(a_i(IJ) + \left(K_{ij}^{pot} \right)^{n_i/n_j} a_i(IJ)^{1-(n_i/n_j)} a_j(IJ) \right) \quad (2.37)$$

Appendix 3. Complementary information of chapter 3

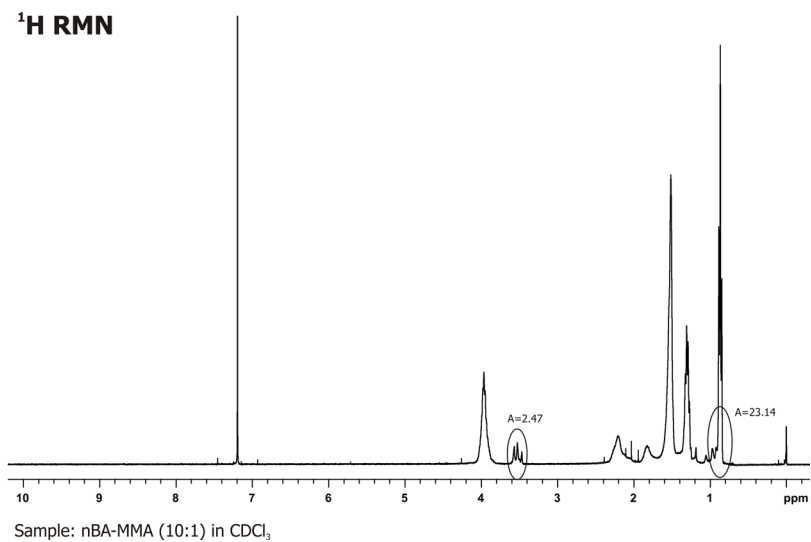


Figure 1 – Proton RMN spectrum of the acrylic membrane nBA-MMA (10:1).

UNIVERSITAT ROVIRA I VIRGILI

SOLID CONTACT ION SELECTIVE ELECTRODES BASED ON CARBON NANOTUBES

Gastón Adrián Crespo Paravano

ISBN:978-84-693-6428-4/DL:T-1630-2010

Appendix 4. Complementary information of chapter 6 (6.5)

Figure 1, 2 and 3 show the calibration curves for NO_3^- , NO_2^- and NH_4^+ solid contact ion selective electrodes based on CNTs in batch conditions respectively. In the same way, in Table 1 are included the LODs and the response time of the sensors.

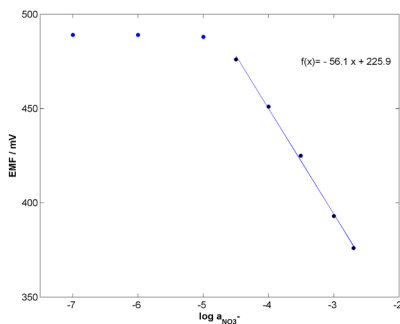


Figure 1 – Calibration curve for NO_3^- SC-ISE in batch conditions obtained by successive addition methodology.

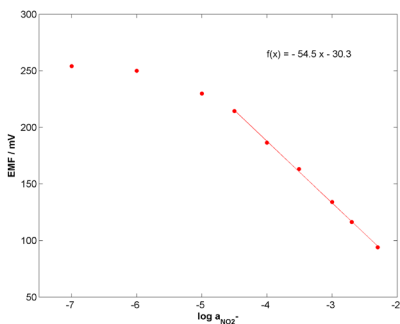


Figure 2 – Calibration curve for NO_2^- SC-ISE in batch conditions obtained by successive addition methodology.

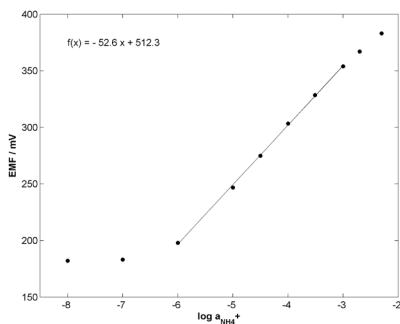


Figure 3 – Calibration curve for NH_4^+ SC-ISE in batch conditions obtained by successive addition methodology.

Sensor	NO_3^-	NO_2^-	NH_4^+
LOD*(mg.L^{-1})	0.5-0.6	0.4-0.5	0.001-0.002
Response time (s)	30	35	20

Table 1 – Main analytical performance parameters for the SC-ISEs obtained in batch conditions are summarized in the table. *LODs were calculated by duplicate.

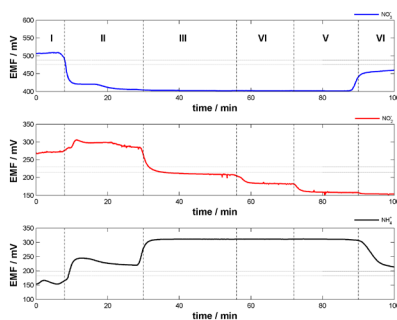


Figure 4- MQ-Water ; II- 49.6 ppm NO_3^- , 18.4 ppm Na^+ ; III-49.6 ppm NO_3^- , 5.6 ppm NH_4^+ , 1.4 ppm NO_2^- , 19.1 ppm Na^+ ; IV- 49.6 ppm NO_3^- , 5.6 ppm NH_4^+ , 4.6 ppm NO_2^- , 20.7 ppm Na^+ ; V- 49.6 ppm NO_3^- , 5.6 ppm NH_4^+ , 14.2 ppm NO_2^- , 25.3 ppm Na^+ ; VI- 1.9 ppm NO_3^- , 0 ppm NH_4^+ , 14.2 ppm NO_2^- , 7.85 ppm Na^+

Figure 4 shows a selectivity plot in the working conditions of this process. Usually the concentration of the nitrate is two orders higher than nitrite and ammonium concentrations. Therefore, various set of experiments were done to explore as the system response in the extreme conditions. In the same figure are plotted the three sensors and the horizontal dot-line represent a

zone of the LODs (there is a small range between two lines, where the sensors starts to respond and the signals are discriminated of the baseline noise).

From I to II can be inferred the effect of 18.4 ppm of sodium over ammonium signal reaching a biased concentration of 0.01 ppm of ammonium. This value is found under the expected concentration of ammonium in the process. Nitrite sensor changes are placed under the LOD of the sensor.

From II, III, IV and V experiments show as nitrite can be quantified for different concentrations (1.4, 4.6 and 14.2 ppm NO_2^-) at high background concentration of nitrate. Stable ammonium signal is also observed, although the concentration of sodium changes in 5 ppm.

From V to VI, ten times of nitrite over nitrate are kept. There is a negligible effect over the nitrate signal reaching a value around 455 mV belongs to 2 ppm nitrate. Ammonium decrease nearby of its limit of detection.

Conversion and selectivity equations.

$$\begin{aligned} & \% \text{ Conversion nitrate} && (1) \\ & (\text{initial } \text{NO}_3^- \text{ moles} - \text{final } \text{NO}_3^- \text{ moles}) \cdot 100 / (\text{initial } \text{NO}_3^- \text{ moles}) \end{aligned}$$

$$\begin{aligned} & \% \text{ Selectivity Nitrite} && (2) \\ & (\text{Converted } \text{NO}_3^- \text{ moles}) \cdot 100 / \text{final } \text{NO}_2^- \text{ moles} \end{aligned}$$

$$\begin{aligned} & \% \text{ Selectivity Ammonium} && (3) \\ & (\text{Converted } \text{NO}_3^- \text{ moles}) \cdot 100 / \text{final } \text{NH}_4^+ \text{ moles} \end{aligned}$$

$$\begin{aligned} & \% \text{ Selectivity Nitrogen} && (4) \\ & 100 - (\% \text{ Selectivity Nitrite} + \% \text{ Selectivity Ammonium}) \end{aligned}$$

UNIVERSITAT ROVIRA I VIRGILI

SOLID CONTACT ION SELECTIVE ELECTRODES BASED ON CARBON NANOTUBES

Gastón Adrián Crespo Paravano

ISBN:978-84-693-6428-4/DL:T-1630-2010

Appendix 5. Short CV

1980. Born on the 25th of August in Buenos Aires, Argentina.
- 1986-1993. Primary school education - Nº18, Buenos Aires.
- 1994-1999. Secondary school education - Don Zeno Institute, Buenos Aires.
- 2000-2005. Undergraduated education at Buenos Aires University (UBA). Chemistry degree.
- 2006-2007. Nanoscience and Nanotechnology MSc. degree. Rovira I Virgili University (URV), Spain.
- 2007-2010. Ph.D studies in the group of Prof. F. Xavier Rius (URV) on nanostructured chemical sensors.

Papers directly resulting from the Doctoral Thesis

- [1] Crespo, G.A., S. Macho, and F.X. Rius, *Ion-selective electrodes using carbon nanotubes as ion-to-electron transducers*. Analytical Chemistry, 2008. 80(4) 1316-1322.
- [2] Crespo, G.A., S. Macho, J. Bobacka, and F.X. Rius, *Transduction Mechanism of Carbon Nanotubes in Solid-Contact Ion-Selective Electrodes*. Analytical Chemistry, 2009. 81(2) 676-681.
- [3] Ampurdanes, J., G.A. Crespo, A. Maroto, M.A. Sarmentero, P. Ballester, and F.X. Rius, *Determination of choline and derivatives with a solid-contact ion-selective electrode based on octamide cavitated and carbon nanotubes*. Biosensors & Bioelectronics, 2009. 25(2) 344-349.
- [4] Crespo, G.A., D. Gugsá, S. Macho, and F.X. Rius, *Solid-contact pH-selective electrode using multi-walled carbon nanotubes*. Analytical and Bioanalytical Chemistry, 2009. 395(7) 2371-2376.
- [5] Kirf, M., Crespo, G.A., Rius, F.X. and Wehrli, B. "New robust potentiometric sensors for dissolved ions in the water column". Limnology & Oceanography. In preparation.
- [6] Crespo, G.A., Gyurcsanyi R., Geza, N., Macho, S., and Rius F.X. "Nano-solid contact ion-selective electrode using carbon nanotubes as tranducer". In preparation.

Papers indirectly resulting from the Doctoral Thesis

- [1] Parra, E.J., G.A. Crespo, J. Riu, A. Ruiz, and F.X. Rius, "Ion-selective electrodes using multi-walled carbon nanotubes as ion-to-electron transducers for the detection of perchlorate". Analyst, 2009. 134(9) 1905-1910.
- [2] Düzgün, A., Zelada, G., Crespo, G.A., Macho, S., Riu, J and Rius, F.X. "Nanostructured materials in potentiometry" Analytical and Bioanalytical Chemistry, 2010. In press.
- [3] Rius-Ruiz, F.X., Crespo, G.A., Berenjano, D., Katakis, I., Riu, J., and Rius, F.X. "Screen-printed potentiometric cell based on carbon nanotubes". In preparation.
- [4] Alemayehu, W.P., Macho, S., Crespo, G.A. and Rius, F.X. "Potentiometric on-line detection of aromatic hydrocarbons in aqueous phase using carbon nanotube-based sensors". Submitted 2010.

- [5] Parra, E.J., Blondeau P, Crespo, G.A and F.X. Rius, "Lead-ionophore covalently bonded on carbon nanotubes used as recognition-transducer nanostructured assembly in potentiometric sensors". In preparation.

Patents

Gastón A. Crespo, Santiago Macho, Jordi Riu, F. Xavier Rius. "Electrodos selectivos de iones de contacto sólido basados en nanotubos de carbono". Spanish Patent (P200701468) being internationally expanded. The patent has been licensed to the company NT Sensors S.L.

Oral communications

1. F.Xavier Rius-Ruiz, Gastón A. Crespo, Diego Berenjano, Ionais Katakis, Jordi Riu and F.Xavier Rius. "Screen-printed ion selective electrodes based on carbon nanotubes". III Workshop of Nanoscience and Nanotechnology 2009. Oviedo (Spain).
2. Gastón A. Crespo, Santiago Macho, Johan Bobacka and F. Xavier Rius. "Transduction mechanism of carbon nanotubes in solid contact ISEs". Mátrafüred 2008—International Conference on Electrochemical Sensors-Dobogókő (Hungary).
3. Gastón A. Crespo, Santiago Macho and F. Xavier Rius. "Ion selective electrodes based on CNTs". SENSONAT 2008. Alicante (Spain).
4. Gastón A. Crespo, Santiago Macho and F. Xavier Rius. "Carbon Nanotubes Based Solid Contact Electrode". I Workshop of Nanoscience and Nanotechnology 2007. Cordoba (Spain). Flash presentation.

Posters

1. Jordi Ampurdanés, Gastón A. Crespo, Alicia Maroto, M. Angeles Sarmentero, Pau Ballester and F. Xavier Rius. "Determination of choline and derivatives using a solid-contact CNT-based ISE". Mátrafüred 08 – International Conference on Electrochemical Sensors - Dobogókő (Hungary).
2. Gastón A. Crespo, Santiago Macho, Johan Bobacka and F. Xavier Rius. "Electrochemical Impedance Spectroscopy of SWCNTs films". II Workshop of Nanoscience and Nanotechnology 2008. Tarragona (Spain).
3. Jordi Ampurdanes, Gastón A. Crespo, Alicia Maroto, M. Angeles Sarmentero, Pau Ballester and F. Xavier Rius. "Solid-contact CNTs based electrode for the determination of trimethylammonium ions". II Workshop of Nanoscience and Nanotechnology 2008. Tarragona (Spain).
4. Enrique Parra, Gastón A. Crespo, Jordi Riu and F. Xavier Rius. "Electrodo selectivos de iones para la determinación de perclorato utilizando nanotubos de múltiples capas como transductores". II Workshop of Nanoscience and Nanotechnology 2008. Tarragona (Spain).
5. Derese Gugsu Desta, Gastón A. Crespo, Santiago Macho and F. Xavier Rius. "Development of a solid state hydrogen ion selective electrode based on multi-walled carbon nanotubes". II Workshop of Nanoscience and Nanotechnology 2008. Tarragona (Spain).

UNIVERSITAT ROVIRA I VIRGILI

SOLID CONTACT ION SELECTIVE ELECTRODES BASED ON CARBON NANOTUBES

Gastón Adrián Crespo Paravano

ISBN:978-84-693-6428-4/DL:T-1630-2010

UNIVERSITAT ROVIRA I VIRGILI

SOLID CONTACT ION SELECTIVE ELECTRODES BASED ON CARBON NANOTUBES

Gastón Adrián Crespo Paravano

ISBN:978-84-693-6428-4/DL:T-1630-2010

UNIVERSITAT ROVIRA I VIRGILI

SOLID CONTACT ION SELECTIVE ELECTRODES BASED ON CARBON NANOTUBES

Gastón Adrián Crespo Paravano

ISBN:978-84-693-6428-4/DL:T-1630-2010

UNIVERSITAT ROVIRA I VIRGILI

SOLID CONTACT ION SELECTIVE ELECTRODES BASED ON CARBON NANOTUBES

Gastón Adrián Crespo Paravano

ISBN:978-84-693-6428-4/DL:T-1630-2010

UNIVERSITAT ROVIRA I VIRGILI

SOLID CONTACT ION SELECTIVE ELECTRODES BASED ON CARBON NANOTUBES

Gastón Adrián Crespo Paravano

ISBN:978-84-693-6428-4/DL:T-1630-2010

UNIVERSITAT ROVIRA I VIRGILI

SOLID CONTACT ION SELECTIVE ELECTRODES BASED ON CARBON NANOTUBES

Gastón Adrián Crespo Paravano

ISBN:978-84-693-6428-4/DL:T-1630-2010